CRITICAL ROLE OF EUKARYOTIC TRANSLATION INITIATION FACTOR 4G DEGRADATION IN MEDIATING ISCHEMIA-INDUCED NEURONAL DEATH

by

Peter S. Vosler

B.S. in Psychobiology, Quinnipiac University, Hamden, CT, 2000

Submitted to the Graduate Faculty of

School of Medicine in partial fulfillment

of the requirements for the degree of

Doctorate of Philosophy in Neurobiology

University of Pittsburgh

2009

UNIVERSITY OF PITTSBURGH

SCHOOL OF MEDICINE

This dissertation was presented

by

Peter S. Vosler

It was defended on

June 26, 2009

and approved by

Brian M. Davis, PhD, Professor of Medicine and Neurobiology

Donald J. DeGracia, PhD, Associate Professor of Research, Wayne State University

Donald B. DeFranco, PhD, Professor and Vice Chair of Pharmacology and Chemical Biology and Neuroscience

Lewis Jacobson, PhD, Professor of Biological Sciences

Xiaoming Yin, MD, PhD, Professor of Pathology

Committee Chair: Teresa G. Hastings, PhD, Associate Professor, Neurology and Neuroscience

Thesis Advisor: Jun Chen, MD, Professor of Neurology and Director of the Center for Cerebrovascular Research

CRITICAL ROLE OF EUKARYOTIC TRANSLATION INITIATION FACTOR 4G DEGRADATION IN MEDIATING ISCHEMIA-INDUCED NEURONAL DEATH

Peter S. Vosler, PhD

University of Pittsburgh, 2009

Stroke is the third leading cause of death in the United States and the second leading cause of death in the world. Despite the epidemiological significance of this disease, there are few treatment options. The purpose of this dissertation is to expand the understanding of underlying mechanisms mediating neuronal death caused by stroke, or cerebral ischemia. Two major metabolic disturbances occur due to ischemia—persistent protein synthesis inhibition and secondary energy depletion. All ischemia-affected neurons experience protein synthesis inhibition. However, neurons that recover protein synthesis live, while neurons that fail to recover die. This makes protein synthesis a robust predictor of neuronal death. However, the underlying mechanisms of persistent protein synthesis inhibition remain unknown. The hypothesis of this dissertation is that persistent protein synthesis inhibition is caused by activation of the calcium-sensitive protease calpain, which degrades eukaryotic translation initiation factor (eIF) 4G. Inhibition of calpain or overexpression of eIF4G results in increased protein synthesis and increased neuronal viability following the *in vitro* model of ischemia oxygen glucose deprivation in rat primary cortical neurons. Importantly, the neuroprotective effect of preservation of eIF4G is only partly due to its restoration of protein synthesis. Potential protein synthesis-independent mechanisms eIF4G-mediated protection are discussed.

Neurons subjected to ischemia suffer an initial loss of energy in the form of ATP, which returns to baseline within fifteen minutes of restoration of blood flow. However, ischemia-sensitive neurons undergo secondary energy depletion prior to delayed neuronal death. The cause of secondary energy failure is hypothesized to be due to DNA recognition enzyme poly(ADP)-ribose polymerase (PARP)-1 depletion of the energy substrate NAD^+. Evidence is

presented linking PARP-1 activation to mitochondrial calcium dysregulation with subsequent calpain activation and apoptosis-inducing factor release.

The results of these two findings are discussed in depth and future experiments are outlined. The potential of role of eIF4G in mitochondrial biogenesis, inhibition of autophagy and prevention of secondary energy loss is postulated. The research presented in this dissertation provides a novel perspective regarding the mechanisms underlying delayed neuronal death and may eventually lead to the development of clinically applicable neuroprotective strategies.

TABLE OF CONTENTS

LIST OF FIGURES

PREFACE

The path to obtaining a Ph.D. in neurobiology in an MD/PhD program is both tumultuous and rewarding. In addition to the rigorous training in terms of coursework, clinical training, grant and paper writing and execution of experiments, life happens. I never would have predicted that I would be called to active duty in the Army to serve in Iraq just five months after entering medical school. The repercussions of my experience affected all aspects of my life. Fortunately, I was able to perform well in medical school. Unfortunately, during my PhD training I got married and soon thereafter divorced. This was a very dark period of my life and for my graduate training.

In spite of the negative occurrences in my life, I was able to emerge to complete my PhD training. This could not have been accomplished without the support of a number of family and friends. I owe a tremendous amount of gratitude first, and foremost, to my family. My mother and father, Karen and Steve Vosler, are the foundation from which all I have achieved has been built. Their omnipresent love and guidance has made me into the man I am today. I thank you Mom and Dad for raising me well as a child and becoming my friends and continued mentors as an adult. My brother Dan has proven to be a great friend. He has helped me immensely throughout my life, especially during the last ten years. I cherish the support and laughter you have provided me throughout the years.

I also owe appreciation to some influential teachers and professors that have guided me and nurtured my intellectual development. In high school, I have to thank Mr. Dominico for challenging me to push my creativity to new limits. Dr. Cornelius Meyer at Quinnipiac University was instrumental in the initial phases of my higher education compelling me to pursue Psychobiology as a major and I believe provided me with the foundation for my future academic success. Dr. Joan Bombace, also at Quinnipiac University, provided me with my introduction to research. If she had not approached me to conduct research with her, I probably would not have pursued a PhD. I thank you Joan.

More recent influential mentors include my two research advisors at Pittsburgh. Dr. Clifton Callaway has been an excellent mentor who provided me with an outstanding and nurturing environment immediately after I returned from Iraq for my first research rotation. Importantly, I have to thank Dr. Jun Chen, my thesis advisor, for all he has done for me. Performing my dissertation work in his lab has permitted me to attain goals I never thought possible. Thank you for your guidance Dr. Chen.

I also want to thank some friends that helped me along the way. Thank you to Sam Clanton and Dr. Justin McCray for helping get through some difficult times by providing me with laughter, high jinks, and much needed distraction. Thank you to Dr. Joshua Hrabosky for being a tremendous and perseverant friend, and for your support and guidance. Finally, and most importantly, thank you to the love of my life, Mae Gould. You have been my rock and are the one who restored me to the man I was meant to be. I cherish you and the life we will spend together.

The path to this achievement has been tumultuous, but the support of my family, friends and mentors has made it rewarding and worthwhile. I feel a tremendous sense of accomplishment at my intellectual development over the past several years, and I look forward to continued growth in my career and in my life. And, despite the unfortunate occurrences in my life, I still strive to attain my childlike aspiration:

To see a world in a grain of sand
And a heaven in a wild flower,
Hold infinity in the palm of your hand,
And eternity in an hour.

-William Blake, Auguries of Innocence

Perhaps, with continued introspection and support from loved-ones, some day I'll achieve this goal.

1.0 Overview of Ischemic Stroke

1.1 INTRODUCTION

Brain tissue relies virtually solely upon oxygen and glucose for its energy requirements. Despite only comprising 2% of total body weight, the brain receives 15% of the cardiac output and it consumes approximately 20% (160μmol/100g/min) of the blood's oxygen content. Because the CO_2 output of the brain is nearly identical to the oxygen consumption, carbohydrates are the main substrate for energy production. This is exemplified by the brain utilizing a quarter of the body's glucose content. The continuous supply of glucose is also critical for brain function because it lacks substantive glycogen stores to replenish any glucose deficit. The brain is thus exquisitely sensitive to perturbations in energy homeostasis, making it highly susceptible to conditions that reduce flow of the oxygen and glucose carrying blood (Magistretti PJ, 1995).

Cerebral blood flow (CBF), the product of cerebral perfusion pressure divided by cerebral vascular resistance, normally ranges between 50 and 57 ml/100g/min in primates. Reductions in cerebral perfusion pressure caused by decreased arterial pressure (as in cardiac arrest) or focally due to embolic or thrombotic occlusion are initially compensated by autoregulatory vasodilation to diminish cerebrovascular resistance. Once autoregulation is maximal, the brain extracts increasing amounts of glucose and oxygen from the blood to

preserve its energy requirements. The CBF must remain above the critical threshold of 15-20 ml/100g/min to maintain normal metabolism. Below this threshold, the brain is no longer able to function normally and clinical symptoms of ischemia are observed (Magistretti PJ, 1995).

Neurologic disorders such as ischemic and hemorrhagic stroke, cardiac arrest and traumatic brain injury are all related by substantial cerebral ischemia resulting in neuronal damage, brain tissue loss, physical, behavioral and cognitive impairment and potentially death. Greater understanding of the pathophysiology underlying the deficits caused by cerebral ischemia will serve to mitigate the negative neurological sequelae following the insult. Of the aforementioned insults, ischemic stroke is the predominant form of cerebral ischemia in the United States (Hirtz et al., 2007).

This dissertation will thus address ischemic stroke in detail, outlining the epidemiological statistics and the pathophysiology of the insult at the tissue, cellular and molecular level. Although the etiology of cardiac arrest greatly differs from ischemic stroke, the global ischemia model of cardiac arrest is also discussed due the common characteristics of the pathophysiology to ischemic stroke. Furthermore, the findings of the basic science models of ischemic stroke and cardiac arrest are commonly generalized to both conditions. The dissertation will go into detail regarding ischemia-induced, caspase-independent programmed cell death. Novel research addressing the mechanisms underlying this phenomenon is presented in Chapter 2, Calcium dysregulation induces apoptosis-inducing factor release: Cross-talk between PARP-1- and calpain-dependent signaling pathways.

Another phenomenon common to both ischemic stroke and cardiac arrest is the impairment of protein synthesis in ischemia-affect brain tissue. The past research is reviewed in detail with an attempt to support the supposition that the failure to reinstate protein synthesis is a

causative factor in delayed neuronal death. A detailed article is provided in Chapter 3, Critical role of eukaryotic initiation factor 4G degradation in mediating ischemia-induced neuronal death, with novel findings delineating an important mechanism responsible for ischemia-induced protein synthesis inhibition.

The dissertation will culminate with a thorough discussion of the implications of the findings of Chapters 2 and 3. Future directions for the understanding of delayed neuronal death are explored with a discussion of novel avenues for understanding delayed neuronal death with the aim of developing novel clinically translatable therapeutics.

1.2 ISCHEMIC STROKE

1.2.1 Epidemiology of Ischemic Stroke

Ischemic stroke comprise 80% of all clinical strokes with hemorrhagic stroke making up the remaining 20%. Stroke affects approximately 795,000 people each year with 75% of patients suffering their first incident and the remainder experiencing recurrent attacks (Lloyd-Jones et al., 2009). Ischemic stroke, herein referred solely as stroke, ranks as the third leading cause of death in industrialized nations (including the U.S.) and the 2nd leading cause of death worldwide (Lloyd-Jones et al., 2009). According to the most recent stroke statistics available, every 40 seconds someone in the U.S. suffers a stroke. The U.S. death rate due to stroke in 2006 was 43.6

people per 100,000 people in the U.S. population during the given year, and 1 out of 17 deaths were due to stroke.

Stroke, however, does not uniformly result in death, and stroke survivors are subjected to debilitating physical, mental and cognitive dysfunction. Stroke is thus a major cause of long-term disability ((CDC), 2001), and approximately one third of stroke survivors receive outpatient rehabilitation. The substantial disability caused by stroke is predicted to cost the U.S. $68.9 billion in 2009 when the costs of inpatient care, rehabilitation and follow-up care for enduring deficits are totaled (Lloyd-Jones et al., 2009).

The incidence of stroke is similar across genders; however, data is emerging suggesting a rise in stroke incidence in middle aged women, and outcomes in women may be worse in women (Towfighi et al., 2007). Ethnicity is an established factor as there is a nearly two-fold increase in stroke incidence in blacks compared with whites. In addition to greater incidence, the severity of stroke in blacks is greater accompanied by an increased mortality rate (Stansbury et al., 2005).

1.2.2 Etiology

Strokes were traditionally categorized as arising from either embolic or thrombotic infarcts. Embolic infarcts are caused by a portion of a substance, usually a blood clot, formed in a distant vessel or organ, which becomes dislodged and travels to a distal region where it occludes a vessels. Thrombotic events are caused by blood clots that form locally, usually due to atherosclerosis, and occlude the blood vessel. A more comprehensive classification system was established in 1993 categorizing strokes resulting from cardioembolism, large-artery

atherosclerosis, small vessel occlusion, stroke of other determined etiology or idiopathic (unknown) origins (Adams et al., 1993).

Cardioembolism occurs when a thrombus formed in the heart becomes dislodged and occludes a cerebral vessel. This can occur following atrial fibrillation, release of a thrombus formed on the wall of the heart (mural thrombus), ventricular akinesis (following a heart attack), dialated cardiomyopathy or a disease of the valves of the heart (Adams et al., 1993).

Large-artery atherosclerosis can result in substantial restriction of blood flow in major extracranial and intracranial arteries. Atherosclerosis commonly occurs at branches of major vessels, such as the carotid artery or at the origins of vessels. Infarction can occur locally as the atherosclerotic plaque immediately occludes its resident vessel. A portion of the plaque or clot can also become dislodged and occlude another distal artery, or it may simply causes hypoperfusion that results in clinically significant symptom generation. The predominant presentation of patients with large-artery atherosclerosis is a recurrence of clinical symptoms due to the occlusion of blood flow to the same cerebral territory (Blumenfeld, 2002).

The final major classification of stroke etiology is small-vessel occlusion. This is when the small-penetrating branches off the major cerebral arteries that supply the deeper regions of the brain become occluded (Adams et al., 1993). These structures include the basal ganglia, thalamus, and internal capsule within the cerebral hemispheres. Occlusions of these vessels are also called lacunar infarcts due to their resemblance of small lakes on pathological section (Blumenfeld, 2002). The other two classifications of stroke are very infrequent and will not be discussed here.

The etiology of transient ischemic attacks (TIAs) should also be discussed briefly. As the name implies, TIAs are merely short term deficits in neurologic function wherein the patient has

complete recovery. Originally TIAs were considered any neurologic deficit that lasts less than 24 hours. That definition has been substantially revised because it is known in animal models and imaging studies that ischemic episodes lasting longer than ten minutes can result in permanent damage. Thus, the duration of TIA has been refined to lasting approximately 10 minutes. Although TIAs are temporary, they are not completely benign. The highest risk of stroke occurs within a few days of TIA (Johnston et al., 2000). The occurrence of TIAs is thus useful clinically to determine underlying cerebrovascular disease.

1.2.3 Risk Factors

The risk factors for stroke mainly include patients with vascular diseases. These include hypertension, diabetes, hypercholesterolemia, cigarette smoking, having a family history of stroke and a prior history of having a stroke. Any evidence of cardiac disease, including atrial fibrillation or having a low ejection fraction due to congestive heart failure, is also a risk factor for stroke. Less commonly, stroke is caused by patients with hypercoagulable states. Any patient with an increased risk for forming random clots is at a higher risk for stoke, myocardial infarction, pulmonary embolism and deep venous thrombosis (Lloyd-Jones et al., 2009).

1.2.4 Anatomy of Stroke

In addition to etiology, stroke is characterized by the major vessel or portion of the vessel occluded and the area of the brain damaged. This section will provide a succinct overview of the vascular supply of the brain and the classic symptoms that arise from infarcts to the major

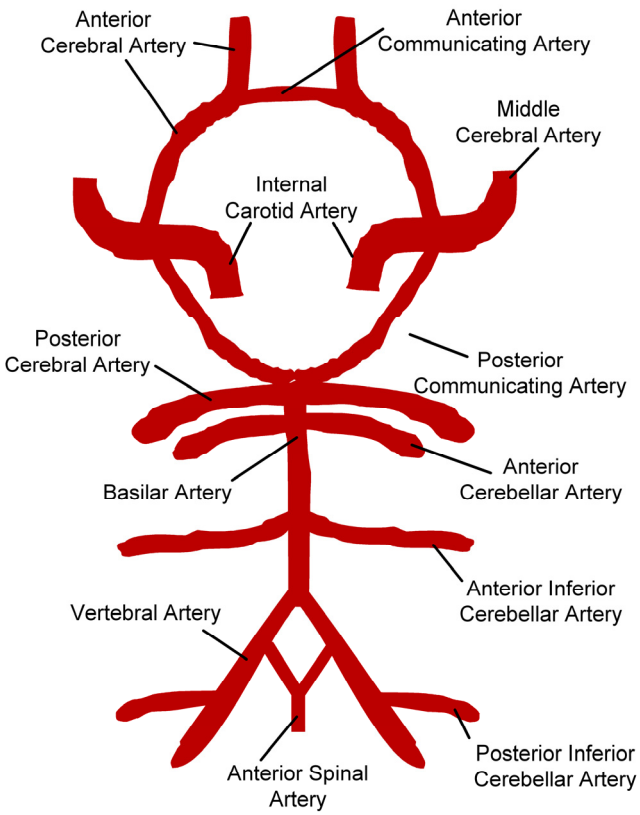

Figure 1.1 Circle of Willis. This is a depiction of the anastamotic relationship between the anterior and posterior cerebral circulation. A full circle of Willis is present in only 25% of people.

vessels. The major cerebral vessels can be divided into many segments, each having its unique clinical characteristics. This is beyond the scope of this dissertation, and the general brain area affected and the clinical symptoms produced by ischemia will suffice to provide an understanding of the significance of knowing cerebrovascular anatomy. Greater detail can be found elsewhere (Blumenfeld, 2002).

The blood supply to the brain is derived from two sets of systemic vessels. The anterior circulation is supplied by the internal carotid artery and the posterior circulation is supplied by the vertebral arteries. The right and left carotid arteries arise from the aortic arch where they

branch into the internal and external carotids at the carotid bifurcation. The internal carotid has two terminal branches located within the brain—the anterior cerebral artery (ACA) and the middle cerebral artery (MCA). The vertebral arteries arise from the subclavian arteries, course through the transverse processes of the cervical vertebrae, enter the skull through the foramen magnum and join to form the basilar artery. The anterior and posterior circulations anastomose at a vascular ring name the circle of Willis (**Figure 1.1**). The anterior circulations of the left and right hemispheres are joined by the anterior communicating arteries. The posterior circulation joins the anterior segment via the posterior communicating arteries. The circle of Willis provides substantial collateral blood flow in the advent of occlusion. Interestingly, a complete circle is only present in approximately 25% of people (Blumenfeld, 2002).

1.2.4.1 Anterior Cerebral Artery. The ACA runs medially and anteriorly between the cerebral hemispheres to supply the inferior surface of the frontal lobe (**Figure 1.2**). It then courses posteriorly over the corpus callosum to supply the medial portion of the primary motor and sensory cortices. Occlusion of the ACA results in contralateral motor weakness and sensory deficits of the lower extremity. Frontal lobe abnormalities and aphasia can also be present (Blumenfeld, 2002).

1.2.4.2 Middle Cerebral Artery. Of the cerebral arteries, the MCA supplies the largest area. This is possibly one of the reasons strokes are more common in the MCA territories than in the anterior or posterior cerebral artery territories. Logically, due to it being the most frequent infarct in humans, the most common animal model of stroke is performed by occluding the MCA.

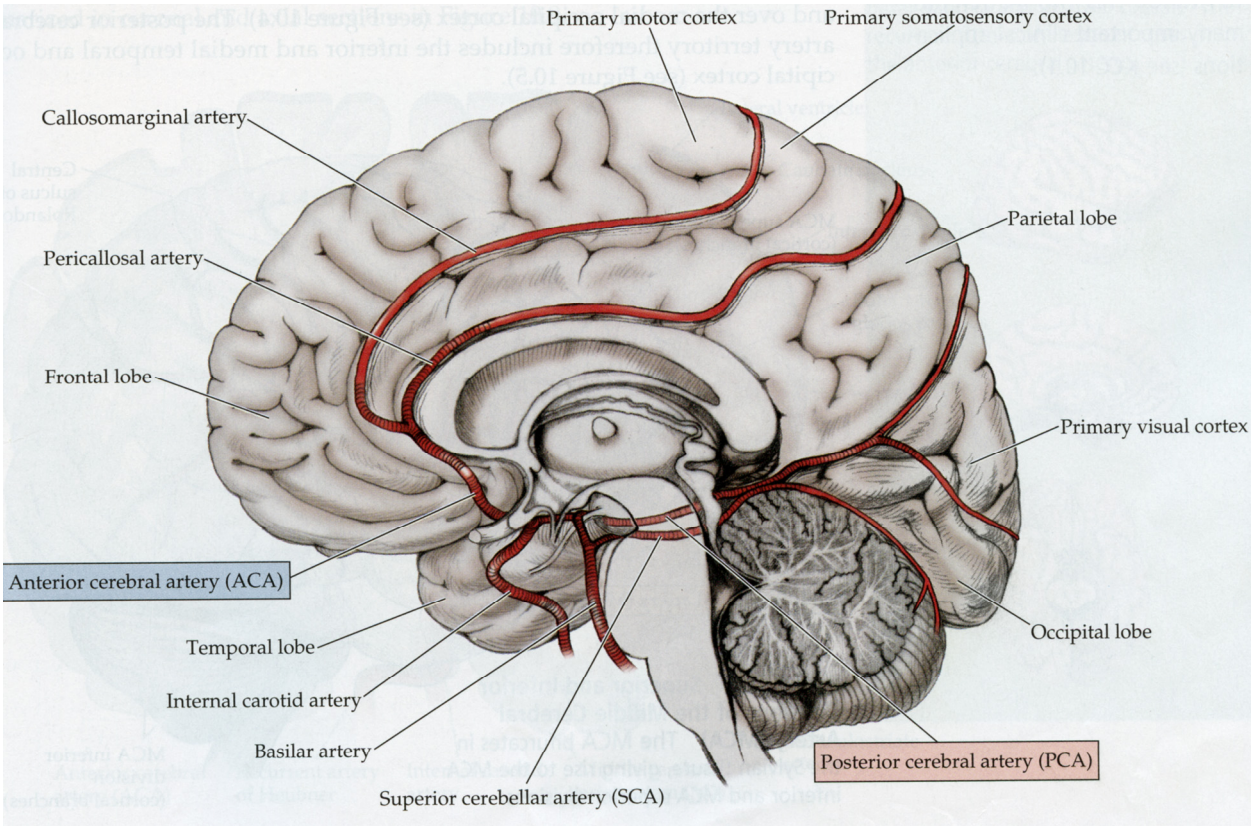

Figure 1.2 Anterior Cerebral Artery Territory. The anterior cerebral artery supplies the medial aspect of the cerebral hemispheres (from H. Blumenfeld. In *Neuroanatomy Through Clinical Cases*, Copoyright 2002 by Sinauer Associates, Inc. Used by permission of Sinauer Associates, Inc.).

The MCA supply can be divided into three regions: superior division, inferior division and deep territory. From the circle of Willis, the MCA runs laterally where its initial branches are the lenticulostriate arteries. These arteries supply the deep territory of the MCA including the basal ganglia and the internal capsule. Distal to the lenticulostriate arteries, the MCA courses into the Sylvian fissure and bifurcates into superior and inferior divisions (**Figure 1.3 and 1.4**). The superior division accordingly supplies the cortex above the Sylvian fissure while the inferior division supplies the cortex below the Sylvian fissure and a portion of the parietal cortex.

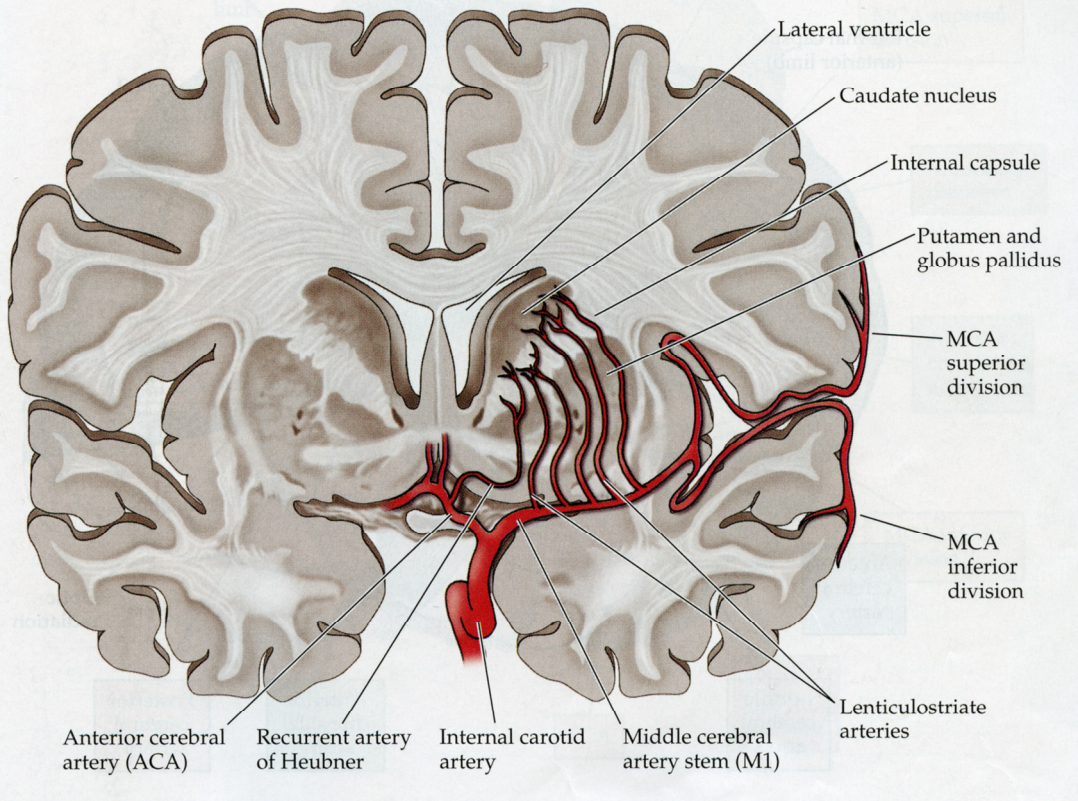

Figure 1.3 Internal Middle Cerebral Artery Territory. The middle cerebral artery supplies structures such as the thalamus and basal ganglia internally via the lenticulostriate arteries. It courses toward the external surface of the cerebral hemisphere in the Sylvian fissure. (from H. Blumenfeld. In *Neuroanatomy Through Clinical Cases*, Copoyright 2002 by Sinauer Associates, Inc. Used by permission of Sinauer Associates, Inc.).

Occlusion of the superior division of the MCA can result in Broca's aphasia (left-sided occlusion), contralateral face and arm weakness and possible contralateral face and arm sensory loss. Damage to the inferior division can cause Wernicke's or fluent aphasia (left-sided occlusion), left hemineglect (right-sided occlusion), and possibly contralateral weakness. Deep territory MCA infarcts result in complete contralateral motor hemiparesis as this territory supplies the internal capsule. Finally, patients with occlusion to the MCA proximal to the region

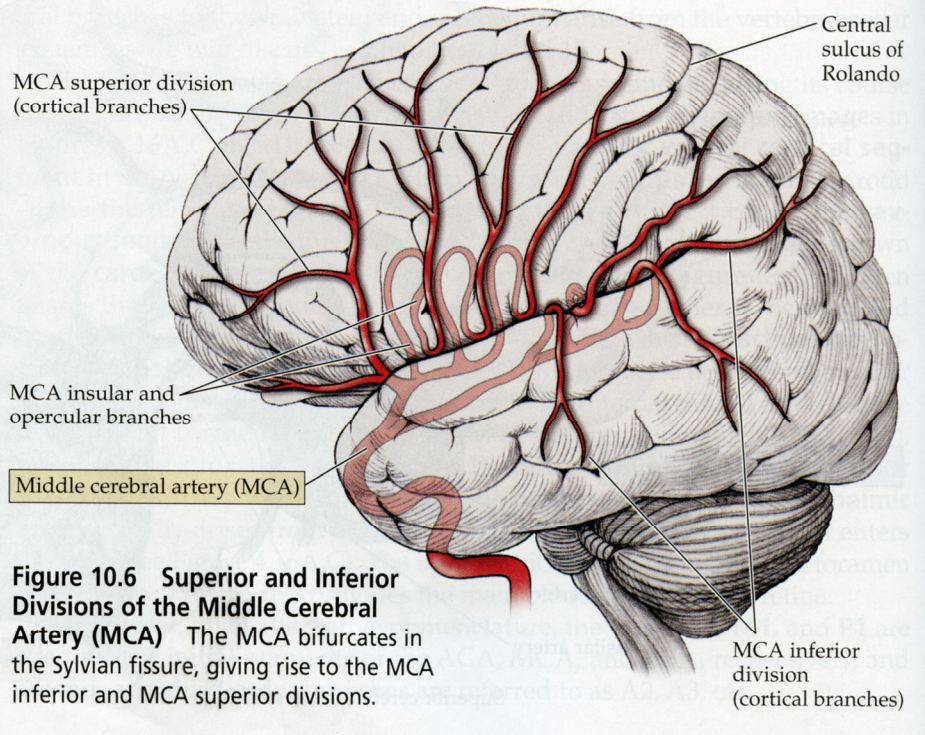

Figure 1.4 External Middle Cerebral Artery Territory. The external territory of the MCA supplies the lateral aspect of the cerebral hemisphere including areas responsible for speech. (from H. Blumenfeld. In *Neuroanatomy Through Clinical Cases*, Copoyright 2002 by Sinauer Associates, Inc. Used by permission of Sinauer Associates, Inc.).

divisions, or the MCA "stem" will present with a combination of the aforementioned symptoms, contralateral hemiplegia, contralateral sensory loss, global aphasia (left-sided occlusion), and left hemineglect (right-sided occlusion) (Blumenfeld, 2002).

1.2.4.3 Posterior Cerebral Artery. The PCA courses posteriorly over the basilar artery and supplies the inferior and medial temporal lobes, and the medial occipital cortex. Occlusion of the PCA results in contralateral visual field deficits (Blumenfeld, 2002).

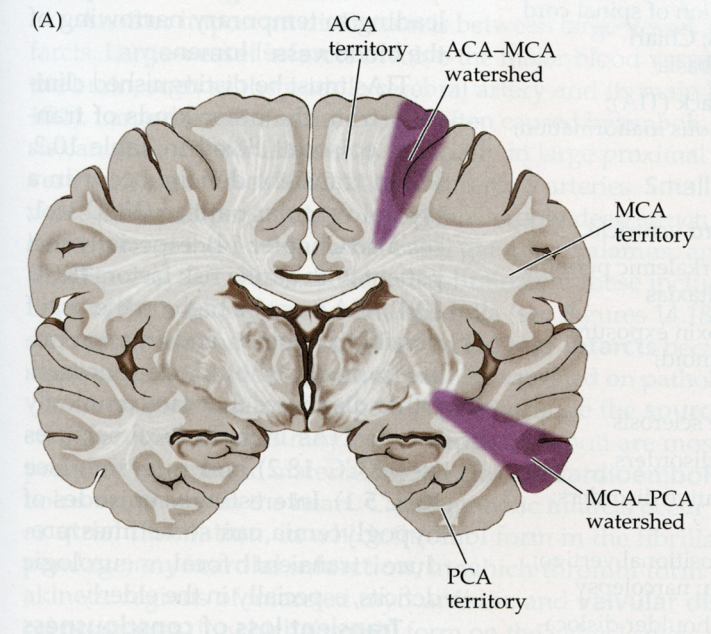

Figure 1.5 Watershed Zones. These areas of the brain generally receive sufficient collateral blood flow to suffer minimal damage from ischemia of any one cerebral artery. However, occlusions that occur in the watershed zones cause infarcts of the entire watershed area. (from H. Blumenfeld. In *Neuroanatomy Through Clinical Cases*, Copoyright 2002 by Sinauer Associates, Inc. Used by permission of Sinauer Associates, Inc.).

1.2.4.4 Watershed Zones. The regions between cerebral arteries are called watershed zones as they receive collateral blood from two arteries. Under conditions where one artery is occluded, watershed areas are protected or have reduced damage due to collateral flow. In contrast, when the occlusion occurs near the junction of the two vessels, the watershed zone is the most susceptible to ischemia. Other causes of watershed infarction are sudden drop in systemic blood pressure and sudden carotid artery occlusion. The latter infarct occurs in the ACA-MCA watershed zone because both the ACA and MCA are supplied by the internal carotid artery (**Figure 1.5**). Infarcts in the ACA-MCA watershed zone can result in proximal arm and leg weakness and possibly aphasia if the infarct occurs in the dominant hemisphere. The MCA-PCA watershed zone infarcts cause disturbances in visual processing (Blumenfeld, 2002).

1.2.5 Current Treatment Options

Currently, there are three categories of stroke therapy: antiplatelet and antithrombotic therapy, thrombolytic agents, and neuroprotective agents. The vast majority of the current treatment options for stroke revolve around restoration of blood flow. This follows logical reasoning as the etiology of a majority of strokes involve either a local thrombotic occlusion or a thrombus formed distally that becomes dislodged and occludes a cerebral vessel (embolic stroke). The former two categories will be discussed here. Neuroprotective agents are discussed in greater detail later in this introduction.

1.2.5.1 Antiplatelet and Antithrombotic Therapy. The rationale underlying antiplatelet and antithrombotic therapy is that platelets become activated following stroke (Sandercock et al., 2008); therefore, administration of these agents would theoretically reduce the chance of thrombus formation and improve overall blood flow. Aspirin is the prototypical antiplatelet drug, and is currently the only recommended antiplatelet or antithrombotic therapy approved for use for acute stroke; however, aspirin should only be used if there is no known contraindication for patient use of aspirin (i.e. allergic reaction to salicylates) or administration of the antithrombotic heparin or alteplase (discussed further in the following section).

Patients who received 300mg of aspirin within 48h of stroke onset had a reduced risk of recurrent stroke and a slightly improved neurological outcome at 6 month in the International Stroke Trial (IST) (1997). Similar results were found when patients receive the smaller dose of 160 mg of aspirin again within 48h of stroke onset in the Chinese Acute Stroke Trial (CAST). The administration of aspirin reduced mortality 14% at one month following stroke (1997).

Taken together, aspirin administration resulted in the modest reduction of 9-13 nonfatal strokes per 1000 patients (Chen et al., 2000; Sandercock et al., 2008).

Other, more potent antiplatelet therapies and antithrombotic therapies have also been studied for treatment of stroke. Neither heparin nor low molecular weight heparin administration have shown significant benefit (Gubitz et al., 2004). Caution is also urged when using antithrombotics as heparin therapy also significantly increases the incidence of symptomatic intracranial hemorrhage (Gubitz et al., 2004). Another antiplatelet agent used for potential therapy against stroke is the platelet glycoprotein IIb/IIIa receptor inhibitor abciximab. The data yielded from studies using this agent were again disappointing as the AbESST trial demonstrated that abciximab caused a nonsignificant increase in symptomatic intracranial hemorrhage (2005), and the AbESTT-II trial was discontinued because of lack of benefit and significant symptomatic intracranial hemorrhage (Adams et al., 2008).

Collectively, based on the outcomes of the trials using antiplatelet or antithrombotic agents, it is currently recommended by the American Heart Association/American Stroke Association that anticoagulation agents not be used for treatment of acute stroke (Adams et al., 2008). The only caveat to this recommendation is the use of early aspirin therapy when alteplase cannot be administered.

1.2.5.2 Thrombolytic Agents. A breakthrough in stroke research was realized in 1995 when the National Institute of Neurological Diseases and Stroke (NINDS) study of 624 patients suffering stroke benefited from treatment of recombinant tissue plasminogen activator (tPA), or alteplase (1995). Tissue plasminogen activator is a serine protease that is present on the extracellular membrane of vascular endothelial cells. It functions endogenously as a catalyst to convert

plasminogen to plasmin, the predominant enzyme for thrombolysis. The mechanism of action of alteplase in stroke therapy is to break down the clot occluding the cerebral vessel to restore blood flow.

The NINDS trial was the first study to realized clinically significant benefit as patients treated with alteplase within three hours of stroke onset were approximately 30% more likely to have improved clinical outcome (limited or no disability) at three months following stroke (1995). There was, however, no difference in mortality rates at the three month follow up. Another trial published the same year, the European Cooperative Acute Stroke Study (ECASS), examined the benefit of alteplase for stroke treatment with a treatment window of up to six hours (Hacke et al., 1995). Their results were similar to the NINDS study as patients that received alteplase had better neurological outcome three months after stroke. However, the subsequent study by the same group, the ECASS-II study, did not show a statistical significant improvement in neurological outcome with a six hour treatment window (Hacke et al., 1998).

Further clinical trials attempted to examine the effect of alteplase at greater intervals after stroke in order to increase the cohort of patients who would benefit from thrombolytic therapy. The Alteplase ThromboLysis for Acute Nonintervential Therapy in Ischemic Stroke (ATLANTIS) conducted a randomized, double-blind study examining 613 patients that received either placebo or alteplase 3-5 hours after stroke onset (Clark et al., 1999). Patients who received alteplase during the 3-5 hour window, however, did not show any therapeutic benefit over placebo control. Similarly, another study conducted by the same group of investigators examining the effects of alteplase on neurological improvement when it was administered between 0-6 hours after stroke onset found no difference between alteplase-treatment and placebo control (Clark et al., 2000).

A meta-analysis examining the individual patients from the aforementioned trials revealed that alteplase treatment showed decreasing efficacy to improve neurological outcome when administered at greater intervals after stroke onset. They found that the odds ratio (probability that patients who received alteplase would show neurological improvement at a three month follow-up) at the 0-90 minute interval was 2.8. Subsequent intervals examined showed decreased efficacy of alteplase with the odds ratio decreasing to 1.6, 1.4 and 1.2 for 91-180 minutes, 181-270 minutes and 271-360 minutes, respectively (Hacke et al., 2004). This study confirmed the findings of the NINDS trials showing a benefit for alteplase treatment when administered within three hours of stroke onset. It also revealed that the therapeutic window may extend to 4.5 hours (odds ratio of 1.4).

This therapeutic window was recently examined in the ECASS-III trial. The researchers found that alteplase treatment when administered between 3-4.5 hours after stroke onset maintained a modest, but significant, beneficial effect on clinical outcome (52.4% alteplase-treated vs. 45.2% placebo) (Hacke et al., 2008). This trial confirmed the previous meta-analysis that suggested a therapeutic benefit to extending the therapeutic window of alteplase to 3-4.5 hours.

Unfortunately, even with this extension, alteplase is only given to 3-8.5% of patients (Reeves et al., 2005). This is likely due to the fact that the median arrival time to the hospital for treatment of acute stroke is within 3-6 hours after stroke onset (Evenson et al., 2001). Another reason for the lack of treatment with alteplase is that its major side effect is intracerebral hemorrhage (ICH). Within the three hour therapeutic window there was a 6.5% chance of ICH in patients receiving alteplase versus a 0.6% chance in the placebo group in the NINDS trial

(1995). The increased risk of ICH was also found in the ATLANTIS trials and the ECASS I, II and III trials.

Other thrombolytic agents and methods of recanalization have been attempted given the limited patient population that benefits from alteplase treatment. Intra-arterial administration of the thrombolytic prourokinase (Prolyse) in the Prolyse in Acute Thromboembolism (PROACT-II) trial demonstrated a 15% increase in clinical improvement in patients receiving intra-arterial thrombolysis up to 6 hours after stroke onset (Furlan et al., 1999). As with the alteplase trials, this benefit also came at the risk of symptomatic ICH (10% prourokinase versus 2% placebo) (Furlan et al., 1999).

An even greater therapeutic window for recanalization therapy was demonstrated with mechanical embolectomy in the MERCI trials. Mechanical embolectomy in the first MERCI trial resulted in recanalization in 46% of patients when attempted up to 8 hours after stroke onset. Improved neurological outcome was realized in patients where recanalization was attained compared to patients whose recanalization was not successful (46% versus 10%). Unlike the alteplase trials, there was also a decrease in mortality in the patients whose recanalization was successful (32% versus 54%; successful recanalization versus unsuccessful recanalization, respectively) (Smith et al., 2005). Newer mechanical embolectomy devices implemented since the first MERCI trial have improved the success rate of recanalization; however, improvement in neurological outcome and mortality is not significantly different from older generation techniques (Smith et al., 2008). Regardless, these trials demonstrate a more practical therapeutic window for recanalization and therapy for acute stroke.

Evidence is mounting from the trials outlined here and others that clinically effective neuroprotection is only going to be attained with successful recanalization. This is because the

brain needs an adequate energy supply to repair and maintain neurons and other brain cells. Sole use of recanalization therapy, however, is unlikely to completely prevent brain damage and subsequent neurological impairment. This is due to the pathophysiological nature of the insult. In order to minimize the damage caused by stroke, adjunct therapy must be implemented to repair and salvage neurons that are programmed to die. The development of these adjuvant therapies can only be attained by having a comprehensive understanding of the mechanisms underlying delayed neuronal death. The following section outlines the pathophysiological mechanisms fundamental to programmed neuronal death and discusses the concept of the ischemic penumbra in detail.

1.3 PATHOPHYSIOLOGY OF STROKE

1.3.1 Origins of the Penumbra Concept

Dysfunction caused by cerebral ischemia is intimately related to cerebral blood flow. It was originally established in both experimental and clinical studies that a threshold exists between cerebral blood flow and electrical activity of the brain. In the clinical setting, patients undergoing carotid endarterectomy were shown to have inhibition of electrical activity measured by electroencephalograph (EEG) when CBF was reduced below 16-17ml/100g/min (Sharbrough et al., 1973; Trojaborg and Boysen, 1973). Measurement of evoked potential (EP), an analogous measure of brain electrical function, in baboon cortex was also shown to be inhibited at a similar

threshold of CBF—15ml/100g/min (Branston et al., 1974). It is interesting that the threshold for other species such as cats and rodents is similar to the primate threshold (Heiss, 1992).

The mechanism underlying inhibition of electrical activity due to surpassing the CBF threshold was initially thought to be caused by ion pump failure and massive release of intracellular K^+ or due to extracellular acidosis. In a seminal paper by Astrup and colleagues (1977), it was determined that brain electrical failure was not due to intracellular K^+ release as the threshold for K^+ release was 10ml/100g/min—noticeably lower than the threshold for electrical inactivity. Additionally, there was no direct relation between tissue acidosis and electrical inactivity as no critical level of H^+ concentration and electrical inactivity or recovery was established (Astrup et al., 1977). The concept of two ischemic thresholds was thus established. The upper threshold being electrical inactivity and the lower being K^+ release.

The relationship between electrical failure, energy state, K^+ release and ion pump failure was never directly studied in ischemia models before the concept of penumbra was introduced. Using controlled hypotension and bicuculline-induced seizures in rats, it was determined that reductions in blood flow that abolished seizures (and thus electrical activity) did not result in K^+ release. In fact, at the point of electrical failure, extracellular K^+ was reduced, suggesting there was sufficient ATP levels for pump function (Astrup et al., 1979). Thus, electrical inactivity was not due to energy failure. However, further reductions in CBF did reduce ATP levels and were related to ion pump failure and massive K^+ release.

On the basis of the above rationale the lower ischemic threshold was refined to become energy failure and ion pump failure (Astrup et al., 1981). Thus, the brain region immediately supplied by the occluded vessel where the blood flow drops below 10ml/100g/min suffers from energy failure, ion pump failure and ultimately membrane failure. This ischemic center is what

is now known as the core of the infarct. Surrounding the ischemic center residual blood flow from collateral circulation is sufficient to maintain cellular structural integrity, but not electrical activity. Since this level of CBF occurred in a ring around the ischemic center, much like light radiating around the moon in a solar eclipse, this region was named the penumbra (Astrup et al., 1981).

This is an extremely important concept in stroke research as it posits that there are damaged neurons that do not die immediately due to ischemia, and are potentially salvageable. Astrup and colleagues (1981) argued that the abolition of electrical activity served as a potential protective mechanism and that the CBF threshold that resulted in energy and pump failure was a lethal threshold. Indeed, recovery of electrical activity was possible following 2-3 hours of focal ischemia only in brain regions that maintained CBF above 10-12ml/100g/min (Jones et al., 1981). The reality that neurons in the penumbra regain electrical function has been lost in the stroke field over the past three decades. It is true that electrical activity and energy state respond nearly immediately to lowering of CBF below their respective thresholds. However, it has been repeatedly reported that restoration of blood flow allows for nearly complete recovery of electrical activity even after 1 hour of ischemia (Hossmann, 1971; Hossmann and Zimmermann, 1974; Hossmann et al., 1987; Kataoka et al., 1987). Therefore the original penumbra definition of electrically silent but structurally intact neurons only pertains to the ischemic period. During reperfusion, EPs return and then gradually disappear as delayed neuronal death occurs (Heiss, 1992).

The concept of the penumbra has been refined over the past three decades. The initial definition of electrically silent but structurally intact only represented a small amount of brain tissue. The narrow threshold difference between CBF of 16-17ml/100g/min for electrical silence

and the CBF of 10ml/100g/min for loss of membrane integrity, however, does not account for the total infarct observed 24h after ischemia. Penumbra was thus defined as the difference between the infarct area that had developed at 1h after ischemia and the final infarct volume at 24h after ischemia (Memezawa et al., 1992). This definition is conceptually correct, but it does not include an understanding of the underlying mechanisms resulting in the delayed infarct. Later, Hossmann (1994) posited two commonalities to all penumbra definitions: 1) area of the brain where blood flow is reduced but 2) where the brain tissue remains viable (Hossmann, 1994). He thus defined the penumbra as brain regions with decreased blood flow that maintain energy metabolism.

1.3.2 Functional Thresholds of Ischemia

A more comprehensive understanding of the penumbra is gained by examining the various physiological, biochemical and functional thresholds induced by reductions in CBF (**Figure 1.6)**. As discussed above, the thresholds for energy and ion pump failure were approximately 10-12ml/100g/min, and the threshold for electrical failure was 16-17ml/100g/min. Measurement of ATP levels indicates a sharp decline at CBF below 26ml/100g/min with complete loss of ATP between 10-18ml/100g/min (Heiss, 1992). Glucose utilization exhibits a biphasic curve. When CBF falls below 35ml/100g/min, glucose utilization increases to compensate for decreases in ATP. Due to the increasingly hypoxic state of the brain tissue, glucose is metabolized by anaerobic glycolysis and results in increased lactate production. Glucose extraction is increased until approximately 25ml/100g/min, where it sharply declines. The CBF range of 35-

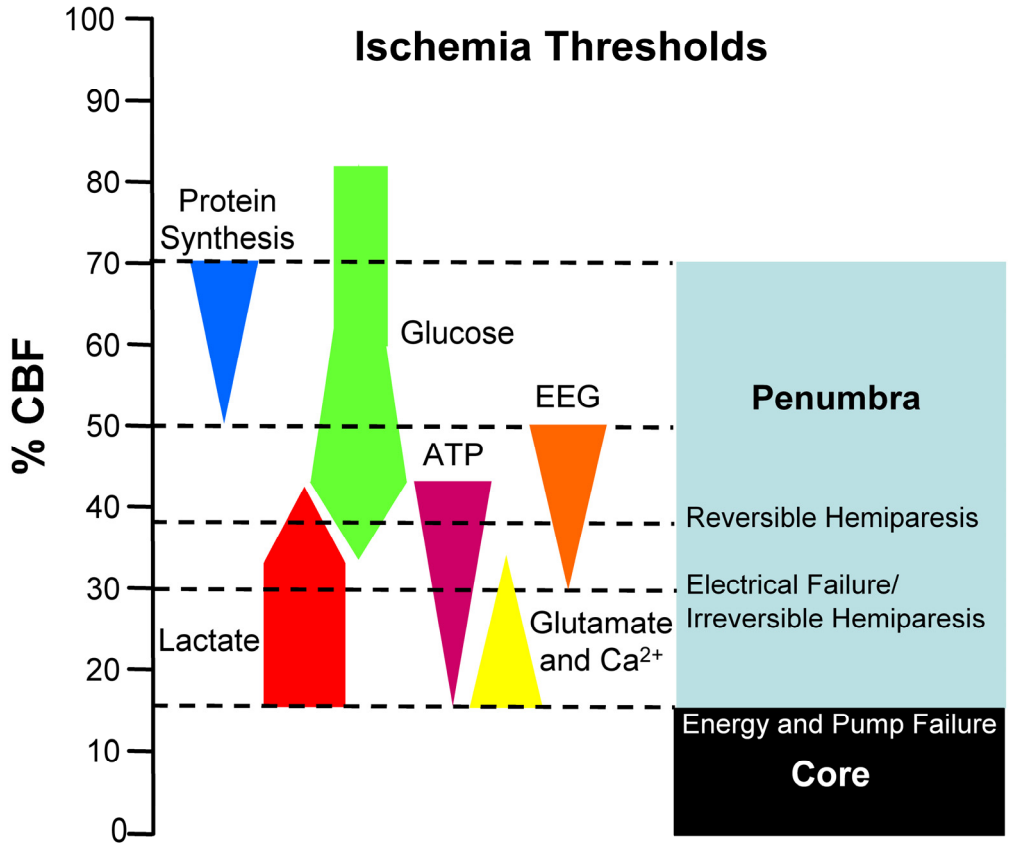

Figure 1.6 Ischemic Thresholds of Stroke. The percentage of cerebral blood flow was calculated based on individual species' baseline CBF (see references provided in text). The ranges of disturbance are depicted in this figure. Definitions of the penumbra and core are based on the metabolic disturbances studied. Note that the inhibition of protein synthesis has the highest threshold at approximately 70% CBF. This sensitive metabolic function is a robust predictor of eventual infarction, and is therefore a good definition of penumbra. [Figure was adapted from (Astrup et al., 1977; Hossmann, 2006)].

25ml/100g/min corresponds to the beginning of tissue acidosis (Paschen et al., 1992). Of note, the decline in glucose utilization is at the same point that ATP levels diminish and where tissue acidosis is prominent. The threshold for protein synthesis is much higher than the thresholds for alterations in energy metabolism and glucose utilization. Protein synthesis is inhibited by 50% at flow rates of 55ml/100g/min (approximately 50% of control CBF in rat) and is completely inhibited below 35-40ml/100g/min (Xie et al., 1989; Mies et al., 1991).

Release of neurotransmitters also follows the threshold for electrical and energy failure. Increases in extracellular concentrations of the excitatory amino acids glutamate and glycine are observed at CBF rates below 20ml/100g/min (Shimada et al., 1990). This corresponds to an increase in intracellular calcium levels, which also have a threshold of approximately 20ml/100g/min (Greenberg et al., 1990). Interestingly, there are also increases in the inhibitory neurotransmitters GABA and adenosine at a similar threshold (Shimada et al., 1990; Matsumoto et al., 1992). It therefore seems that neurotransmitter release is nonspecific and is probably a function of impaired energy metabolism.

Examination of the functional disturbances caused by reductions in CBF show a threshold similar to the threshold of electrical inactivity and loss of energy metabolism. Mild paralysis in monkeys was established below CBF of 22ml/100g/min with complete and irreversible paralysis occurring below 12ml/100g/min (Jones et al., 1981). In humans, decreases in EEG signal begin at CBF of 23ml/100g/min and are completely suppressed below 16-17ml/100g/min (Sharbrough et al., 1973; Trojaborg and Boysen, 1973). This demonstrates remarkable consistency between electrical activity and functional outcome.

A synopsis of the CBF thresholds is as follows: protein synthesis is inhibited at flow rates below 55ml/100g/min. This is followed by a transient increase then sharp decrease of glucose utilization between 35-26ml/100g/min. At the point where CBF reaches 26ml/100g/min, acidosis becomes prominent. When CBF falls below 22ml/100g/min, mild hemiparesis sets in. At approximately 20ml/100g/min, neurotransmitter release ensues and intracellular calcium increases. Electrical activity is abolished at flow rates below 16-17ml/100g/min as measured by EP or EEG. Finally, ion pump failure and complete energy failure, otherwise known as anoxic depolarization, take place below 12ml/100g/min.

It is well established that final infarct volume is directly related to the period of ischemia. Accordingly, the thresholds for the respective metabolic disturbances previously discussed nearly uniformly increase with increasing periods of ischemia. An ischemic period of 30 minutes has a threshold for ATP depletion of 12ml/100g/min. This threshold rises to 19ml/100g/min at 2 hours of ischemia and is further increased to 23 and 32ml/100g/min at 6 and 12 hours of ischemia, respectively (Mies et al., 1991). Glutamate release thresholds also increase with ischemic period. The threshold at 1 hour of ischemia for glutamate release is 20ml/100g/min, and this rises to 30ml/100g/min between 6-15 hours of ischemia (Hossmann, 1994). The neuronal electrical activity CBF threshold is similarly increased from 16-17ml/100g/min at 30 minutes ischemia to 20ml/100g.min at 2 hours ischemia (Heiss, 1992). The only caveat to the phenomenon of increasing thresholds with increasing ischemia periods is regarding protein synthesis. The threshold for protein synthesis stays remarkably consistent (55ml/100g/min) up to 12 hours of ischemia (Mies et al., 1991). This is an important discovery that is implicated with the development of neuronal injury and prediction and definition of the penumbra following focal ischemia.

1.3.3 Protein Synthesis Inhibition and Penumbra

Further examination of energy state, tissue acidosis and cerebral protein synthesis when establishing a mouse model of focal ischemia promoted the notion that areas protein synthesis inhibition delineated the infarct area (Hata et al., 1998). Indeed, the regions of protein synthesis inhibition were larger than that of tissue acidosis and ATP depletion and indicated the penumbral area of eventual infarct. Use of the permanent MCA occlusion model of focal ischemia

demonstrated that the region of ATP depletion gradually increased in the ischemic hemisphere from 40.1% to 58.9% of the contralateral hemisphere when examined at 1 hour to 3 days of ischemia, respectively (Hata et al., 2000b). In contrast, the region of protein synthesis inhibition remained consistent ranging from 58.9% of the contralateral hemisphere at 1h to 60.2% at 3 days. The penumbra in this study was thus defined as the difference in the regions of protein synthesis inhibition and preserved ATP, and the penumbral area was calculated to decrease from 20% of the contralateral hemisphere at 1 hour of ischemia to 3% after 3 days. It was therefore concluded that the area of eventual infarct size was robustly predicted by the region of protein synthesis inhibition (Hata et al., 2000b).

The transient MCA occlusion model of focal ischemia was studied next to compare the role of metabolic disturbances observed in this model with the disturbances in the permanent MCA occlusion model. Levels of ATP and protein synthesis were measured following 1 hour of transient ischemia with subsequent reperfusion at 1, 3 and 6 hours and 1 and 3 days. As in the permanent ischemia model, protein synthesis inhibition was consistently inhibited in the ischemic hemisphere (54-57% of the non-ischemic contralateral hemisphere) for 6 hours of reperfusion. Unlike in permanent MCA occlusion, protein synthesis improved to 49% and 37% at 1 and 3 days of reperfusion, respectively (Hata et al., 2000a).

Again, similar to permanent MCA occlusion, ATP was depleted in 40% of the ischemic hemisphere compared to the contralateral control hemisphere. In contrast to permanent MCA occlusion and protein synthesis after transient ischemia, ATP levels returned to control levels after 1 hour reperfusion. However, longer periods of reperfusion resulted in secondary ATP depletion resulting in 35% of the ischemic hemisphere depleted of ATP at 3 days of reperfusion. Remarkably, the region of final ATP depletion completely corresponded with the region where

protein synthesis inhibition persisted. This area of persistent protein synthesis inhibition and eventual ATP depletion also coincided with the eventual infarct area (Hata et al., 2000a).

It can therefore be concluded that failure to recover translation or persistent protein synthesis inhibition is a robust predictor of eventual neuronal death following ischemia. Importantly, this phenomenon is consistent regardless of the focal ischemia model employed. The phenomenon that recovery of protein synthesis is vital to the recovery of neurons following ischemia is reinforced in the next section outlining the effect of protein synthesis following global ischemia.

1.3.4 Protein Synthesis Inhibition and Global Ischemia

The link between persistent protein synthesis inhibition and eventual neuronal death was originally discovered using the global ischemia model. Briefly, this model reproduces the effect of cardiac arrest on the brain by either transiently occluding the common carotid combined with coagulation of the vertebral arteries (4-vessel occlusion) (Pulsinelli and Buchan, 1988) or combining transient carotid artery occlusion with hypotension (2-vessel occlusion) (Smith et al., 1984). Both methods severely restrict blood flow to the entire brain. Accordingly, durations of global ischemia are usually between 5-30 minutes as longer periods of global ischemia are lethal.

The pathological hallmark of global ischemia is the delayed neuronal death of a select group of neurons. Neuronal death is initially seen within 12 hours and progresses dramatically between 1 and 3 days specifically in the rat CA1 field of the hippocampus and layers 2 and 5 and 6 of the cortex, and hilar neurons (Pulsinelli and Brierley, 1979; Pulsinelli et al., 1982). The phenomenon of delayed neuronal death in the hippocampal CA1 field is also seen in gerbils

using a two vessel occlusion model (Kirino, 1982). (Occlusion of only two vessels are required in gerbils to obtain global ischemia because a posterior communicating artery is absent from their cerebral vasculature and therefore their forebrain receives little collateral circulation from the vertebral arteries.)

Global ischemia reduces the CBF to less than 10% of normal values. However, the duration of ischemia is brief enough so there is no necrotic damage as seen in the core of focal ischemia. The residual flow is therefore above the time threshold of anoxic depolarization and below the threshold for electrical activity. Glucose utilization is decreased and energy levels measured by ATP decrease to between 10-15% of control. However, energy levels, glucose utilization (Suzuki et al., 1983b) and neuronal activity (Suzuki et al., 1983a) are restored within 10-15 minutes in all brain regions. Importantly, the energy levels are sustained at control values in the CA1 field until the time that neuronal death is observed (Arai et al., 1986).

It has been repeatedly shown that protein synthesis is inhibited in all ischemia affected areas of the brain during global ischemia (Kleihues and Hossmann, 1971, 1973; Cooper et al., 1977; Morimoto et al., 1978; Dienel et al., 1980; Morimoto and Yanagihara, 1981; Nowak et al., 1985; Bodsch et al., 1986; Thilmann et al., 1986; Xie et al., 1988; Araki et al., 1990). In contrast to the rapid restoration of energy metabolism, protein synthesis is slower to recover and even fails to recover in the ischemia-susceptible brain regions (Dienel et al., 1980; Bodsch et al., 1986; Thilmann et al., 1986; Araki et al., 1990). It has thus been concluded that it is not the inhibition of protein synthesis that is detrimental to post-ischemic neurons. Rather, it is the persistence of protein synthesis inhibition that results in delayed neuronal death.

This phenomenon is exemplified by examining other insults that result in protein synthesis inhibition. Application of chemical protein synthesis inhibitors such as cycloheximide

(Kesner et al., 1981), cortical spreading depression (Avaria and Krivanek, 1973; Krivanek, 1978), pharmacologically or electrically-induced seizures (MacInnes and Luttges, 1973; Wasterlain, 1974; Collins et al., 1980; Kiessling and Kleihues, 1981; Dwyer and Wasterlain, 1984), hyperthermia (Heikkila and Brown, 1979b, a) and hypoglycemia (Metter and Yanagihara, 1979; Kiessling et al., 1984; Kiessling et al., 1986) all inhibit protein synthesis. In contrast to the pathological insults of global or focal ischemia, the suppression of protein synthesis is transient (Avaria and Krivanek, 1973; MacInnes and Luttges, 1973; Krivanek, 1978; Kesner et al., 1981). It can be argued that protein synthesis inhibition is a general metabolic response to perturbations of brain tissue. The duration of protein synthesis inhibition seems to be a major predictor of whether neurons live or die.

The turnover of proteins as measured by protein half-life in brain ranges from 3 to 9 days (Chee and Dahl, 1978). The onset of delayed neuronal death following global ischemia encroaches upon the lower limit of brain protein half-life, and neuronal death in this model is plausibly due to the failure of susceptible neurons to regenerate old proteins. The onset of neuronal death is much more rapid following focal ischemia as infarct area is established within 24 hours of ischemia. An alternate hypothesis as to the importance of protein synthesis is not to solely replace proteins that have reached their shelf-life, but to replace proteins that have been degraded by resident proteases activated by the pathological insult. Finally, protein synthesis inhibition could impair the ability of ischemia-affected neurons to produce stress-induced proteins that will protect neurons from the damaged caused by ischemia.

1.3.5 Excitotoxicity

The previous sections describe the physiological and metabolic disturbances caused by cerebral ischemia. However, there is controversy as to whether it is protein synthesis inhibition or the eventual failure of energy metabolism that directly contributes to neuronal death. In order to address the involvement of these two ischemia-induced phenomena one should understand the mechanistic underpinnings of delayed neuronal death. The following sections outline the currently known cellular and molecular mechanisms of delayed neuronal death. In particular, the mechanisms potentially contributing to secondary energy failure and alterations to mechanisms governing protein synthesis are emphasized.

One of the major hypotheses instigating progressive neuronal death in the penumbra is the phenomenon of excitotoxicity. The inception of excitotoxicity as a mediator of neuronal death occurred in 1957 when administration of the excitatory amino acid glutamate to mice resulted in retinal degeneration (Lucas and Newhouse, 1957). In the ensuing decade, neurotoxicity due to exogenous glutamate exposure was linked to activation of excitatory amino acid receptors (Olney, 1969). Excitotoxicity was eventually connected with ischemia in 1984 when it was discovered that addition of the excitatory amino acid antagonist γ-D-glutamylglycine abrogated neuronal death induced by anoxia and glutamate in primary rat hippocampal neuronal cultures (Rothman, 1984).

The origin of excitotoxicity in ischemia is the depolarization of neurons in the core and the surrounding tissue of the infarct with CBF less than 20ml/100g/min that results in massive release of glutamate. The uncontrolled release of glutamate in the infarct core initiates depolarizations that spread into the penumbra (Nedergaard and Astrup, 1986). This phenomenon

is aptly named per-infarct spreading depression or per-infarct depolarizations. In normal brain, this phenomenon is referred to cortical spreading depression and is found in epilepsy and migraine headaches in addition to cerebral ischemia (Rogawski, 2008). Metabolic studies show that in normal brain cortical spreading depression results in increased energy demand due to activation of ion pumps, which is facilitated by an increase in blood flow. In the ischemic brain, however, blood flow to the depolarized tissue is severely reduced and cannot accommodate the increased energy demand (Back et al., 1994). The importance of this phenomenon is shown by the direct relationship between the number of peri-infarct depolarizations and infarct volume (Mies et al., 1993a). This phenomenon could cause the secondary energy failure seen following focal ischemia.

The mechanism underlying peri-infarct depolarizations are the continued release of glutamate from presynaptic terminals to activate glutamate receptors post-synaptically to induce depolarizations. This produces a domino-effect that radiates depolarizations from the core to the peripheral brain tissue. The exposure to supranormal glutamate causes excitotoxic neuronal death via activation of *N*-methyl-D-aspartate (NMDA) and α-amino-3-hydroxy-5-methyl-4-isoxazoleproprionic acid (AMPA) receptors. The role of glutamate-induced excitotoxicity in ischemic injury is evident via the robust neuroprotection provided by NMDA and AMPA receptor antagonists in animal models (Simon et al., 1984; Gill et al., 1987; Mies et al., 1994; Dirnagl et al., 1999).

An interesting, yet unheralded study, examined the effect of the neuroprotective NMDA antagonist MK-801 treatment on ischemia thresholds. Antagonism of NMDA receptors with MK-801 was shown to significantly decrease the threshold for protein synthesis from 51ml/100g/min to 19ml/100g/min following MCA occlusion in rats. In stark contrast, NMDA

antagonism did not change the threshold for energy failure, which remained constant around 15ml/100g/min (Mies et al., 1993b). This important study provides three major findings: 1) there is a direct link between neuroprotection and blocking protein synthesis inhibition in the ischemic brain, potentially via inhibiting Ca^{2+} influx, 2) the mechanism underlying protein synthesis inhibition may be dependent on the NMDA receptor, and 3) the unaffected threshold of energy metabolism suggests this is the lower limit of CBF wherein neurons are irreversibly damaged.

Greater understanding of the intracellular mechanisms of excitotoxicity introduces potential mechanisms underlying both protein synthesis inhibition and secondary energy failure caused by cerebral ischemia. Glutamate receptor activation results in increased influx of calcium--the degree of which is positively linked to infarct development (Uematsu et al., 1988). Moreover, it is established that delayed neuronal death due to glutamate exposure is calcium dependent (Choi, 1987). Both NMDA and AMPA receptors regulate calcium entry into neurons—NMDA activation results in immediate calcium influx wherein AMPA receptors contribute to delayed calcium-influx (Liu et al., 2006; Peng et al., 2006). The importance of calcium influx in neuronal death is underscored by the fact that calcium channel inhibitors also provide neuroprotection (Uematsu et al., 1991b; Uematsu et al., 1991a); however, calcium channel inhibition is a less potent neuroprotective mechanism (Uematsu et al., 1991a).

Calcium ion, the universal second messenger, is tightly regulated under physiological conditions. The extracellular calcium concentration is approximately 1.2mM, while the physiological intracellular calcium concentration ranges between 0.1 to 1μM. Cerebral ischemia, via activation of glutamate receptors and calcium channels, increases the calcium concentration to 50-100μM (Edvinsson, 2002). This exceeds the endogenous buffering capacity

of the cell and has myriad consequences. A consequence of increased calcium that has been studied extensively is activation of the protease calpain. Additionally, increased calcium concentrations increase the production of free oxygen radicals and nitric oxide (NO) formation.

1.4 CALPAIN [1]

Calcium-dependent protease with papain-like activity, or calpain, is a cytoplasmic cysteine protease that is activated by calcium. It is a highly evolutionarily conserved protease with homologues present in invertebrates, plants, fungi and mammals, and it consists of 15 ubiquitous and tissue-specific isoforms in humans (Goll et al., 2003). The catalytic subunits found in the CNS include isoforms 1, 2, 3, 5, and 10 (Wu et al., 2007). The typical calpain isoform consists of an 80kDa catalytic subunit and a 30kDa regulatory subunit. The regulatory subunit possesses a hydrophobic, glycine-rich domain for membrane association. Each subunit contains an EF hand domain, characteristic of most calcium binding proteins (Blanchard et al., 1997). For extensive reviews on the structure, tissue and subcellular localization of calpain see references (Goll et al., 2003; Wu et al., 2007; Bevers and Neumar, 2008).

There are two prototypical calpains, μ-calpain and m-calpain. Mu-calpain, or calpain I, is located in the cytosol or near the membrane and is activated by μM concentrations of calcium *in vitro*. In contrast, m-calpain, or calpain II, is located at the membrane and requires mM concentrations of calcium for activation. Calcium sensitivity is functionally important as

[1] This section (subsections 1.4.1 through 1.4.4) was adapted from Vosler PS, Brennan CS, Chen J (2008) Calpain-Mediated Signaling Mechanisms in Neuronal Injury and Neurodegeneration. Mol Neurobiol..

physiologic concentrations of calcium range from 100-1000nM (Chan and Mattson, 1999) and rise to 5-10μM during excitotoxic conditions (Hyrc et al., 1997). Therefore, it is expected that μ-calpain would be affected by small changes in calcium concentrations, while m-calpain is likely activated by intracellular signaling via phosphorylation by protein kinase A (PKA) (Wu et al., 2007) and other yet undefined kinases. Following calcium stimulation, the 80kDa subunit is autocatalytically processed to a 76kDa fragment, and the 30kDa regulatory subunit is processed to 18kDa (Goll et al., 1992). The regulatory subunit is critical for calpain activity; for example, it is necessary for embryonic development as genetic deletion of the subunit is embryonic lethal at E11.5 (Arthur et al., 2000). The requirement of m-calpain for development has also been demonstrated as it is necessary for embryo implantation (Dutt et al., 2006).

Calpain activity is modulated *in vivo* by one known endogenous inhibitor, calpastatin. This cytosolic protein contains 4 calpain inhibitor domains and a consensus phosphorylation site for PKA, which increases calpastatin's specificity for m-calpain (Pontremoli et al., 1992). Both calpain and caspase-3 can cleave calpastatin. The calpain cleavage products retain their calpain-inhibitory activity (DeMartino et al., 1988), while caspase cleavage abrogates the calpain inhibition of calpastatin.

The prototypical calpain substrate is the cytoskeletal protein α-spectrin (for review see (Czogalla and Sikorski, 2005)). Calpain cleaves this protein into characteristic 150 and 145kDa fragments that are detectable by an antibody directed against α-spectrin for Western blot and immunohistochemistry (Siman et al., 1984; Nixon, 1986), and is stimulated by calmodulin binding of α-spectrin (Seubert et al., 1987). Thus, α-spectrin-cleavage is a straightforward surrogate to detect calpain cleavage *in vitro* and *in vivo*, and has been used extensively as a quantitative measure of calpain activity. Despite numerous attempts to predict a preferential

sequence of calpain cleavage (Tompa et al., 2004; Cuerrier et al., 2005), it has been determined that calpain likely cleaves via recognition of protein secondary or tertiary structure making substrate identification unpredictable.

1.4.1 Calpain Activation Following Ischemia

Calpain activation was initially thought to cause only necrotic cell death, while activation of caspases led to programmed cell death. However, calpain does play a role in apoptotic cell death in mixed glial and primary cortical neuronal cultures following oxygen-glucose deprivation (OGD) that is just as important as caspases (Newcomb-Fernandez et al., 2001). Moreover, calpain has been shown to cleave and activate caspase-3 following maitotoxin treatment (McGinnis et al., 1999) and OGD (Malagelada et al., 2005). The role of calpain in necrotic versus apoptotic cell death is still not without controversy. The calpain-cathepsin hypothesis posits calpain activation due to excitotoxic stimulus disrupts lysosomal membranes. This is ensued by the release of the lysosomal proteases, including cathepsins, the breakdown of cellular proteins and, ultimately,necrosis (Yamashima et al., 1998; Yamashima et al., 2003). In support of this model, the sequential activation of calpain, cathepsins and caspases occurs in a model of focal ischemia (Chaitanya and Babu, 2008), while the administration of E64d, a combined μ-calpain-cathepsin B inhibitor, decreases infarct volume, edema and neurologic deficit following focal ischemia in rats (Tsubokawa et al., 2006a; Tsubokawa et al., 2006b).

A large number of proteins are cleaved by calpain following an ischemic or excitotoxic insult [for reviews see (Chan and Mattson, 1999; Goll et al., 2003; Verkhratsky, 2007; Bevers

and Neumar, 2008)]. A comprehensive list of calpain substrates found in neurons thus far is available (for review see (Vosler et al., 2008)). Below are the recently identified, novel substrates and new signaling consequences of calpain stimulation.

1.4.2 Membrane and Receptor Targets

Briefly, calpain activation following excitotoxic insult positively regulates its own activity via cleavage of a number of proteins involved the homeostatic control of intracellular calcium. Calpain cleavage of the plasma membrane calcium ATPase (PMCA) (Pottorf et al., 2006), sodium-calcium exchanger (NCX) (Bano et al., 2005), L-type calcium channel (De Jongh et al., 1994; Hell et al., 1996), ryanodine receptor (RyR) (Rardon et al., 1990), sarcoplasmic/endoplasmic reticulum calcium ATPase (SERCA) (Parsons et al., 1999; French et al., 2006) and inositol (1, 4, 5) triphosphate receptor (Magnusson et al., 1993) and inositol triphosphate kinase B (Pattni et al., 2003) all result in the maintenance of elevated intracellular calcium levels. Cleavage of the C-termini of NMDA (Guttmann et al., 2001; Guttmann et al., 2002; Simpkins et al., 2003; Gascon et al., 2008) and AMPA (Bi et al., 1998a; Bi et al., 1998b; Bi et al., 2000) receptor subunits results in decreased glutamatergic transmission through these channels by disabling downstream signaling mechanisms (Wu et al., 2005). The effect of cleavage on calcium transmission, if any, remains unknown, as the proteins forming the calcium channel are not altered by calpain. Similar to calpain mediated C-terminal truncation of the metabotropic glutamate receptor mGluR1α disrupting coupling to the pro-survival PI3K-Akt

pathway (Xu et al., 2007), cleavage of the C-terminus of the NMDA NR2A subunit and post-synaptic density (PSD) 95 uncouples synaptic NMDA receptors from CREB-mediated prosurvival expression (Gascon et al., 2008).

1.4.3 Cytosolic Targets

Calpain also cleaves key cytosolic enzymes involved with calcium homeostasis such as Ca^{2+}/calmodulin-dependent protein kinase (CaMK) type IV (Tremper-Wells and Vallano, 2005) and the protein phosphatase calcineurin (CaN) A (Wu et al., 2007). Although the effect of CaMKIV cleavage on neuronal death has not been determined, regulation of CaN A has been examined in ischemia due to the neuroprotective effects of the CaN inhibitor FK506 (Sharkey and Butcher, 1994). This may be due to blocking the dephosphorylation and activation of the proapoptotic protein Bad by CaN A (Uchino et al., 2002). Calpain-cleavage of CaN A also results in increased phosphatase activity leading to the translocation of the transcription factors nuclear factor of activated T-cells (NFAT) and forkhead in rhabdomyosarcoma (FKHR), and increased expression of proapoptotic Bim and Fas-ligand (Shioda et al., 2006; Shioda et al., 2007). Further experiments are necessary to determine if inhibition of the downstream effectors of CaN A can provide neuroprotection.

Calpain may also cleave eukaryotic initiation factor 4G (eIF4G), a scaffolding protein critical for the delivery of mRNA cap-binding protein to the ribosome for translation. Decreases in eIF4G levels were demonstrated to be calpain-mediated following decapitation ischemia, as the pharmacological calpain inhibitor, MDL-28,170, abrogated diminished protein levels (Neumar et al., 1998). Calpain-mediated decreases in eIF4G were also shown following NMDA

toxicity in primary neuronal culture as the calpain inhibitor calpeptin also blocked reductions in eIF4G protein levels (Petegnief et al., 2008). Reduced eIF4G levels were correlated with inhibition of protein synthesis; however, in this model, although calpain inhibition was neuroprotective, it did not restore protein synthesis, leaving the significance of eIF4G reduction for neuronal survival in excitotoxicity unknown. Further studies are necessary to definitively show that eIF4G is a direct substrate of calpain as decreased protein levels could be indirectly linked to calpain via release of cathepsins or due to proteasomal degradation.

1.4.4 Nuclear Targets

Calpain can alter the availability of a number of transcription factors, including those of the Sp-family proteins. These transcription factors regulate the expression of "housekeeping genes" and are critical for development and survival (Suske, 1999). Following glutamate exposure, a decrease in Sp transcription occurs in cortical neurons (Mao et al., 2002) that is due to calpain cleavage of Sp3 and Sp4 (Mao et al., 2007). The direct effects of diminished Sp-mediated transcription are unknown, but it has been suggested that they may indirectly mediate decreased expression of the NR1 subunit following NMDA-mediated excitotoxicity (Gascon et al., 2005).

Pathologic proteolytic activation of calpain also occurs with the N-terminal cleavage of the collapsing response mediator proteins 1-5 (CRMP 1-5) (Hou et al., 2006; Jiang et al., 2007). Nuclear translocation of CRMP N-terminal cleavage products has been implicated in neuronal death (Hou et al., 2006), as well as with the alteration of NMDA NR2B subunit expression at the neuronal surface (Bretin et al., 2006). Cyclin-dependent kinase 5 (Cdk5) is physiologically

activated by p35 (Tsai et al., 1994); however, under conditions of calcium dysregulation and calpain activation, p35 is cleaved to form p25 (Patrick et al., 1999; Jamsa et al., 2006). This truncated form of p35 does not contain the membrane localization sequence of p35 and has a longer half-life, leading to increased activity often in abnormal subcellular locations, including the nucleus (Patrick et al., 1999). Calpain-mediated increased activity of Cdk5 following excitoxicity leads to phosphorylation of the NMDA NR2A subunit and increased neuronal death (Rashidian et al., 2005). Overactivation of Cdk5 has also been implicated with the accumulation of hyperphosphorylated tau in ischemic areas (Wen et al., 2007).

Thus, the acute insult of cerebral ischemia rapidly overactivates glutamate receptors, sharply increases intracellular calcium concentrations and results in pathological calpain activation. Calpain potentiates its own activation via cleavage of calcium regulatory proteins at the membrane (L-type calcium channels, PMCA and NCX) and ER (RyR, SERCA and IP3R) resulting in further increases in intracellular calcium. Calpain-mediated cleavage uncouples NMDAR from prosurvival cascades (PI3K/Akt and PKA) and propagates mitochondrial dysfunction. Another consequence of ischemia-induced calpain activation is alteration of transcription through direct cleavage of transcription factors (Sp3 and Sp4) or through modification of phosphatase (CaN A) and kinase (Cdk5) activity. Finally, calpain-mediated CRMP N-terminal cleavage product translocation to the nucleus results in neuronal death—a phenomenon shared by many of the neurodegenerative diseases.

1.4.5 Calpain and Apoptosis-Inducing Factor [2]

Apoptosis-inducing factor (AIF) is a flavoprotein that functions as an oxidoreductase within the mitochondrial intermembrane under physiologic conditions. Under periods of excitotoxic stress, however, there is an increase in nitric oxide (NO)-dependent oxygen free radicals, leading to DNA damage (Hara and Snyder, 2007). Increased DNA damage activates PARP, resulting in NAD depletion, PAR polymer formation, and release of AIF from the mitochondria (Yu et al., 2006). The Bcl-2 proteins Bax and Bid are also necessary for AIF release (Cregan et al., 2002; Culmsee et al., 2005). Liberated AIF translocates to the nucleus, a necessary event for AIF-induced cell death (Cheung et al., 2006). Despite the fact that AIF has no inherent endonuclease activity, it causes distinctly high molecular weight (~50kb) fragmentation of DNA (Susin et al., 1999). This is in contrast to the finer oligonucleosomal DNA degradation seen following caspase activation. Mechanistically, it is known that AIF possesses DNA binding capability, which is necessary for AIF-induced cell death (Ye et al., 2002). Binding of AIF to DNA causes chromatin condensation, a factor that possibly increases DNA susceptibility to endonucleases.

The importance of AIF in neuronal cell death is exemplified by examining the ischemia-resistant phenotype of Harlequin mice. These mice possess a proviral insert within the AIF gene rendering an 80% reduction in total AIF compared to wild-type controls (Klein et al., 2002). Despite retinal and cerebellar degeneration likely due to reduced tolerance to oxidative stress, these mice have an approximate 40% reduction in infarct volume following a focal ischemic insult (Culmsee et al., 2005).

[2] This sub-section was adapted from Vosler P, Chen J (2009) Calpain-modulation of programmed cell death pathways in cerebral ischemia. In: Experimental Stroke (Yang G, Jin K, eds), pp 1-8. Oak Park, IL: Bentham Science Publishers, Ltd.

Calpain activation is directly linked to programmed neuronal death following excitotoxicity in a caspase-independent manner (Cregan et al., 2002; Ray, 2006). Since calpain prevents caspase activation, calpain must induce an alternate pathway. For a brief synopsis see **Figure 1.7** (Vosler and Chen, 2009). Until recently, AIF release was linked to PARP activation (Du et al., 2003; Yu et al., 2006; Moubarak et al., 2007) and to Bax and Bid translocation to the mitochondria (Cregan et al., 2002; Culmsee et al., 2005); however, a direct mechanism tying these disparate mechanisms together was lacking. Calpain activation is a common phenomenon to these signaling mechanisms.

First tested in isolated mitochondria from brain and liver, calpain mediates truncation of AIF and release from mitochondria in response to truncated Bid (Polster et al., 2005). In both *in vitro* and *in vivo* models of ischemia, it was determined that μ-calpain located in the intermitochondrial space is activated and mediates cleavage of AIF, which is responsible for its translocation to the nucleus (Cao et al., 2007). While Bid and Bax are not required for AIF truncation, Bid enhances calpain-mediated AIF release.

The identification of a mitochondrial calpain, calpain 10, substantiates the above findings. Although it is an atypical calpain lacking domain IV (calcium binding domain), it is present in the mitochondrial outer membrane, intermembrane space, inner membrane and matrix (Arrington et al., 2006). Furthermore, mitochondrial calpain has similar calcium activating requirements, as μ-calpain and antibodies directed against μ-calpain recognize the mitochondrial form (Ozaki et al., 2007).

Calpain activation induced by cerebral ischemia thus acts upon many substrates, and AIF has received considerable attention concerning ischemia-induced neuronal death. As will be discussed in Chapter 2, there is controversy over the mechanism of AIF release. In addition to

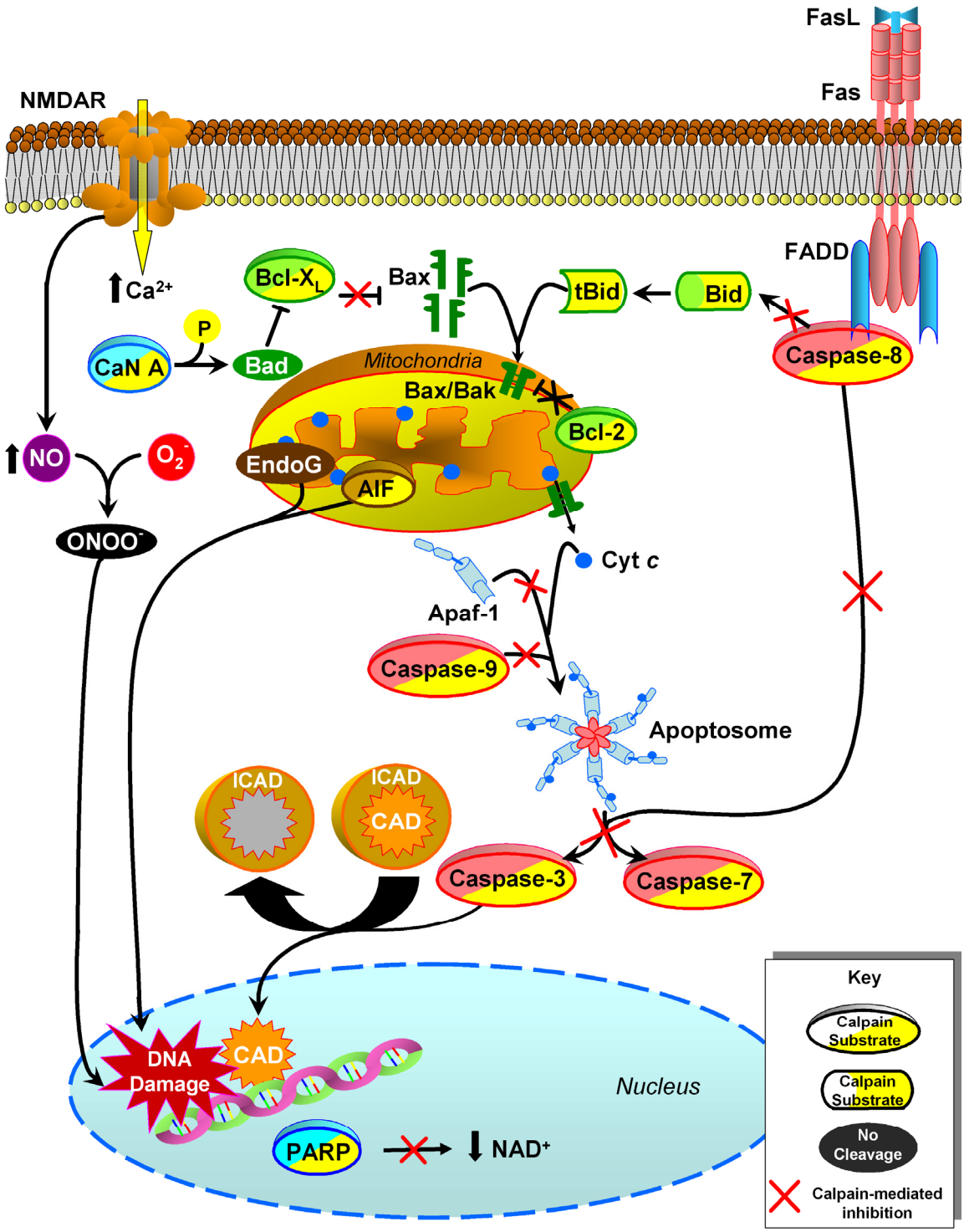

Figure 1.7 Ischemia-induced calpain modifications of intrinsic and extrinsic pathways.

Figure 1.7 (continued). Traditionally, ischemia was thought to activate both the intrinsic and extrinsic pathways. Activation of the pro-apoptotic Bcl-2 family proteins Bax and Bak lead to mitochondrial membrane depolarization and release of cytochrome *c*. Cytochrome *c* release into the cytosol combines with Apaf-1 and dATP, forming the apoptosome. This complex recruits and activates caspase-9, which results in cleavage and activation of effector caspases-3 and -7. Active effector caspases cleave ICAD, releasing CAD to cleave DNA. Inflammation caused by ischemia results in release of pro-inflammatory cytokines such as FasL into the extracellular milieu. The cytokines bind to their respective receptors, causing recruitment of FADD and dimerization of caspase-8. Active capsase-8 cleaves Bid causing further mitochondrial membrane disruption. Additionally, caspase-8 directly cleaves effector caspases. Excitotoxicity due to ischemia, however, causes overactivation of NMDA receptors, leading to increased intracellular calcium and NO activation. Increased intracellular calcium directly activates cytosolic calpain, hijacking both the intrinsic and extrinsic pathways to enact its own neuronal death cascade. Calpain directly cleaves the anti-apoptotic Bcl-2 proteins Bcl-X_L and Bcl-2, and the pro-apoptotic Bcl-2 proteins Bax and Bid. Indirectly, calpain cleaves CaN A, causing dephosphorylation of Bad and sequestration of Bcl-X_L. Combined, these events result in calpain-mediated mitochondrial membrane permeabilization, mitochondrial Ca^{2+} dysregulation, and activation of mitochondrial calpain with cleavage of AIF. Once cleaved, AIF translocates to the nucleus along with EndoG and results in DNA damage. Calpain also cleaves Apaf-1 and apical caspases-8 and -9 to inhibit activation of effector caspases. Finally, rapid induction of NO to form peroxynitrite results in PARP overactivation caused by DNA damage. Overactivated PARP is cleaved by calpain to abrogate detrimental decreases in NAD^+ levels to ensure that programmed neuronal death continues. Abbreviations: AIF, apoptosis-inducing factor; Apaf-1, apoptosis-activating factor 1; CAD, caspase-activated DNase; CaN A, calcineurin A; Cyt *c*, cytochrome *c*; EndoG, endonuclease G; FADD, Fas-associated death domain protein; FasL, Fas ligand; ICAD, inhibitor of caspase-activated DNase; NAD, nicotinamide adenine dinucleotide; NMDAR, *N*-methyl-D-aspartate receptor; NO, nitric oxide; $ONOO^-$, peroxynitrite; PARP, poly (ADP-ribose) polymerase.

the connection between AIF release and calpain, there is also evidence that AIF release is linked to activation of poly(ADP-ribose) polymerase (PARP)-1. As discussed in the following section, PARP-1 overactivation following ischemia can result in AIF release. Moreover, ischemia-induced PARP-1 activation can contribute to neuronal secondary energy failure.

1.5 MOLECULAR MECHANISMS OF ISCHEMIA-INDUCED ENERGY FAILURE AND DELAYED NEURONAL DEATH

1.5.1 Nitric Oxide Induction

Calcium influx into neurons via NMDA receptors also induces NO production. Increased calcium binds to calmodulin, which binds and activates neuronal nitric oxide synthase (nNOS) (Knowles and Moncada, 1994). Activated nNOS converts L-arginine into citrulline and NO. Neuronal NO has many physiological functions mediated by increasing cyclic GMP (cGMP) concentrations via activation of soluble guanylyl cyclase. Increased levels of cGMP then activate cyclic GMP-dependent kinases which modulate vascular smooth muscle relaxation and learning and memory (Schlossmann and Hofmann, 2005).

Pathological activation of NMDA receptors can also result in NO-mediated neuronal death as both NO inhibitors (Dawson et al., 1991) and genetic deletion of nNOS (Dawson et al., 1996) abrogated excitotoxic neuronal death. There are many potential mechanisms mediating NO pathology. Increased NO produced by glutamate receptor activation is known to reversibly block mitochondrial ATP production by inducing disruption of mitochondrial membrane potential (Almeida and Bolanos, 2001). Additionally, glutamate receptor activation results in increased mitochondrial calcium, which contributes to loss of mitochondrial membrane potential (White and Reynolds, 1996) and opening of the mitochondrial membrane permeability transition pore (Almeida and Bolanos, 2001; Alano et al., 2002).

Glutamate receptor activation also results in production of reactive oxygen species, including the potent DNA damaging peroxynitrite via the combined actions of increased

mitochondrial calcium and NO production. Increased mitochondrial calcium results in production of superoxide radicals, and superoxide reacts with NO to form peroxynitrite (Stout et al., 1998; Urushitani et al., 1998). Peroxynitrite then diffuses into the nucleus where it causes severe DNA damage (Hara and Snyder, 2007). Recently, in an elegant series of experiments, it was determined that glutamate-mediated calcium dysregulation induced DNA damage with subsequent activation of PARP-1 via in mitochondrial-derived ROS and NO-dependent manner (Duan et al., 2007). These experiments delineate the sequence of events leading to PARP-1 activation. The following section outlines the role of PARP-1 in excitotoxic and ischemia-related neuronal death.

1.5.2 PARP-1 Activation

Poly(ADP-ribose) polymerase-1 is a nuclear enzyme that uses nicotinamide adenine dinucleotide (NAD^+) to form long branched negatively charged poly(ADP-ribose) polymers (PAR) on proteins. The targets of PARP-1 are histones and multiple transcription factors, but over 90% of PAR is found on PARP-1 itself (D'Amours et al., 1999). Regulation of PAR formation is governed by poly(ADP-ribose) glycohydrolase, which cleaves PAR to produce free ADP-ribose (Davidovic et al., 2001). The most studied function of PARP-1 is its role in DNA damage repair. PARP-1 recognizes multiple forms of DNA damage as it is involved in the single and double strand break and base excision repair pathways, making it a versatile DNA damage detector (Kim et al., 2005). Identification of damaged DNA occurs via its double zinc finger domain, which activates self-polymerization of ADP-ribose (D'Amours et al., 1999).

Activity of PARP-1 is important for cellular survival as it functions to repair moderate levels of DNA damage. Animals with genetic deletion of PARP-1 are defective in repairing single and double strand break, have increased deletion, insertion and rearrangement mutations (de Murcia et al., 1997; Shibata et al., 2005; Shibata et al., 2009). PARP-1 is also involved in the maintenance of genomic stability as mice lacking PARP-1 have an increased incidence of tumors when exposed to alkylating agents (Shibata et al., 2005) and have an increased incidence of spontaneous brain and liver tumors with advancing age (Shibata et al., 2009). Finally, PARP-1 has been implicated in learning and memory as PARP-1 activity is increased in long-term memory tasks and learning is inhibited with pharmacological inhibition of PARP-1 in aplysia (Cohen-Armon et al., 2004).

In contrast to its physiological function, when high levels of DNA damage occur, PARP-1 activation is associated with cellular death. This has been shown in many stress models, including neurons (Hara and Snyder, 2007). Specifically, PARP-1-mediated neuronal death is implicated in NMDA excitotoxicity via NO and peroxynitrite formation (Mandir et al., 2000). In addition, pharmacological PARP-1 inhibition or genetic deletion is known to attenuate infarct volume caused by focal ischemia (Eliasson et al., 1997; Endres et al., 1997).

The mechanism of PARP-1 overactivation-induced neuronal death has not been fully delineated. PARP-1 activation caused by exposure of neurons to the DNA damaging agent MNNG were shown to induce neuronal death via release of AIF (Yu et al., 2002). Further examination of the mechanism of PARP-mediated neuronal death demonstrated that PAR polymer, which translocates from nucleus to cytosol upon PARP-1 activation, is neurotoxic (Andrabi et al., 2006). Moreover, formation of PAR polymer was associated with mitochondrial AIF release and AIF-mediated neuronal death (Yu et al., 2006).

Another plausible hypothesis underlying PARP-mediated neuronal death is that PARP-1 overactivation leads to severe NAD^+ depletion causing eventual energy failure. Formation of PAR polymer by PARP-1 requires substantial amounts of NAD^+. PARP-1 cleaves the glycosidic bond between nicotinamide and ADP-ribose of NAD^+ to produce the ADP-ribose needed for polymerization. Processing NAD^+ in this manner requires re-synthesis of the energy substrate rather than reduction of oxidized NAD, as is seen in other cellular processes including glycolysis and the tricarboxylic acid cycle (Kim et al., 2005). Severe PARP-1-mediated energy depletion has been suggested as a possible mechanism underlying ischemic neuronal death (Endres et al., 1997). Loss of NAD^+ and energy depletion could also compromise mitochondria, also leading to AIF release. However, a link between NAD^+ and AIF release has not been established.

In summary, ischemia and excitotoxic injury results in calcium dysregulation, NO formation, and increases in ROS including peroxynitrite leading to DNA damage and PARP-1 activation. PARP-1 activation, either by formation of PAR polymer or NAD depletion, results in AIF release and eventual neuronal death. As discussed in previous section, calpain is also associated with AIF release and neuronal death following excitotoxic or ischemic insults. Since the same insults lead to the activation of both PARP-1 and calpain, it is probable that there is a common mechanism linking PARP-1 and calpain to AIF release. Additionally, PARP-1 depletion of NAD^+ is potentially responsible for secondary energy depletion observed with delayed neuronal death.

1.6 PROTEIN SYNTHESIS AND ISCHEMIA

1.6.1 Regulation of Protein Synthesis

The manufacturing of proteins is a fundamental cellular process essential to the growth, development and maintenance of all cells. The central focus behind protein synthesis involves correctly translating a sequence of messenger RNA (mRNA) transcribed from the DNA into a series of amino acids. There are three stages to protein synthesis—initiation, elongation, and termination. The process of protein synthesis initiation involves two key steps: 1) recruiting the appropriate transfer RNA (methionine-tRNA) with its associated amino acid into the 40S ribosomal complex, and 2) the binding and incorporation of the mRNA to the ribosome for translation (**Figure 1.8**).

Initiation begins with the attachment of the eukaryotic initiation factors (eIF) eIF1, eIF1A eIF3, and eIF5 along with a methionine-charged tRNA connected to eIF2 to the 40S ribosomal subunit. This forms the 43S preinitiation complex. This complex is then brought to the mRNA by the formation of eIF4F—a composite of eIF4A, eIF4E, and eIF4G. eIF4E binds the 7-methyl guanosine cap of the mRNA at the 5'end, eIF4A is a helicase that unwinds the mRNA secondary structure, and eIF4G is a scaffolding protein that binds the other three proteins. The 43S preinitiation complex is brought to the mRNA subsequent to eIF4F binding forming the canonical 48S preinitiation complex. The 48S complex scans the 5' untranslated region (UTR) of the mRNA stopping at an initiation codon that is recognized by an anticodon methionine-connected tRNA ($tRNA^{Met}$). The recognition of the initiation codon triggers eIF2-associated GTP hydrolysis, a reaction that is catalyzed by eIF5. The eIFs then dissociate from the ribosome

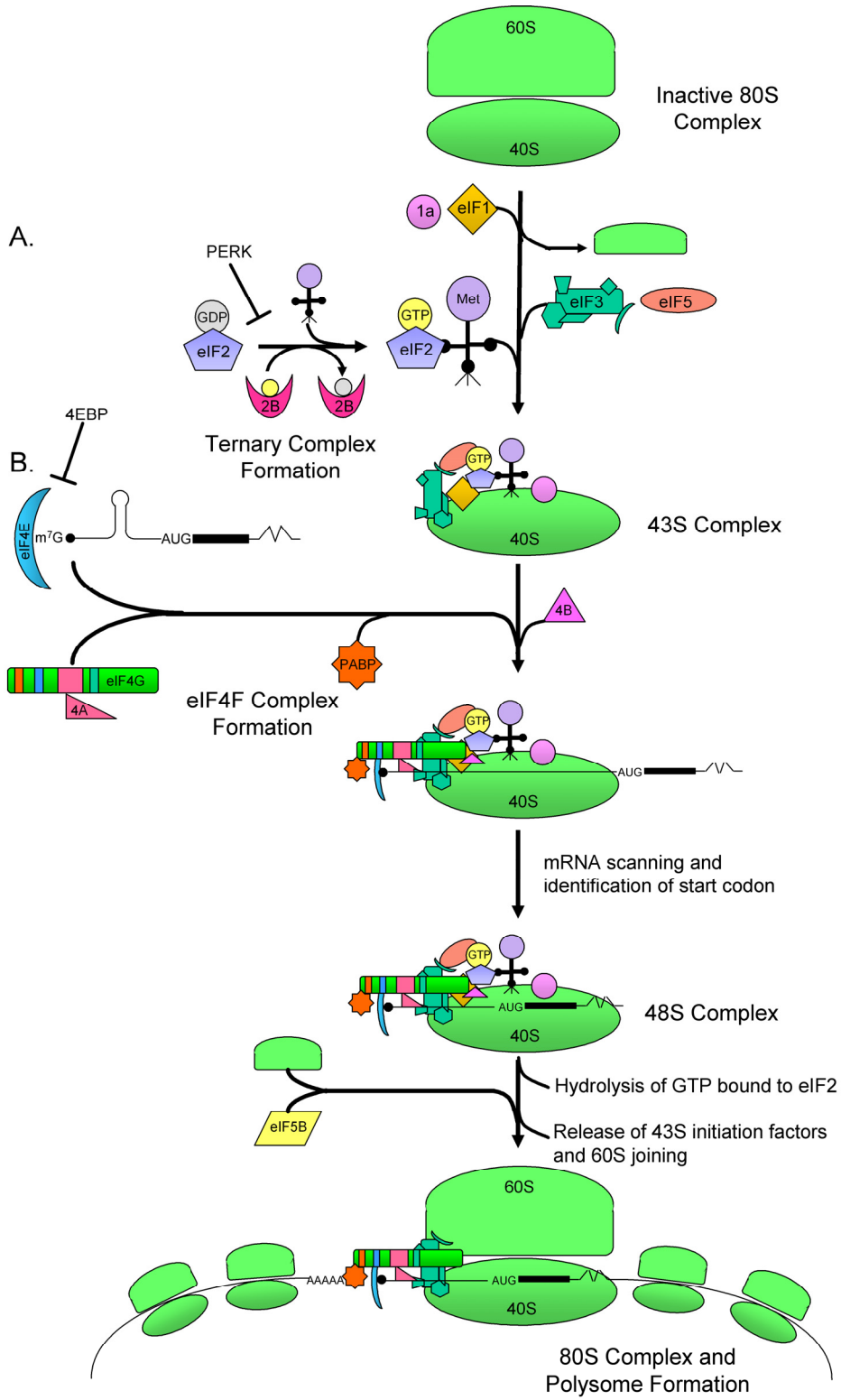

Figure 1.8. Protein Synthesis Initiation.

Figure 1.8 (continued). Translation initiation begins with either a single 40S ribosomal subunit, or as an 80S complex. Initiation factors eIF1 and 1a are recruited to the 40S ribosome. In the presence of an 80S complex, the large ribosomal subunit is removed. Initiation factors 3 and 5 then bind 40S. One of the main regulatory mechanisms is the formation of the eIF2-GTP-methionyl tRNA ternary complex (A). This proceeds by the exchange of GDP for GTP on eIF2 by eIF2B, allowing the binding of the met-tRNA to bind eIF2. This process is regulated by eIF2α kinases, such as PERK. PERK phosphorylates the alpha subunit of eIF2, blocking the exchange of GDP for GTP by eIF2B. The ternary complex then binds the ribosome forming the 43S preinitiation complex. The second main regulatory step in initiation is brining the mRNA to the ribosome for translation (B). This is regulated by the eIF4F complex. eIF4E binds the methyl-7-guanine cap of the mRNA and then binds the 4E binding domain of the scaffolding protein eIF4G. Cap binding is regulated by 4EBP, which in its unphosphorylated state will sequester 4E inhibiting cap binding. eIF4G, 4E, the RNA helicase eIF4A, and PABP combine to form the eIF4F complex that binds to 40S via the eIF3 binding domain of 4G. Another helicase, eIF4B, also joins the initiation complex. The mRNA undergoes scanning until the start codon is reached. This signifies formation of the 48S preinitiation complex. The hydrolysis of the GTP on eIF2 catalyzed by eIF5 is followed by eIF5B-GTP, which removes all of the 43S preinitiation complex factors except eIF3. Translation then proceeds with the addition of more ribosomes translating the same mRNA, forming the polysome. The mRNA is circularized via PABP binding the poly-A-tail of the RNA, a step that greatly enhances translation of the message.

leaving the tRNA bound to the initiator codon in the P site of the 40S ribosomal subunit, allowing for the binding of the 60S ribosomal subunit to the 40 subunit. This forms the functional 80S ribosome. Comprehensive reviews of protein synthesis are available (Sonenberg et al., 2000; Anderson and Kedersha, 2002; Thornton et al., 2003).

The key regulatory proteins in this process are eIF2 and eIF4F. eIF2 binds $tRNA^{Met}$ during formation of the 43S preinitiation complex, and it is regulated by phosphorylation. Regulatory serine/threonine kinases activated under varying stressors will phosphorylate the α subunit of eIF2 on serine 51 (Kimball, 2001). Phosphorylation of eIF2α increases the affinity of eIF2 to eIF2B—a GDP-GTP exchange factor that charges the eIF2-GTP- $tRNA^{Met}$ ternary

complex. The phosphorylated eIF2α acts as a competitive inhibitor of eIF2B and therefore reduces the concentration of the .ternary complex. This inhibits the formation of the 43S preinitiation complex and essentially arrests protein synthesis (Kimball, 2001).

Regulation of eIF4F function is also important in controlling protein synthesis initiation. The binding of eIF4E is modulated by at least two sets of proteins—eIF4E binding protein 1 (4EBP1), 4EBP2, and 4EBP3 and MAP kinase-interacting kinase 1(Mnk1). eIF4E is initially bound to 4EBP1, and when 4EBP1 is phosphorylated it releases eIF4E and allows it to bind to the 5' end of the mRNA (Takei et al., 2001). Phosphorylation of 4EBP1 is mediated through the PI3K/AKT/mTOR pathway (Takei et al., 2001; Takei et al., 2004). Mnk1, alternatively, phosphorylates and activates eIF4E even when it is bound by 4EBP1(Waskiewicz et al., 1999). Mnk1 activation is mediated through the MAP kinase/ERK pathway (Waskiewicz et al., 1997).

1.6.2 Molecular Mechanisms Underlying Protein Synthesis Inhibition

Following an ischemic insult the brain uniformly shuts down protein synthesis in all ischemia-affected areas (Kleihues and Hossmann, 1971). During ischemia, the arrest of protein synthesis is due to depletion of energy stores in the form of ATP and GTP and the direction of the little energy available to the execution of more essential cellular processes. However, energy depletion cannot be the cause of the entire duration of protein synthesis as energy stores are repleted by fifteen minutes after reperfusion despite continued protein synthesis inhibition (PSI) (Kleihues and Hossmann, 1971; Nowak et al., 1985). Protein synthesis eventually recovers within 6-24 hours in most, but not all brain regions (Dienel et al., 1980; Thilmann et al., 1986; Araki et al., 1990). In selectively vulnerable brain regions, namely the CA1 field of the

hippocampus, PSI persists, and this enduring PSI is correlated with eventual cell death in this region (Hossmann, 1993). Furthermore, since PSI occurs uniformly throughout the brain, it is not the loss of protein synthesis that produces damage after ischemia—it is the specific inability to recover the function of protein synthesis (Hossmann, 1993).

The initial inhibition of protein synthesis after an ischemic insult can be isolated to the inhibition of the initiation step of protein synthesis. This is supported both by experiments examining the role of protein synthesis initiation and elongation in PSI. In one study, inhibiting protein synthesis initiation using Poly (I) in an *in vitro* assay of ischemic brain tissue and observing no further decreases in protein synthesis (Cooper et al., 1977). Other studies have shown there was no correlation between the activity of the rate-limiting elongation factor, eEF2, and protein synthesis rate in both an *in vitro* and an *in vivo* model of transient global ischemia (Althausen et al., 2001; Garcia et al., 2004a; Owen et al., 2005). Hence, the regulation of protein synthesis initiation has been studied in much greater depth.

1.6.2.1 ER Stress and Ischemia. Recently, post-ischemia PSI research focused on the regulation of protein synthesis via the unfolded protein response (UPR) due to endoplasmic reticulum (ER) stress. ER stress (i.e. ER depletion of calcium or ATP, or blockade of protein glycosylation), is defined as an accumulation of misfolded proteins in the ER lumen (Kaufman, 1999). The accumulation of misfolded proteins leads to the dissociation of the ER chaperone glucose-regulated protein 78 (GRP78) from the effector proteins PERK, ATF6, and IRE1α, which are normally inhibited by GRP78 binding (Bertolotti et al., 2000; Shen et al., 2002). Release of PERK autophosphorylates, then phosphorylates eIF2α and results in inhibition of protein synthesis (Harding et al., 1999; Harding et al., 2000). Under conditions where eIF2α is

phosphorylated there is increased transcription of ER stress transcripts. Under sublethal stresses, the UPR is thought to be transiently induced to reverse ER stress. In contrast, prolonged UPR activation is associated with a failure to reduce ER stress and results in cell death (Kaufman, 1999; McCullough et al., 2001).

Ischemia has been shown to induce ER dysfunction on multiple occasions (Paschen et al., 1998b; Paschen et al., 1998a; Hu et al., 2000; Hu et al., 2001; Kumar et al., 2001). However, the UPR is not induced following either focal (Paschen et al., 2003) or global ischemia (Kumar et al., 2003). Focal ischemia resulted in pronounced expression of IRE1α-processed xbp1 mRNA; however, the normal increase in translation of the transcription factor following UPR induction was not observed (Paschen et al., 2003). Therefore, in focal ischemia, the UPR was induced, but it could not proceed due to the global inhibition of protein synthesis. There was even less evidence of the UPR following global ischemia. Measurements of xbp1 revealed no increase in IRE1α-processed xbp1, and there was no increase in translation of the UPR effector proteins XBP1, CHOP or ATF4 (Kumar et al., 2003). Again, this indicates that impairment to protein synthesis following ischemia prevents neurons from mounting an UPR. It also demonstrates a failure of ischemia-sensitive neurons to mount a functional stress response.

1.6.2.2 Ischemia-induced eIF2 Regulation. Although the UPR is not activated following ischemia, ER stress-induces activation of PERK after cerebral ischemia (Kumar et al., 2001; Kumar et al., 2003), which is necessary for ischemia-induced phosphorylation of the α subunit of eIF2 (Owen et al., 2005). Examination of the phosphorylation of eIF2α, and thus the inhibition of eIF2B, has been shown on multiple occasions to be involved with at least the initial suppression of translation during reperfusion after ischemia (DeGracia et al., 1996; DeGracia et

al., 1997; Althausen et al., 2001; Kumar et al., 2001; Martin de la Vega et al., 2001; Kumar et al., 2003; Garcia et al., 2004a; Owen et al., 2005). While there is substantial evidence regarding eIF2 phosphorylation, and this has been shown to inhibit protein translation, the time course of phosphorylation of this initiation factor does not correspond to the duration of PSI after cerebral ischemia. Phosphorylated eIF2α is at its maximal levels approximately 10 minutes after reperfusion and stays elevated between 90 minutes and 2 hours; however, phosphorylated eIF2α has returned to baseline levels in brainstem, cortex, and hippocampus by 6 hours after reperfusion (Althausen et al., 2001; Martin de la Vega et al., 2001; Kumar et al., 2003). Transient phosphorylation of eIF2α was also observed following 1 hour of MCA occlusion. Phosphorylated eIF2α was increased after 15 minutes of reperfusion, peaked at 3 hours and returned to baseline by 24 hours of reperfusion (Mengesdorf et al., 2002). Therefore, since protein synthesis has not returned in most areas of the brain by 3-6 hours post-reperfusion, then phosphorylation of eIF2α cannot be responsible for persistent PSI.

Tangential to eIF2α phosphorylation state returning to baseline after ischemia is the finding that the protein levels of growth arrest and DNA damage protein 34 (GADD34), an eIF2α phosphatase, are elevated after focal (McCaig et al., 2005) and global ischemia reaching maximum expression around 24 hours after ischemia (Garcia et al., 2004a; Paschen et al., 2004). Increased GADD34 protein levels are specific to the cortex, the whole hippocampus and the penumbral zone of focal ischemia (Garcia et al., 2004a; Paschen et al., 2004; McCaig et al., 2005); however, there is no change in the vulnerable CA1 field of the hippocampus (Paschen et al., 2004). In addition, GADD34 is further increased in the cortex and the whole hippocampus after ischemic preconditioning suggesting a protective role of GADD34 (Garcia et al., 2004a). Interestingly, while GADD34 protein levels are not increased in the CA1 fields, GADD34

mRNA levels are increased within 1 hour of reperfusion (Paschen et al., 2004). This again suggests there is a problem with recovery of protein synthesis initiation in vulnerable brain regions to translate protective proteins.

1.6.2.3 eIF4E and Ischemia. Comparative to eIF2α is the behavior of eIF4E after ischemia and reperfusion. DeGracia et al. (1996) found that there was no change in either phosphorylated eIF4E or total eIF4E after 10 minutes of cardiac arrest followed by 90 minutes of reperfusion. In a 4 vessel occlusion model of global ischemia it was found that there was no change in total eIF4E after 30 minutes of ischemia, but there was a 50% decrease in phosphorylated eIF4E during ischemia that normalized within 30 minutes of reperfusion (Burda et al., 1998). Another study using the 4 vessel occlusion model found a decrease in total eIF4E levels in both cortex and hippocampus after 30 minutes of ischemia that normalized after 4 hours of reperfusion in the cortex but not the hippocampus (Martin de la Vega et al., 2001). Moreover, this study showed that phosphorylation of the eIF4E binding protein, 4EBP1, was significantly decreased after 30 minutes of ischemia, but normalized to control levels by 30 minutes of reperfusion (Martin de la Vega et al., 2001). A follow up study performed by the same lab repeated the finding of normalization of phosphorylated eIF4E by 4 hours of reperfusion following 30 minutes of ischemia in both rats that did and did not receive ischemic tolerance (Garcia et al., 2004a). Together, these findings suggest that regulation of eIF4E is not involved in prolonged PSI due to ischemia. Cumulatively, the role of eIF2 and eIF4E, the two main regulatory molecules involved in protein synthesis under normal conditions do not seem to play a role in the pathogenesis surrounding prolonged PSI. Hence there must be other mechanisms at work.

1.6.2.4 Potential Role of eIF4G in Persistent PSI. One possible target mediating persistent PSI after ischemia and reperfusion is the regulation of eIF4G. DeGracia et al. (1996) found that 90 minutes of reperfusion following 10 minutes of cardiac arrest resulted in the fragmentation of eIF4G. This finding was later confirmed to be caused by μ-calpain, as *in vivo* inhibition of μ-calpain by calpastatin and MDL-28,170 completely blocked eIF4G fragmentation following decapitation ischemia (Neumar et al., 1998). Furthermore, in a 4 vessel occlusion model Garcia et al. (2004b) again found eIF4G fragmentation to be associated with μ-calpain and not caspase-3 activation as measured by α-spectrin cleavage within 4 hours of reperfusion. However, caspase-3 cannot be ruled out as a mediator of further eIF4G fragmentation since proteolytic activation of caspase-3 does not occur until 4-72 hours after ischemia (Chen et al., 1998).

Martin de la Vega et al. (2001) also found that after 4 hours of reperfusion following 30 minutes of 4-vessel occlusion ischemia eIF4G levels were diminished in the CA1 field of the hippocampus, but not in the whole hippocampus or the cortex. This result was also paralleled by the formation of the eIF4F complex, as levels were diminished in the CA1 field compared to the whole hippocampus and cortex (Martin de la Vega et al., 2001).

Phosphorylated eIF4G was also found to parallel Akt phosphorylation, as levels of both phosphorylated proteins were diminished immediately after ischemia but rose substantially after 30 minutes reperfusion (Garcia et al., 2004b). These levels remained elevated over controls even at 4 hours of reperfusion in both the hippocampus and the cortex. They also found a progressive diminution of total eIF4G throughout 4 hours of reperfusion only in rats without ischemic tolerance and the decrease was correlated with calpain activation. Total eIF4G remained diminished but constant in the rats with ischemic tolerance (Garcia et al., 2004a).

Reduced levels of eIF4G were also found in the penumbra following 1 hour of MCA occlusion in mice (Mengesdorf et al., 2002). The reductions in eIF4G levels were pronounced by 3 hours reperfusion and progressively decreased until 24 hours reperfusion. Thus, following both focal and global ischemia, it appears that the brain regions that are subject to persistent PSI coincide with loss of eIF4G.

Given the previous results, the investigation of the regulation of eIF4G after ischemia requires further attention. The fragmentation of eIF4G by μ-calpain after ischemia and reperfusion is also of interest. Fragmentation of eIF4G alters its ability to bind eIF4E and thus alters the type of mRNA's that are translated. If eIF4E is not able to bind to eIF4G, then mRNA's with a 7-methy guanosine cap are not translated, and this shifts the selection of mRNA's that contain an internal ribosomal entry sequence (IRES) that does not require a cap to be translated (Pelletier and Sonenberg, 1988; Gingras et al., 1999). Messages with IRES in their 5' untranslated region (UTR) encode a number of proteins that could modulate the death of neurons after ischemia (Coldwell et al., 2000; Henis-Korenblit et al., 2000). It would be of interest to determine the mRNA being translated after ischemia and reperfusion, and to establish their role in cell death. Finally, on a larger scale, the determination of the discrepancy in temporal changes beyond 4 hours of ischemia and reperfusion of eIF4G between the cortex, whole hippocampus, and the CA1 field of the hippocampus are essential to determining the role of eIF4G in persistent PSI.

1.7 SUMMARY

There are an exorbitant and intimidating number of processes that have been linked to neuronal death following either ischemic insult or *in vitro* excitotoxicity. Dissecting the relevant and important aspects for realizing viable neuroprotective strategies is a daunting task due to the breadth knowledge available. Extensive examination of both the pioneering cerebral ischemia literature scrutinizing the physiological disturbances caused by reduced blood flow and the more recent discoveries of the cellular and molecular mechanisms of ischemic neuronal death exposes two main pathological phenomenon underlying neuronal death—secondary energy failure and persistent protein synthesis inhibition.

Secondary energy failure is seen *in vivo* in penumbral neurons following focal ischemia and in the selectively vulnerable hippocampal CA1 neurons following global ischemia immediately prior to death of these neurons. The intracellular phenomenon implicated in this dissertation causing secondary energy failure is PARP-1 activation. Increased PARP-1 activation rapidly depletes NAD^+ and disrupts mitochondria to release AIF. Depletion of NAD^+ and mitochondrial disruption concomitantly contribute to secondary energy failure. Translocation of AIF to the nucleus produces DNA damage and is associated with delayed neuronal death.

The other major phenomenon linked with delayed neuronal death is persistent protein synthesis inhibition. Elegant physiological experiments have repeatedly shown that ischemia-affected neurons that do not recover protein synthesis die. Importantly, but unappreciated in the field, is the complimentary finding that neuroprotection realized by NMDA antagonism maintained protein synthesis by lowering the CBF threshold for inhibition (Mies et al., 1993b).

Examination of the underlying mechanisms of ischemia-induced protein synthesis inhibition consistently demonstrates that physiological means of inhibition are not responsible for causing persistent inhibition. Rather, the degradation of the scaffolding protein eIF4G is repeatedly shown to be correlated with both persistent protein synthesis inhibition and delayed neuronal death. However, direct evidence linking ischemia-induced eIF4G degradation with protein synthesis inhibition and neuronal death is lacking.

The subsequent chapters will address these two issues independently. Chapter 2 provides experimental evidence demonstrating a connection between PARP-1 activation and calpain-mediated truncation of AIF via mitochondrial calcium disruption. Chapter 3 examines the role of eIF4G degradation by calpain in persistent protein synthesis inhibition and delayed neuronal death following *in vitro* ischemia. Finally, the implications of these findings are discussed.

2.0 CALCIUM DYSREGULATION INDUCES APOPTOSIS-INDUCING FACTOR RELEASE: CROSS-TALK BETWEEN PARP-1- AND CALPAIN- SIGNALING PATHWAYS[1]

2.1 INTRODUCTION

Over the past decade, increasing evidence suggests that caspase-independent pathways play a critical role in neuronal death, and apoptosis-inducing factor (AIF) is emerging as a predominate mediator (Culmsee and Landshamer, 2006; Boujrad et al., 2007). Apoptosis-inducing factor is a mitochondrial flavoprotein that functions as an oxidoreductase within the inner membrane (Miramar et al., 2001). Cell death stimuli that disrupt the mitochondrial membrane, such as excitoxicity, oxidative stress, DNA damage and cerebral ischemia cause AIF release from the mitochondria and subsequent translocation to the nucleus (Susin et al., 1999; Cregan et al., 2002; Yu et al., 2002; Cao et al., 2003; Zhu et al., 2003; Plesnila et al., 2004). The presence of AIF in the nucleus is necessary for AIF-induced cell death (Cheung et al., 2006), where AIF binds

[1] This chapter was previously published: Vosler PS, Sun D, Wang S, Gao Y, Kintner DB, Signore AP, Cao G, Chen J (2009b) Calcium dysregulation induces apoptosis-inducing factor release: Cross-talk between PARP-1- and calpain- signaling pathways. Exp Neurol..

directly to DNA and causes chromatin condensation and high molecular weight (~50kb) DNA fragmentation (Susin et al., 1999; Ye et al., 2002).

There are two hypotheses regarding the mechanism of AIF release from mitochondria. The first involves a byproduct of the activation of the DNA repair enzyme poly(ADP-ribose) polymerase-1 (PARP-1), the poly(ADP-ribose) (PAR) polymer. Activation of PARP-1 is essential for AIF release (Wang et al., 2004; Culmsee et al., 2005; Moubarak et al., 2007), and results in the production of high levels of neurotoxic PAR polymer (Yu et al., 2006). Moreover, PAR polymer has been directly linked to the induction of AIF translocation (Andrabi et al., 2006), thus providing a death signaling mechanism that links the nucleus and mitochondria in neurons.

The second hypothesis governing AIF release and translocation entails activation of the calcium-dependent cysteine protease calpain (Cao et al., 2007). Calcium dysregulation is nearly a ubiquitous facet of neuronal injury and death (Vosler et al., 2008). Accordingly, calpain activation has been implicated in the pathology of most neurodegenerative diseases [for review see (Vosler et al., 2008)]. Stemming from this fact, it was discovered that calpain was necessary for AIF truncation and release from isolated brain and liver mitochondria (Polster et al., 2005). We have demonstrated that calpain activation and N-terminus cleavage of AIF is also essential for AIF translocation and ischemia-induced neuronal death (Cao et al., 2007).

The purpose of the present study was to determine whether PARP-1-mediated AIF release is sequentially linked to calpain-dependent AIF release. To this end, we studied the potential interaction between PARP-1 and calpain signaling pathways using the excitotoxic NMDA exposure model in primary neurons. Our results suggest that PARP-1 and calpain work in concert following calcium dysregulation to induce AIF release.

2.2 METHODS

2.2.1 Gene transfection in primary neurons by AAV vectors

Construction and production of adeno-associated virus (AAV) vectors carrying either the short hairpin siRNA AIF targeting sequence (AAV–AIFt), its scrambled control sequence (AAV–AIFs) or the calpastatin cDNA (AAV–Cps) have been described elsewhere (Cao et al., 2007). The neuronal cultures were infected with the AAV–AIFt, AAV–AIFs, or AAV–Cps vector or the control vector [AAV–green fluorescent protein (GFP) or empty AAV] at the particle/cell ratio of 1 x 10^5/liter for 6 h in serum-free media, and then incubated in vector-free normal media for 72 h. The overexpression of calpastatin in neurons was confirmed by Western blot using the anti-hemagglutinin (HA) antibody. The AIF knockdown effect by AAV–AIFt in neurons was examined using Western blot with the anti-AIF antibody.

2.2.2 Primary neuronal culture and NMDA neurotoxicity

Primary cultures of cortical neurons were prepared from 17 d Sprague Dawley rat embryos. Experiments were conducted at 12-14 d *in vitro* (DIV), when cultures consisted primarily of neurons (97%) as determined using cell phenotype-specific immunocytochemistry (Cao et al., 2001). To induce NMDA neurotoxicity, cultures were incubated with NMDA at the concentration of 100 μM for 30 min and then returned to normal culture media.

Fluorescence of Alamar blue (Accumed International, Westlake, OH), an indicator that changes from blue to red and fluoresces when reduced by cellular metabolic activity, was used to

measure the viability of the cultured neuron at 24 h after induction of NMDA neurotoxicity. One-half of the culture medium was replaced with MEM-Pak containing 10% Alamar blue (v/v), and cultures were incubated for 1.5 h at 37°C in humidified 95% air and 5% CO_2. Fluorescence was determined in a Millipore (Billerica, MA) CytoFluor 2300 automated plate-reading fluorometer, with excitation at 530 nm and emission at 590 nm.

NMDA-induced cell death was quantified by measuring lactate dehydrogenase (LDH) release from damaged cells into the culture medium (Cao et al., 2007). In brief, 10 µl aliquots of medium taken from the cell culture wells were added to 200 µl of LDH reagent (Sigma, St. Louis, MO). Using a spectrophotometer plate reader (Molecular Devices, Sunnyvale, CA), the emission was measured at 340 nm, which is proportional to the amount of LDH in the medium. The data is expressed as the percentage change of LDH release and we used NMDA toxicity alone as maximum toxicity (100%).

2.2.3 Subcellular fractionation and Western blot analysis

Nuclear and mitochondrial protein extracts were prepared from cultured neurons at 0.5, 2, 6, and 24 h after NMDA exposure. The cells were first suspended in a hypotonic buffer containing 50 mM Tris-HCl (pH 8.0), 25 mM MgCl2, and 0.1 mM phenylmethylsulfonyl fluoride and kept on ice for 15 minutes. The nuclear and mitochondrial fractions of protein were separately isolated by centrifugation as previously described (Cao et al., 2003). The nuclear protein samples were then immunoreacted with the rabbit monoclonal anti-AIF antibody at a dilution of 1:1000, and immunoblotting of Histone-1 served as the protein loading control.

Western blotting was performed using standard methods and the enhanced chemiluminescence detection reagents (GE Healthcare). The following antibodies were used: rabbit monoclonal anti-AIF antibody (clone E20, 1:1000) was purchased from Epitomics (Burlingame, CA); mouse monoclonal anti-cytochrome *c* oxidase IV antibody (1:1000) was from Invitrogen (Carlsbad, CA); rabbit polyclonal antibody histone-1 (1:500) was from Santa Cruz Biotechnology (Santa Cruz, CA).

2.2.4 Calpain activity assay

Calpain activity assay was performed using a fluorescent calpain I substrate as described previously (Cuerrier et al., 2005). In brief, mitochondrial proteins (30 μg) were incubated with calpain reaction buffer [20 mM HEPES, pH 7.6, 1 mM EDTA, 50 mM NaCl, and 0.1% (v/v) 2-mercaptoethanol] containing 10 μM calpain I fluorescent substrate H-E(EDANS)PLF~AERK(DABCYL)-OH (Calbiochem, La Jolla, CA). The reaction was initiated by addition of $CaCl_2$ (final concentration of 5 μM) and incubated at 37°C for 30 min. The activity of calpain was measured by detecting the increase in fluorescence using excitation/emission wavelengths of 335/500 nm. Calpain activity was calculated quantitatively based on the standard curve generated using recombinant calpain I (Calbiochem) and expressed as units per milligram protein.

2.2.5 Mitochondrial Ca^{2+} (Ca^{2+}_m)

Neurons on coverslips were incubated at 37°C for 60 min with 9 μM Rhod2-AM (Invitrogen, Carlsbad, CA) which was reduced with a minimum of sodium borahydride and 3 mM sodium

succinate in an HCO_3^--MEM buffer solution as described before (Marks et al., 2005; Kintner et al., 2007). Cells were then loaded with 200 nM MitoTracker green (Invitrogen, Carlsbad, CA) in HEPES-MEM buffer for 30 min at 37°C. The coverslip was placed in a perfusion chamber (Warner Instruments, Hamden, CT) on the stage of a Leica DMIRE2 confocal microscope (Exton, PA). Cells were visualized with a 100X oil-immersion objective. Cells (2-3 in the field) were scanned sequentially for MitoTracker green (ex. 488 nm argon laser line, em 500-545 nm) and Rhod-2 (ex. 543 HeNe laser, em 544-677). The MitoTracker green signal was used to maintain focus before each sequential scan. Sequential scans were analyzed using Leica confocal software. Average grayscale values were collected from regions of interest (ROI) around perinuclear mitochondrial clusters which exhibit colocalization of MitoTracker green and Rhod-2 signals (typically, 5-6 ROIs were selected in each cell). $Ca^{2+}{}_m$ values were expressed as relative change of Rhod-2 signals from the baseline values and summarized data represents the average of the calculated values from 4-5 cells. Rhod-2 AM (K_d ~ 580 nM) was taken up into the mitochondria electrophoretically where it was de-esterified and trapped. At the end of each experiment, 1 μM FCCP was applied in order to depolarize mitochondria and the subsequent loss of Rhod-2 fluorescence signal verified its specific localization in mitochondria.

2.2.6 Statistical Analysis

Data are presented as mean ± SE. Statistical assessment was performed using analysis of variance (ANOVA) with *post hoc* Scheffe's tests. A level of $p<0.05$ was considered statistically significant.

2.3 RESULTS

2.3.1 NMDA toxicity induces AIF truncation and AIF-dependent neuronal death

Previously we have established that calpain mediates AIF truncation as a prerequisite for release from mitochondria (Cao et al., 2007). However, it is known that both full length and truncated AIF can bind to DNA to cause DNA damage (Yu et al., 2002; Cao et al., 2003). Therefore, we wanted to confirm that NMDA-mediated toxicity induced the release of the truncated form of AIF. In rat primary cortical neurons, 30 minutes of NMDA exposure resulted in progressive appearance of truncated AIF in whole-cell extracts beginning at 2 h after exposure (**Figure 2.1A**). In parallel with increases in truncated AIF in whole-cell extracts, there was an increased presence of truncated but not full length AIF in the nuclear fraction of NMDA exposed neurons (**Figure 2.1B**). These results support previous findings that truncated AIF is released from the mitochondria and translocates to the nucleus following excitotoxic stress.

In order to confirm that AIF translocation is neurotoxic (Wang et al., 2004), we infected neurons using an adeno-associated viral (AAV) vector expressing AIF-targeting shRNA (shRNAt) to inhibit AIF expression. **Figure 2.2A** demonstrates a nearly complete loss of AIF expression in shRNAt-infected but not in the control scrambled shRNA (shRNAs)-infected neurons. We employed measures of cell death and cell viability to test if AIF knock down was neuroprotective. Abrogation of AIF expression both significantly reduced LDH release and increased neuronal viability over controls (**Figures 2.2B and C**, respectively). Although the protective effect of AIF knock down was not complete, these data confirm that AIF plays a role in NMDA-induced neurotoxicity.

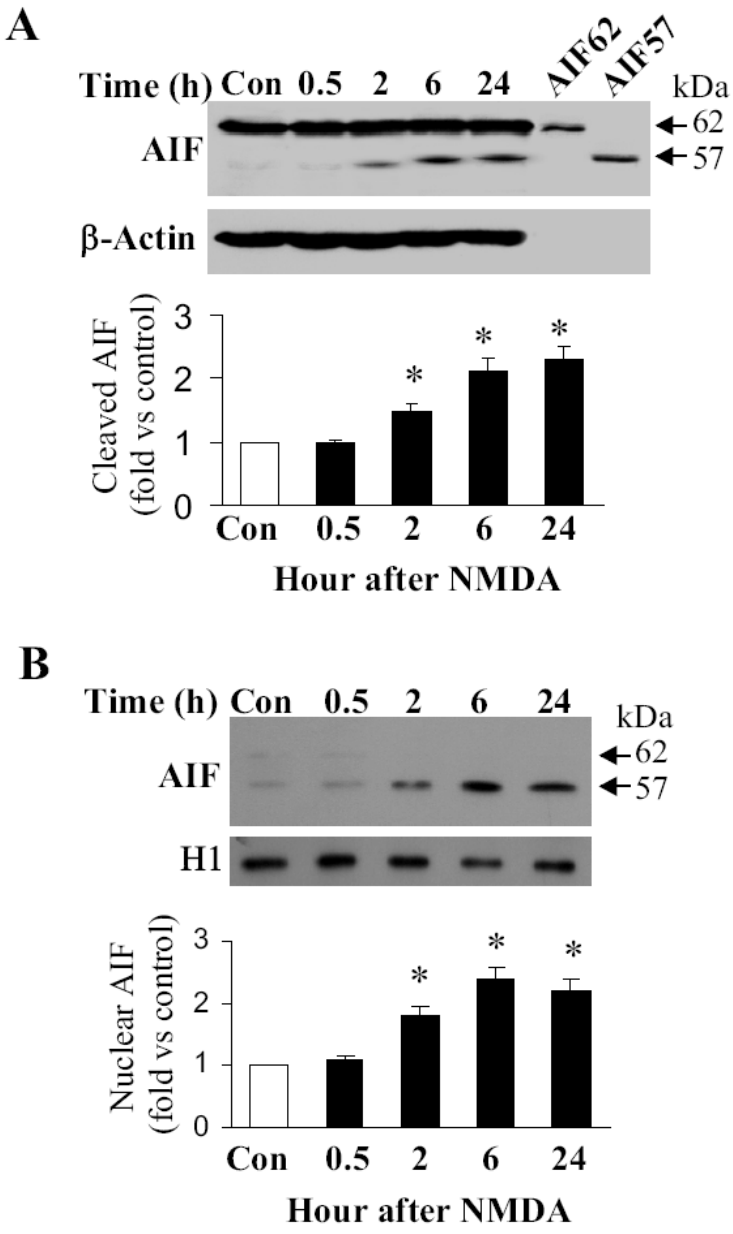

Figure. 2.1. Translocation of truncated AIF in neurons after NMDA neurotoxicity. ***A***, Western blots based on total-cell extracts show that AIF was truncated to yield the 57 kDa fragment in neurons at 2, 6, and 24 h after NMDA exposure (100 μM). Recombinant proteins AIF62 (representing the endogenous AIF) and AIF57 (representing the calpain-truncated AIF) served as size controls. ***B***, Western blots based on nuclear protein extracts show that a truncated AIF at the size of 57 kDa was increased in the nucleus at 2, 6, and 24 h after NMDA exposure (100 μM). The graphs at the bottom of blots illustrate the time-dependent increases in the truncated AIF in both whole-cell extracts (A) and nuclear extracts (B) after NMDA exposure. Data are based on 3 independent experiments. *$p < 0.05$ *versus* control neurons without NMDA exposure.

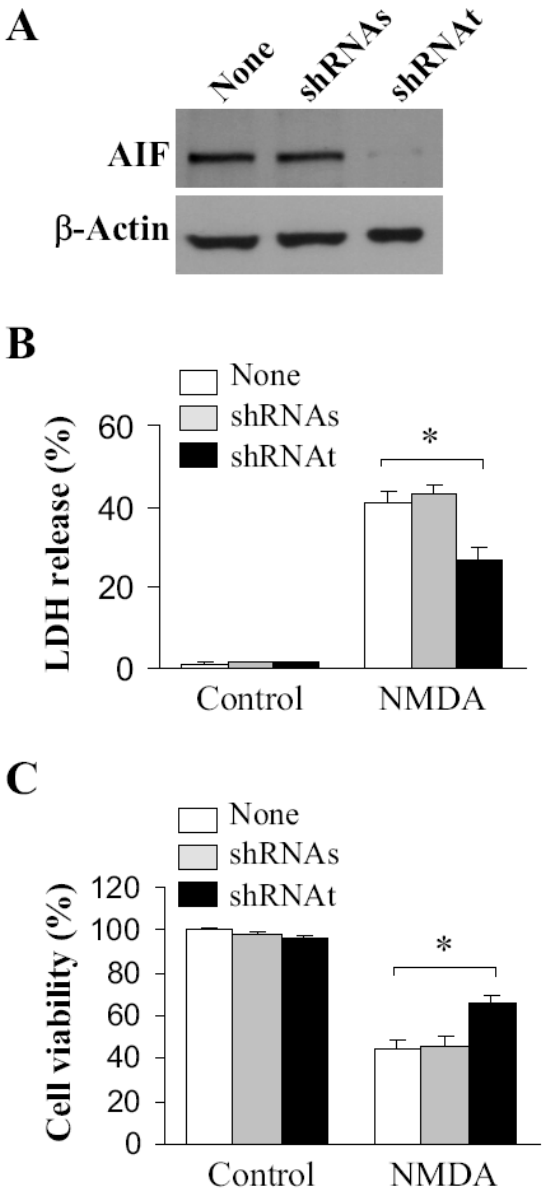

Figure 2.2 Neuroprotective effect of AIF knockdown against NMDA toxicity in primary cortical neurons. ***A***, Western blots show that AIF expression was decreased in neurons infected with AAV expressing the AIF-targeting shRNA sequence (shRNAt), but not in neurons expressing the scramble shRNA sequence (shRNAs). ***B-C***, Cell death and cell viability were measured based on LDH release (B) and Alamar blue fluorescence (C), respectively, at 24 h after NMDA exposure (100 μM). *$p < 0.05$ versus nontransfected neurons. Data are mean ± SE; n = 12 per experimental condition from three independent transfection experiments.

2.3.2 AIF cleavage and translocation is calpain-dependent

We and others have demonstrated that AIF truncation and release is dependent upon calpain activation in isolated mitochondria (Polster et al., 2005), primary neurons and in rat brain (Cao et al., 2007). We next sought to demonstrate involvement of calpain in AIF truncation and translocation to the nucleus following NMDA exposure. Calpastatin, the only known endogenous inhibitor of calpain (Murachi et al., 1980), was transfected into neurons using AAV expressing calpastatin-HA (Figure 3A). Calpastatin overexpression significantly reduced AIF truncation (**Figure 2.3B**) and nuclear translocation (**Figure 2.3C**) following NMDA exposure. In addition, calpain inhibition also resulted in a significant increase in cell viability. These experiments demonstrate the requirement of calpain activation for AIF truncation, translocation and neuronal death following NMDA exposure.

2.3.3 PARP-1 inhibition abrogates AIF translocation and calpain activity

We next confirmed the dependence of AIF release on PARP-1 activation. Using PAR polymer as a marker of PARP-1 activity, we found that exposure of neurons to NMDA resulted in the progressive accumulation of PAR polymer, an effect that was blocked using the PARP-1 specific inhibitor 3-ABA (**Figure 2.4A**). Inhibition of PARP-1 (and PAR polymer formation) also attenuated AIF truncation, nuclear translocation, and neuronal death (**Figures 2.4B, C and E**, respectively). Thus, PARP-1 is also critical for AIF release and neuronal death due to NMDA exposure.

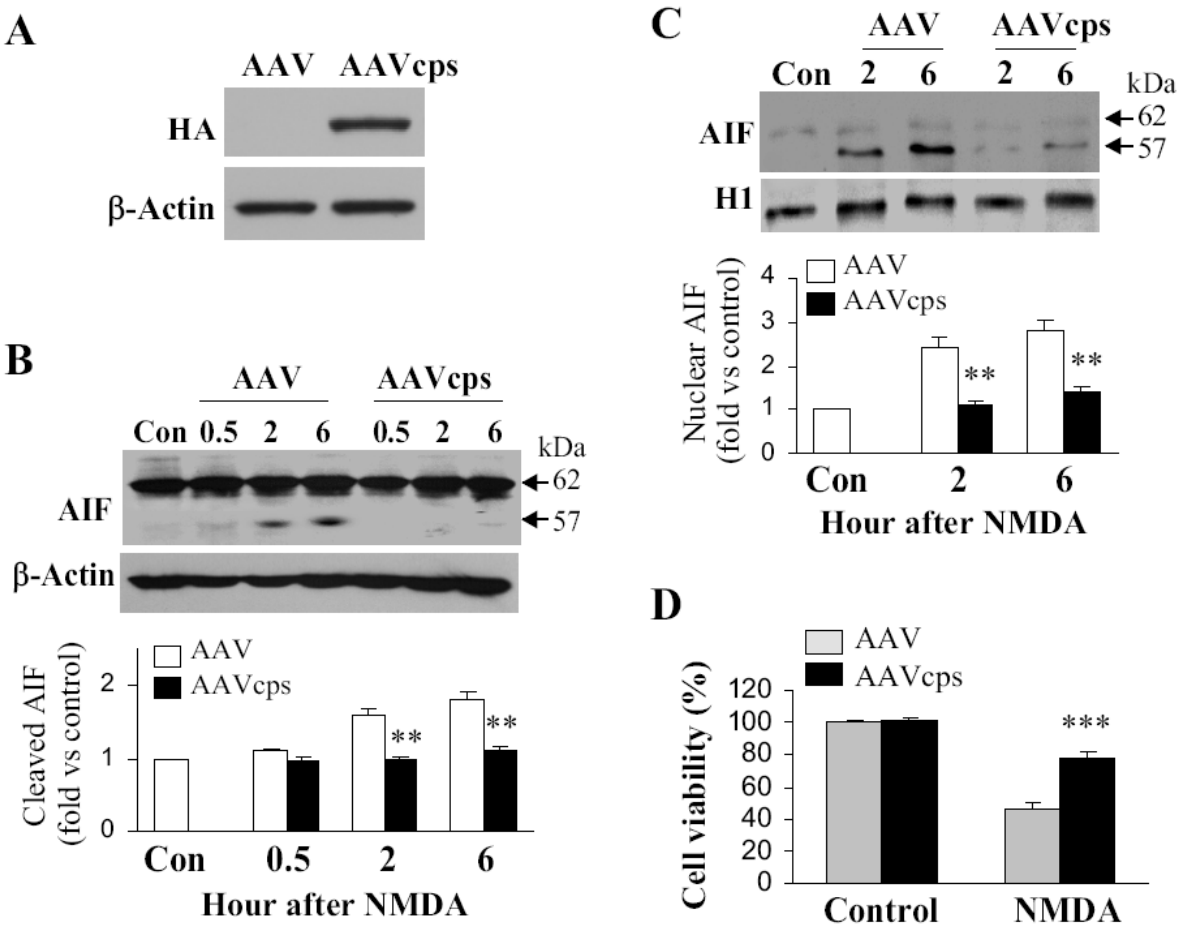

Figure 2.3 Calpain inhibition prevents NMDA-induced AIF truncation and nuclear translocation in neurons. ***A***, Neurons were infected for 3 d with empty AAV or AAV carrying the calpastatin (cps) cDNA (AAVcps), and the expression of cps (tagged with HA) was confirmed by Western blot using the anti-HA antibody. ***B***, Western blots for AIF using whole-cell extracts from control neurons (Con) or 0.5, 2 and 6 h after NMDA exposure (100 μM) in neurons infected with empty AAV or AAVcps. ***C***, Western blots for AIF using nuclear extracts from control neurons (Con) or 2 and 6 h after NMDA exposure in neurons infected with empty AAV or AAVcps. The graphs at the bottom of blots illustrate the effect of cps transfection on NMDA-induced truncation (B) and nuclear translocation (C) of AIF, respectively. ***D***, Cps transfection increases cell viability 24 h after NMDA exposure, based on the Alamar blue assay. All data are mean ± SE, **p<0.01; ***p<0.001 versus neurons infected with empty AAV, based on 3 independent experiments.

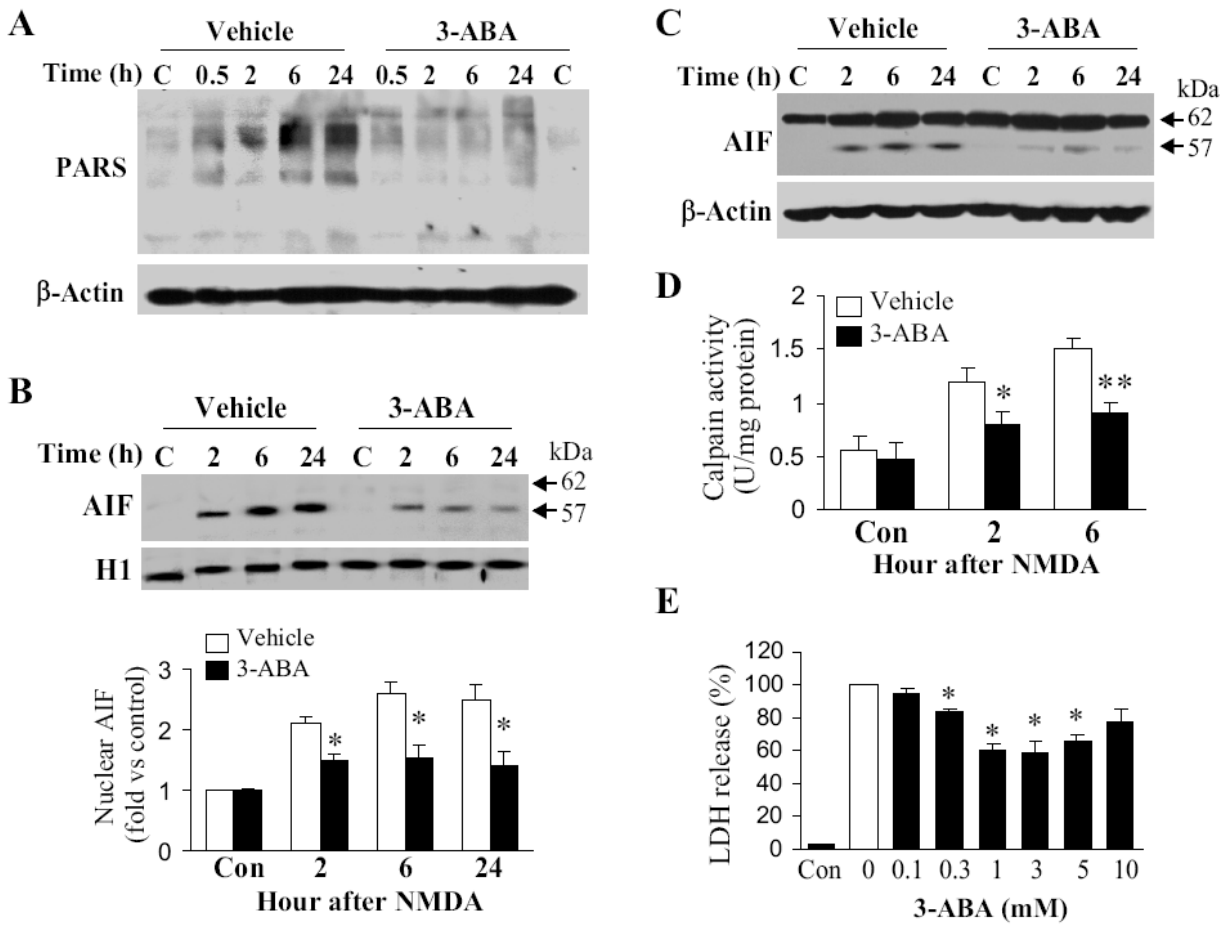

Figure 2.4 PARP-1 inhibition attenuates NMDA-induced AIF truncation and nuclear translocation in neurons. ***A***, Neurons were treated with 3-ABA (1 mM) or vehicle for 30 min and then incubated with NMDA (100 μM). Western blot was performed at 0.5, 2, 6 and 24 h after NMDA exposure to detect the formation of poly(ADP-ribose)polymers (PARS). The blots are representatives of two independent experiments with similar results. ***B***, Western blots for AIF using nuclear extracts from control neurons (C) or 2, 6 and 24 h after NMDA exposure in neurons pre-treated with 3-ABA (1 mM) or vehicle. The graph at the bottom illustrates the effect of 3-ABA on NMDA-induced nuclear translocation of AIF, based on 3 independent experiments. *$p < 0.05$ versus vehicle-treated neurons. ***C***, Western blots for AIF using whole-cell extracts from control neurons (C) or 2, 6 and 24 h after NMDA exposure in neurons pre-treated with 3-ABA (1 mM) or vehicle. The blots are representatives of two independent experiments with similar results. ***D*,** Calpain activity measured in isolated mitochondria (30 μg protein/reaction) before or 2 and 6 h after NMDA exposure from neurons neurons pre-treated with 3-ABA (1 mM) or vehicle. ***E*,** PARP-1 inhibition by 3-ABA decreases cell death 24 h after NMDA exposure, as determined by measuring LDH release. All data are mean ± SE, *$p<0.05$; **$p<0.01$ versus vehicle-treated neurons, from three experiments.

Activation of PARP-1 has also been associated with increased calpain activity in non-neuronal cells (Moubarak et al., 2007). We therefore tested the hypothesis that calpain activity is dependent upon PARP-1. Exposure of neurons to NMDA resulted in elevated calpain activity in mitochondria, which was prevented by PARP-1 inhibition (**Figure 2.4D**). This indicates that calpain-mediated truncation of AIF is contingent upon PARP-1 activity.

2.3.4 Calpain and PARP-1 inhibition attenuates AIF translocation

To confirm that AIF translocation was dependent upon both calpain and PARP-1, we performed immunocytochemistry to visualize AIF. In control neurons, AIF colocalized with the mitochondrial marker cytochrome *c* (**Figure 2.5Aa-c**). At 6h following NMDA exposure, approximately 50% of the neurons had AIF present in the nucleus (**Figure 2.5A, d-f and m-p**). In contrast, treatment with either calpastatin and 3-ABA treatment attenuated AIF translocation to the nucleus (**Figure 2.5A, g-l**). Quantification demonstrated a significant reduction in the number of neurons containing nuclear AIF with calpain and PARP-1 inhibition (**Figure 2.5B and C**, respectively). These results demonstrate that both PARP-1 and calpain activation are involved in AIF translocation to the nucleus.

2.3.5 3-ABA inhibits NMDA-induced Ca^{2+} accumulation in mitochondria

Lastly, we sought to determine the mechanisms governing PARP-1-dependent calpain activation. Since calcium dysregulation is a common phenomenon underlying neuronal demise, and calpain

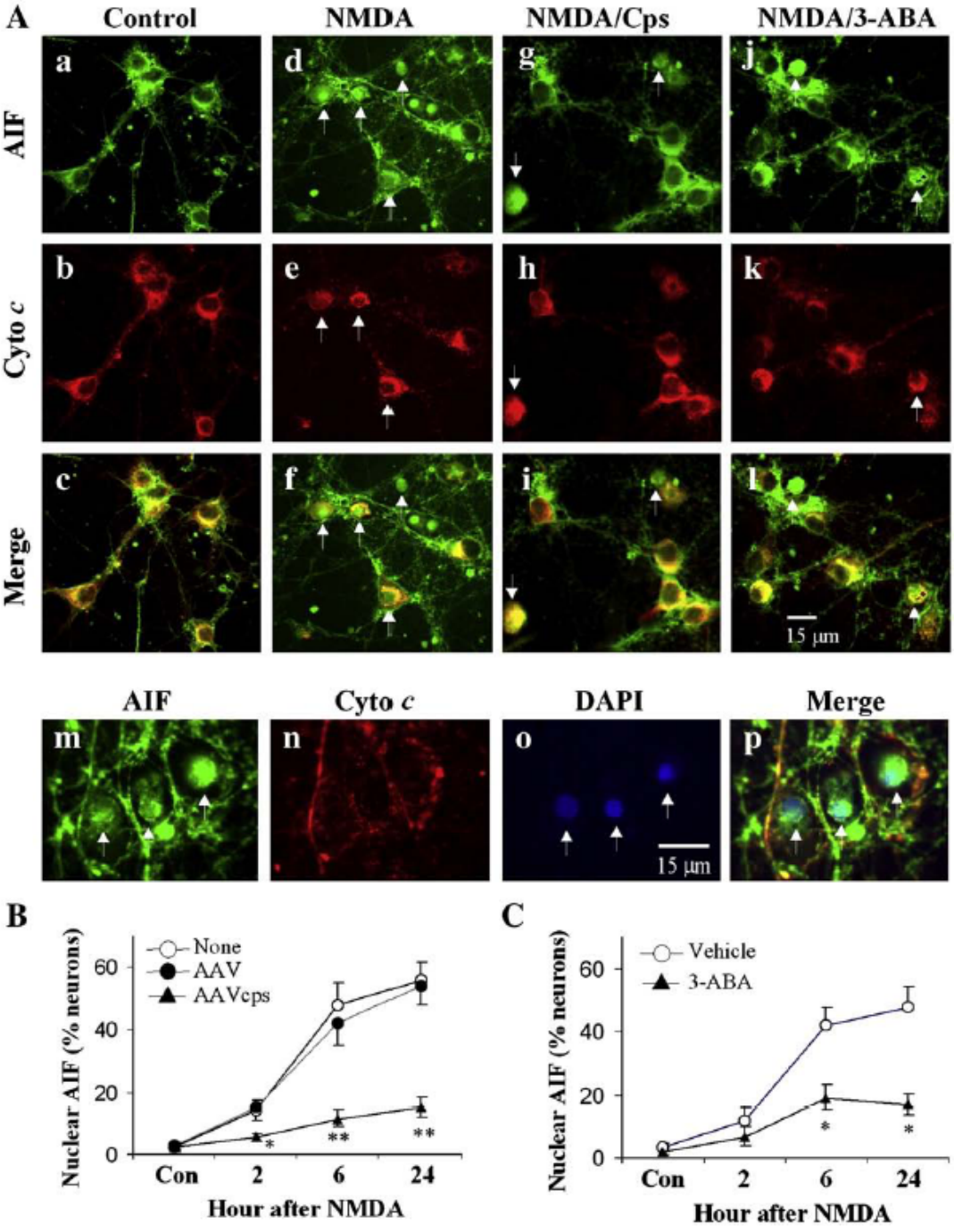

Figure 2.5 Attenuation of NMDA-induced AIF nuclear translocation in neurons by inhibiting calpain or PARP-1. ***A***, Immunostaining for AIF (green) and cytochrome *c* (red). In control neurons (a-c), AIF and cytochrome *c* fluorescence exhibit a coincided cytoplasmic pattern (combined image in panel c). At 6 h after NMDA exposure (100 μM), many neurons

Figure 2.5 (continued). show AIF nuclear localization (arrows in panel d and in combined panel f) in which cytochrome *c* fluorescence remains cytosolic or is lost (e). AIF nuclear translocation is less frequently seen in cultures that are either infected with AAVcps (g-i) or pre-treated with 3-ABA (j-l). The higher power images in panels m-p show the triple-label of AIF (green), cytochrome *c* (red) and DAPI (blue) in NMDA-challenged neurons. Note that AIF and DAPI fluorescence is co-localized in NMDA-challenged neurons (arrows). ***B-C***, Percentages of neurons showing nuclear translocation of AIF at 2, 6, and 24 h NMDA exposure (100 μM). The effects of AAVcps transfection or 3-ABA on AIF translocation are illustrated in B and C, respectively. **p*<0.05, ***p*<0.01 versus control treatment (empty AAV or vehicle), from 4 independent experiments.

is a calcium-dependent protease, we hypothesized that PARP-1 activation contributed to mitochondrial calcium dysregulation and ultimately to calpain activation.

NMDA-induced changes in mitochondrial Ca^{2+} were investigated using Rhod-2. Under control conditions, punctate mitochondrial Ca^{2+} dye Rhod-2 staining colocalized with mitochondrial probe MitoTracker green (**Figure 2.6A**). Exposure to 100μM NMDA resulted in a gradual increase in the mitochondrial Ca^{2+} signal that reached a plateau by 25 min and ~2.5 fold of control (**Figure 2.6B**). Increased mitochondrial Ca^{2+} levels were sustained at 120 min in the presence of NMDA (Figure 6A and B). Loss of Rhod-2 fluorescence signal from mitochondria (>90%) was induced by adding the mitochondrial depolarizing agent FCCP (1μM) to verify that the increased Ca^{2+} localized specifically to the mitochondria (**Figure 2.6A and B**).

To investigate the role PARP-1 plays in mitochondrial dysfunction following NMDA-mediated neurotoxicity, the effects of PARP1 inhibition using 3-ABA on changes in mitochondrial Ca^{2+} was studied. Inhibition of PARP-1 completely abolished the NMDA-induced increases in Rhod-2 fluorescence over the entire 120 min exposure period (Figure 6A-

C). In addition, no mitochondrial swelling was observed with the MitoTracker green signal in the presence of 3-ABA and 100μM NMDA. Together, these data show that PARP-1 activation mediates NMDA-induced elevation of mitochondrial Ca^{2+}.

2.4 DISCUSSION

There are two main contemporary hypotheses regarding the mechanism underlying AIF translocation from the mitochondria to induce caspase-independent neuronal death: PARP-1-induced PAR polymer formation (Yu et al., 2006) and calpain activation (Cao et al., 2007). Here we report the novel finding that PARP-1 induced mitochondrial Ca^{2+} dysregulation mediates calpain activation and subsequent AIF truncation and translocation to the nucleus. This is the first time PARP-1 and calpain activation have been examined simultaneously in the context of neuronal NMDA toxicity. Moreover, it reconciles the two seemingly independent hypotheses.

This study confirmed that ischemia-related injury induces neuronal death via AIF translocation as shown previously (Cregan et al., 2002; Yu et al., 2002; Zhu et al., 2003; Wang et al., 2004; Culmsee et al., 2005). We also demonstrate that both PARP-1 and calpain trigger truncation and nuclear localization of AIF, and that calpain activity is dependent upon PARP-1. This finding is supported by a previous study showing that calpain acts downstream of PARP-1 following MNNG-induced necrosis in mouse embryonic fibroblasts (Moubarak et al., 2007). An important addition to understanding the sequential nature of PARP-1 and calpain activation is

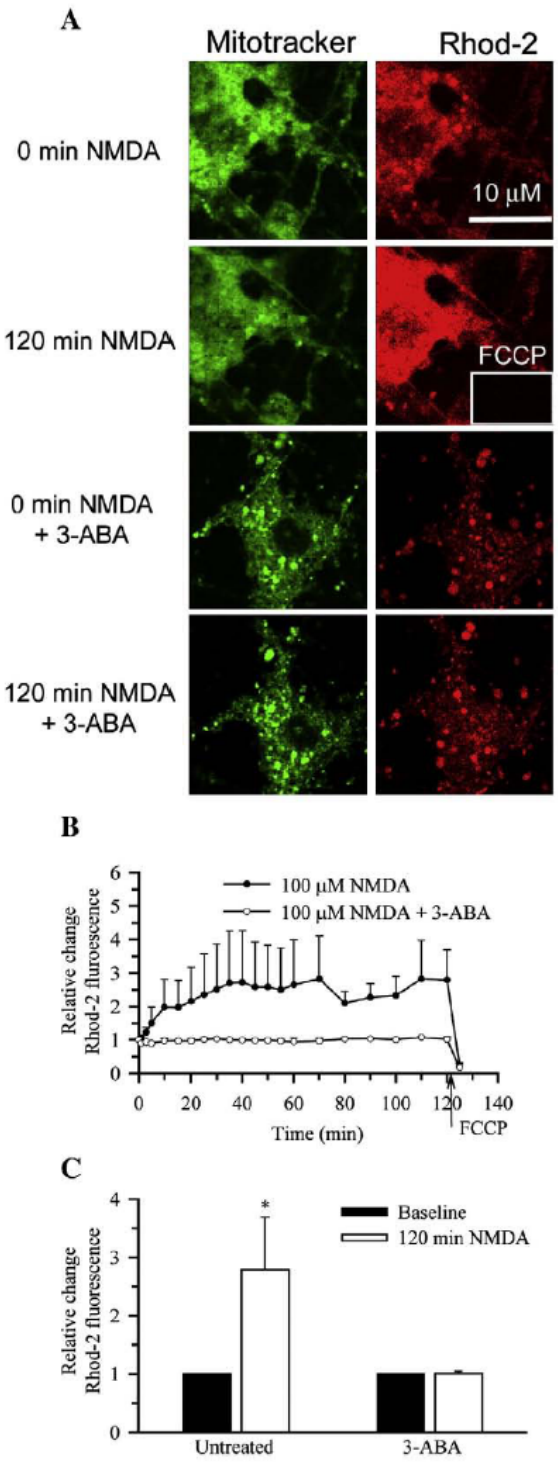

Figure 2.6 PARP-1 activation contributes to mitochondrial Ca^{2+} dysregulation after NMDA neurotoxicity.

Figure 2.6 (continued). Neuronal cultures grown on coverslips were loaded with MitoTracker green and the mitochondrial Ca^{2+} dye Rhod-2. Changes in MitoTracker and Rhod-2 fluorescence were monitored on a confocal microscope. In some studies, cells were incubated with 1.0 mM 3-ABA for 30 min prior to and during the subsequent exposure to NMDA (100 μM). ***A*****,** Representative images showing single neurons loaded with MitoTracker green and Rhod-2. ***B*****,** Time course of changes of Rhod-2 fluorescence signals. ***C*****,** Summary of relative change in Rhod-2 fluorescence in response to 100 μM NMDA with and without 3-ABA treatment. Mean ± S.E.; n = 3-4, *$p < 0.05$.

that PARP-1 activates calpain through PAR polymer-induced mitochondrial Ca^{2+} dysregulation. How PAR polymer induces alterations in mitochondrial Ca^{2+} levels remains unknown. One potential mechanism is that PAR polymer induces mitochondrial permeability pore formation, resulting in Ca^{2+} overload. This is supported by the finding that the mitochondrial permeability pore inhibitor cyclosporine A blocked calpain mediated calcium-induced AIF release in isolated mitochondria (Polster et al., 2005).

The validity of the hypothesis that PARP-1 induces mitochondrial Ca^{2+} dysregulation to induce calpain activation is dependent on mitochondrial calpain. Indeed, the most calcium-sensitive form of calpain, μ-calpain (or calpain I), possesses a mitochondrial localization sequence and is found in the mitochondrial intermembrane space (IMS) (Garcia et al., 2005; Badugu et al., 2008). We have also found μ-calpain to be localized to the IMS under control conditions. However, calpain was also present in both the outer and inner mitochondrial (IM) membrane fractions following ischemia-related injury (Cao et al., 2007). Notably, AIF is normally located in the IM. Ischemic injury therefore results in the colocalization of calpain and AIF.

Mitochondria start accumulating Ca^{2+} when intracellular Ca^{2+} increases to ~400 nM (Szabadkai and Duchen, 2008). Free mitochondrial Ca^{2+} will only increase when the robust Ca^{2+}

buffering capacity of mitochondrial matrix becomes nearly saturated. Therefore, the NMDA-induced increase in free mitochondrial Ca^{2+} levels shown in this study indicates intracellular Ca^{2+}levels increased prior to mitochondrial Ca^{2+} changes and were unremitting, although we did not monitor them concurrently. We believe that sustained increases in free mitochondrial Ca^{2+} leads to opening of the permeability transition pore and release of AIF. Ablation of mitochondrial Ca^{2+} increases by 3-ABA will then reduce AIF release and apoptosis following excitotoxicity.

Neuronal stress induced by NMDA toxicity produced an early (<5 min) increase in mitochondrial Ca^{2+} that was responsible for mitochondria-induced ROS production and PARP-1 activation (Duan et al., 2007). This study complements our findings, and we propose the following two-phase model as shown in **Figure 2.7**. First, excessive NMDA receptor activation leads to massive Ca^{2+} influx. The mitochondria serve as a sink to absorb a portion of this excess Ca^{2+}. However, excessive Ca^{2+} levels overload the oxygen reducing capacity of the mitochondria, and results in release of superoxide radicals into the cytosol. Cytosolic superoxide can then react with the nitric oxide that is concomitantly produced during NMDA receptor activation (Dawson et al., 1991; Dawson et al., 1996) to form peroxynitrite (Stout et al., 1998; Urushitani et al., 1998), a molecule known to produce severe DNA damage (Hara and Snyder, 2007).

Next, DNA damage activates PARP-1 producing PAR-polymer and severe NAD depletion in the second phase of our model (>10 minutes following excitotoxicity). Levels of PAR polymer that exceed the processing capacity of the PAR polymer catabolic enzyme, PAR glycohydrolase (PARG) (Andrabi et al., 2006; Cozzi et al., 2006), result in secondary mitochondrial Ca^{2+} dysregulation. Alternatively, NAD depletion could create a severe energy

crisis (Eliasson et al., 1997; Endres et al., 1997), contributing to mitochondrial Ca^{2+} dysregulation. Abnormal Ca^{2+} homeostasis results in mitochondrial calpain activation, which cleaves AIF located in the inner mitochondrial space. Truncated AIF is then released from the mitochondria and translocates to the nucleus. The final stage is AIF-induced DNA processing and eventual neuronal death.

In summary, we provide novel evidence that PARP-1 activation following NMDA exposure induced mitochondrial Ca^{2+} dysregulation, subsequent calpain activation and AIF release from the mitochondria. This study further reconciles two seemingly disparate hypotheses regarding the mechanisms of AIF-induced neuronal death. Furthermore, it provides the groundwork for future endeavors to investigate how PARP-1 contributes to mitochondrial Ca^{2+} dysregulation. Additional characterization of these mechanisms will lead to greater understanding of neuronal death and potentially to viable therapeutics to combat neurodegenerative diseases.

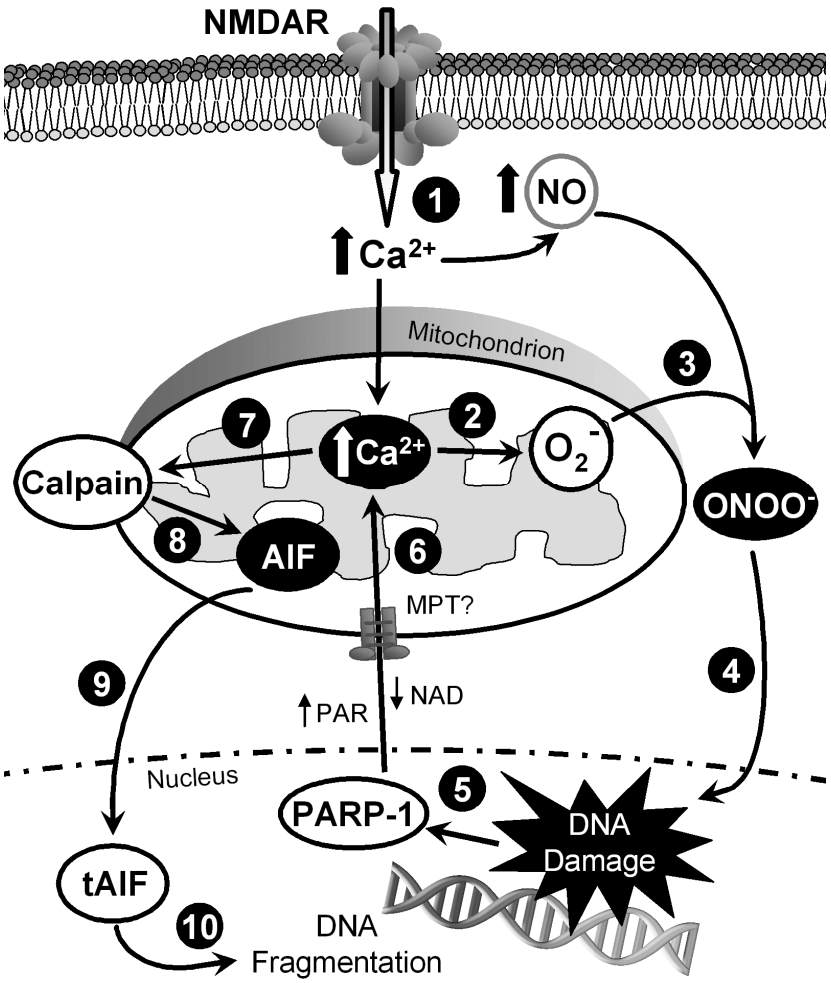

Figure 2.7 Model of PARP-1 and calpain-mediated AIF release. Excitotoxic activation of NMDA receptors result in **1)** massive influx of Ca^{2+} and increased NO production. **2)** Uptake of Ca^{2+} by mitochondria leads to increased O_2^- production that **3)** reacts with NO to form $ONOO^-$. **4)** Production of $ONOO^-$ causes DNA damage, **5)** activating PARP-1. **6)** PARP-1 activation, either by increased PAR polymer formation or decreased NAD cause further mitochondrial Ca^{2+} dysregulation, potentially *via* the MPT. **7)** Further Ca^{2+} dysregulation activates mitochondrial calpain, which **8)** truncates AIF. **9)** Truncated AIF translocates to the nucleus where it causes **10)** DNA fragmentation and neuronal death. *AIF*, apoptosis-inducing factor; *MPT*, mitochondrial permeability transition pore; *NAD*, nicotinamide adenine dinucleotide; *O_2^-*, superoxide radical; *PARP-1*, poly(ADP-ribose) polymerase-1; *$ONOO^-$*; peroxynitrite.

3.0 CRITICAL ROLE FOR EUKARYOTIC TRANSLATION INITIATION FACTOR 4G DEGRADATION IN MEDIATING ISCHEMIA-INDUCED NEURONAL DEATH

3.1 INTRODUCTION

Protein synthesis is a complex and highly regulated process essential for normal growth, development and maintenance of cells. Various cellular stressors including viral infection, nutrient deprivation, heat shock and endoplasmic reticulum (ER) stress uniformly inhibit protein synthesis (Kaufman, 1999; Sonenberg et al., 2000; Anderson and Kedersha, 2002). The degree and nature of the stress is important regarding eventual recovery of protein synthesis. A sublethal insult such as hypoglycemia will initially inhibit protein synthesis, but translation will return upon nutrient repletion (Kiessling et al., 1984). In contrast, inhibition of protein synthesis is unrelenting due to infection or other stimuli that induce programmed cell death (Thilmann et al., 1986; Morley et al., 1998; Gil and Esteban, 2000; Hata et al., 2000b).

Programmed death stimuli are repeatedly shown to inhibit protein synthesis [for review see references (Clemens et al., 2000; Morley et al., 2005)]. Likewise, agents that inhibit protein synthesis are known to induce programmed cell death in various cell types (Cotter et al., 1990;

Martin et al., 1990; Bushell et al., 2000). However, a mechanism directly associating protein synthesis inhibition with cell death has not been identified. The relationship between persistent protein synthesis inhibition and programmed cell death is robustly exemplified by neurons following an ischemic insult, and it provides a useful model to study the interaction between PSI and programmed cell death.

Protein synthesis inhibition (PSI) occurs in all ischemia-affected neurons due to global ischemia (Kleihues and Hossmann, 1971, 1973; Cooper et al., 1977; Morimoto et al., 1978; Dienel et al., 1980; Morimoto and Yanagihara, 1981; Nowak et al., 1985; Bodsch et al., 1986; Thilmann et al., 1986; Xie et al., 1988; Araki et al., 1990). In contrast to the rapid restoration of energy metabolism (Hossmann and Zimmermann, 1974; Kleihues et al., 1975), protein synthesis is slower to recover and even fails to recover in ischemia-susceptible brain regions (Dienel et al., 1980; Bodsch et al., 1986; Thilmann et al., 1986; Araki et al., 1990). This is also poignantly demonstrated in focal ischemia models as the brain regions where protein synthesis is inhibited following 1h of ischemia predict the eventual infarct area at 3 days (Hata et al., 2000b).

Ischemia (Cooper et al., 1977), as well as other programmed cell death stimuli (Morley et al., 1998; Zhou et al., 1998), cause polysome disassociation, indicating inhibition of translation initiation. Examination of the levels and phosphorylation states of a number of critical translation initiation factors following cerebral ischemia collectively suggest that only levels of the scaffolding protein responsible for delivering the mRNA to the ribosome for translation, eukaryotic initiation factor (eIF) 4G, are correlated with persistent PSI (DeGracia et al., 1996; Neumar et al., 1998; Martin de la Vega et al., 2001; Mengesdorf et al., 2002; Garcia et al., 2004b). Excitotoxicity caused by ischemia and other neurodegenerative diseases is known to result in NMDA-induced calcium influx into neurons, resulting in activation of the protease

calpain [for review see (Vosler et al., 2008)]. Calpain is known to degrade eIF4G *in vitro* (Wyckoff et al., 1990), and it has been implicated in ischemia-induced decreases in eIF4G (Neumar et al., 1998; Martin de la Vega et al., 2001).

The purpose of the present study is to determine the underlying mechanisms mediating persistent PSI and to determine if PSI is directly related to neuronal death instigated by an *in vitro* ischemia model, oxygen glucose deprivation (OGD). We hypothesize that persistent PSI following *in vitro* ischemia is caused by calpain-mediated degradation of eIF4G. Our results indicate that eIF4G is degraded following *in vitro* ischemia in a calpain-dependent manner. Moreover, maintenance of critical levels of eIF4G, either by calpain inhibition or eIF4G overexpression, resulted in both protein synthesis-dependent and -independent neuroprotection.

3.2 METHODS

3.2.1 Primary neuronal culture and oxygen-glucose deprivation

Rat primary cortical neuronal cultures were derived from E18 embryos of pregnant Sprague Dawley rats. Cortical neurons were dissociated, suspended in Neurobasal medium supplemented with B27 and plated in 6-well dishes at 2×10^5 cells/cm^2 for immunoblotting and activity assays, 1.6×10^5 cells/cm^2 for cell death assays and protein synthesis assays and 8×10^4 cells/cm^2 for immunocytochemistry. Experiments were performed on DIV 11-12 to ensure development of a mature neuronal phenotype with expression of glutamate receptors (Mattson et al., 1993) and

where cultures consisted of >97% neurons determined by neuron and glial-specific immunocytochemistry (Cao et al., 2001).

Oxygen glucose deprivation (OGD) was used as an *in vitro* model of ischemia. Briefly, maintenance media was replaced with media lacking glucose and other components known to be substrates for glycolysis, culture dishes were placed in an airtight chamber (Billups-Rothenberg, Del Mar, CA) and flushed with 100% argon gas for 3 minutes, and neurons were incubated at 37°C for 0.5, 1.0 or 1.5h. Following OGD, media was replaced and incubated (reperfused) for times indicated (media was not replaced for the "0" time point). Control cultures had their media changed with maintenance media with the same frequency as OGD-treated cultures and were incubated at 37°C in humidified 95% air and 5% CO_2 for equivalent periods.

3.2.2 AlamarBlue, LDH and Hoechst staining

Neuronal viability was assessed by measuring fluorescence of AlamarBlue (Accumed International). AlamarBlue is a blue non-fluorescent dye that fluoresces red when reduced by cellular metabolic activity. The amount of fluorescence is proportional to the number of viable cells (White et al., 1996). Media was replaced with media containing AlamarBlue reagent diluted at 1:30 in Neurobasal media without B27 supplement. Neurons were incubated at 37°C in humidified 95% air and 5% CO_2 for 30 minutes. Fluorescence was read with a Millipore CytoFluor 2300 automated plate-reading fluorometer set at excitation of 530nm and emission at 590nm.

Lactate dehydrogenase (LDH) release is an indicator of cell membrane integrity and correlates with the number of dead cells induced by excitotoxic stimulus (Koh and Choi, 1987).

Aliquots of 100µl were taken from culture wells and were added to 150µl of LDH reagent (Sigma-Aldrich). Absorbance of the reaction was measured at 340nm over a period of 5 minutes. The slope of the absorbance versus time correlates with the amount of cell death.

Nuclear staining with Hoechst 33258 was used to confirm the results of the AlamarBlue and LDH assays. Neurons were fixed with 4% paraformaldehyde for 10 minutes, washed 6 times with PBS, stained with Hoechst for 15 minutes, and washed three more times in PBS (Cao et al., 2003). Cells with normal and condensed nuclei were counted and considered viabile and non-viable, respectively. At least 3000 cells were counted under each condition (three fields per condition, four to six wells per condition, and three independent experiments). Results are presented as the percentage of viable cells relative to experimental control.

3.2.3 Protein Synthesis Assay

Media was replaced with Methionine-free media (Invitrogen) supplemented with 10µCi ^{35}S-methionine (MP Biomedicals) and incubated at 37°C for 15 minutes. This incubation time assured assessment of protein synthesis initiation without appreciable protein degradation. Pulse-labeling was stopped by washing in ice-cold PBS three times. Neurons were lysed in 1M NaOH/2% H_2O_2 and incubated at 37°C for 10 minutes. Lysates were precipitated with 20% TCA and were incubated on ice for 30 minutes. Aliquots were taken from precipitated samples to measure protein content. Pellets were then collected by vacuum filtration on Whatman GF/A glass fiber filters, washed three times with 1ml 5% TCA and once with 1ml acetone, and allowed

to dry. Incorporation of ^{35}S-methionine was measured by scintillation counting. Fold-incorporation over μg protein was calculated, and all data was expressed as a mean percentage of control ± SD.

3.2.4 Caspase and calpain activity assays

Caspase and Calpain activity assays were performed as previously described (Chu et al., 2005; Cao et al., 2007). Briefly, neurons were collected from 6-well plates, centrifuged and lysed by adding 0.15 mL lysis buffer (Cell Signaling). The samples were sonicated and then centrifuged 16 000 *g* for 10 min at 4°C. After centrifugation, protein concentrations of the supernatants were determined using the Bio-Rad Protein Assay Kit (Bio-Rad, Hercules, CA, USA). Samples containing 100 μg protein were mixed with 20 μM of the fluorogenic substrate Acetyl-Asp-Glu-Val-Asp-7-amido-4-trifluoromethyl-coumarin (Chemicon International, Temecula, CA, USA), followed by a 2-h incubation at 37°C. The changes in fluorescence were quantified every 20 min using a luminescence spectrometer (Winlab; Perkin Elmer, Shelton, CT, USA) (excitation 400 nm, emission 505 nm). Results are presented as percentage fluorescence of experimental groups relative to control.

Calpain activity assay was performed as previously described (Cao et al., 2007), and neurons were collected as described in the caspase activity assay. In brief, 100μg of protein were incubated with calpain reaction buffer [20mMHEPES,pH7.6, 1mM EDTA, 50mM NaCl, and 0.1% (v/v) 2-mercaptoethanol] containing 10 μM calpain I fluorescent substrate H-E(EDANS)PLF_AERK(DABCYL)-OH (Calbiochem, La Jolla, CA). The reaction was initiated

by addition of $CaCl_2$ to a final concentration of 5μM and incubated at 37°C for 30 min. The activity of calpain was measured by detecting the increase in fluorescence using excitation/ emission wavelengths of 335/500 nm. Calpain activity as measured by relative fluorescence was presented as percentage fluorescence of experimental groups relative to control.

3.2.5 Western blot analysis

Western blot was performed by gel electrophoresis of cell lysates on SDS-PAGE gels, and detected using enhanced chemiluminescence reagents (GE Healthcare). The following antibodies were used: goat polyclonal antibodies against eIF4G N-terminus (N20) and C-terminus (D-20) (1:400), eIF4A (1:400) and β-actin (1:10,000), purchased from Santa Cruz Biotechnology; rabbit polyclonal antibodies against PABP (1:1000), eIF4B (1:1000), $p70^{S6\ kinase}$ (1:1000), eIF2α (1:1000), S6 (1:1000), 4E (1:1000), 4EBP (1:1000), rabbit monoclonal antibodies for $P\text{-}p70^{S6\ kinase}$ (1:1000) and P-eIF2α (1:1000), and a mouse monoclonal antibody against HA (1:1000), purchased from Cell Signaling; and a rabbit polyclonal antibody for eIF3 (p110) 1:15,000 purchased from Bethyl Laboratories.

3.2.6 Immunocytochemistry

Triple-label staining was performed to examine co-localization of HA tag with the neuronal marker MAP2, along with Hoechst stain in transfected primary neurons. Twenty four hours after OGD neurons were assessed by AlamarBlue and LDH assays, then fixed with 4% paraformaldehyde for 10 min. Cells were washed 6 times with PBS and then blocked for 1h at

4°C in 2% BSA with 0.5% TritonX-100 for cell permeabilization. The cells were incubated overnight at 4°C with rabbit anti-MAP2 antibody (1:1000) (Santa Cruz Biotechnology) and mouse anti-HA (1:1000) (Cell Signaling) diluted in blocking solution. After incubation, cells were washed 6 times and incubated for 1h at 4°C with Alex488-conjugated goat anti-rabbit antibody and Cy3-conjugated rabbit anti-mouse antibody (Jackson ImmunoResearch Inc., West Grove, PA, USA) diluted 1 : 2000. After another three consecutive washes with PBS, cells were stained with Hoechst 33258 to visualize changes in nuclear morphology. Finally, cells were observed and imaged with an inverted fluorescent microscope with a CCD camera. Digital images were captured with the Metavue program (MDS Analytical Technologies).

3.2.7 Recombinant protein preparation

Recombinant myc-tagged eIF4G was a kind gift from Dr. Simon Morley (Sussex University, UK) and the preparation has been described previously (Bushell et al., 2000). The truncated C-terminal His-tagged recombinant eIF4G proteins amino acids 179-675 and 676-1129 were provided by Dr. Nahum Sonenberg (McGill University, Montreal, Canada).

3.2.8 Cell-free proteolytic cleavage of eIF4G by calpain

The cell-free calpain cleavage assay was conducted as previously described (Ghosh et al., 2005; Joy et al., 2006). Briefly, recombinant μ-calpain (Calbiochem, CA) was incubated with either full length or truncated forms of eIF4G in a calpain assay buffer (25mM Tris-HCl, pH 7.3 and 150mM NaCl). Calcium at a concentration of 1mM was added as indicated in the experiments.

Incubation of calpain with eIF4G occurred either in the absence or presence equal molar concentrations of calpastatin or 10μM ALLN. Reactions were incubated for the given times at at 25°C and were stopped by addition of 10mM EDTA. The calpain-treated samples were resolved on SDS-PAGE. The gels were stained with Coomassie blue, and bands were excised for MALDI-TOF mass spectrometry. In other experiments, the gels were transferred to PVDF membranes and probed for the indicated antibodies.

3.2.9 Construction of viral vectors

The HA-eIF4G plasmid was generated as previously described (Imataka et al., 1997; Gradi et al., 1998). Lentiviral vectors overexpressing human full-length HA-eIF4G were constructed by inserting the HA-eIF4G into the FUW transfer vector, which is under control of the ubiquitin promoter. A control vector with the EGFP open reading frame was also constructed and inserted into the FUW transfer vector. The constructed transfer vectors were transformed into JM109 cells (Promega) and isolated using the EndoFree Plasmid Maxi Kit (Qiagen). Large scale production of virus were performed as previously described (Ramezani and Hawley, 2002), with minor modifications. A mixture of plasmids containing 675μg FUW transfer vectors, 435μg pCMVΔR8.9 (packaging construct) and 237μg pVSVG (envelope plasmid) were added to 24ml Opti-MEM (Invitrogen). Lipofectamine 2000 (Invitrogen) solution (900μl in 24ml Opti-MEM) was also prepared, and the plasmid mixture and Lipofectamine 2000 solution were added and incubated at room temperature for 20 minutes. Six ml of plasmid-Lipofectamine solution were added to 15cm plates with 70% confluent monolayer of HEK293T cells. Cells were incubated for 4 hours and media was replaced with fresh culture media. The supernatant was collected 72h

after transfection, filtered through a 0.45μm filter flask, and centrifuged at 21,000 rpm for 1.5h using the SW28 rotor (Beckman Coulter). Further purification of viruses was performed using sucrose gradient ultracentrifugation. The pellet was suspended in 3ml Opti-MEM, loaded on top of 3ml 20% sucrose solution and centrifuged at 22,000rpm for 1.5h using the SW50.1 rotor (Beckman Coulter). The pellet was then resuspended in 200μl Opti-MEM, aliquoted and stored at -70°C.

3.2.10 Gene transfection of calpastatin and viral vectors into primary neurons

Generation of the calpastatin plasmid with the C-terminal 3HA tag in the pcDNA3.1 vector has been described previously (Cao et al., 2007). Transfection of calpastatin was achieved using Nucleofection (Amaxa, Gaithersburgh, MD) according to manufacturer's protocol. The calpastatin plasmid or GFP control plasmid (Amaxa) were transfected immediately prior to plating. Following the rat neuron Nucleofector kit protocol 4 x 10^6 cells were transfected with each reaction. Neurons were then plated at the densities described above. Neurons were allowed to mature to DIV 11 and then transfection efficiency was assessed by immunocytochemistry and Western blot probing for the HA tag.

Biological titer was determined for each batch of lentivirus made. A range of virus volume (1-20μl) was added to individual wells on 24-well plates and incubated for 72h. Transfection efficiency was assessed by immunocytochemistry by probing for the HA tag. Following immunocytochemical detection, virus volume was scaled proportionally to infect the

cells of a 6 well plate, and transfection was assessed by Western blot. For eIF4G overexpression experiments, neurons were infected for 72h with lentivirus. Experiments were then performed on DIV 11.

3.2.11 Lentiviral-shRNA infection

Lentiviral vectors carrying shRNA directed against rat eIF4G and a scrambled control shRNA sequence were purchased from Santa Cruz biotechnology. Virus was stored in aliquots at 5 x 10^3 infections units of virus per µl. Biological titer was performed to determine efficient knock down in primary neurons as assessed by Western blot at indicated incubation times. For neuronal viability and protein synthesis measurements, neurons were transfected with 1.5µl virus per well 72h for before being subjected to OGD. One day after OGD, viability and protein synthesis assays were performed.

3.2.12 Luciferase vectors, in vitro transcription, mRNA transfection and luciferase assays

The β-globin, HCV, EMCV and VEGF reporter plasmids were prepared by cloning various 5'UTRs into pSVN luciferase vector as previously described (Dobrikova et al., 2006; Bradrick et al., 2007). The c-myc and inverse c-myc reporter plasmids had their 5'UTRs cloned into the pUC19 backbone (NEB), also as previously described (Kaiser et al., 2008). Basically, the cloning cassettes consisted of the *Renilla* luciferase ORF and a 50-mer poly(A) tail, and the T7 promoter was inserted in to the various 5'UTRs' promoters.

For *in vitro* transcription, the reporter plasmids were linearlized (β-globin with BamHI; HCV, EMCV and VEGF with ClaI; and c-myc and inverse c-myc with SalI) and transcribed with T7 RNA polymerase (Ambion) to produce mRNAs. Reactions were performed in the presence of either the 7-methyl-guanosine cap (7mG) or the cap analog G(ppp)A to create capped and uncapped mRNA. Enzymatic clean up was performed using an RNeasy kit (Qiagen), mRNA concentration was determined, and each mRNA was inspected on agarose gel to determine correct size and possible degradation.

Transfection of primary neurons was performed using 20µl DMRIE-C reagent (Invitrogen) per well on 24-well plates. A blank control with no transfection reagent and a well with DMRIE-C reagent only (no mRNA) were used for each experimental condition. Immediately prior to transfection, DMRIE-C reagent was mixed with culture media and 1µg mRNA. Culture media was aspirated from neurons and media containing transfection mix was added. Neurons were incubated at 37°C for 2 hours.

Following incubation, neurons were lysed with 100µl *Rluc* assay buffer (Promega) and *Rluc* activity was measured according to manufacturer's protocol (Promega) on a LMaxII luminometer (Molecular Devices). A minimum of three independent experiments were carried out for each mRNA. Background luminescence was determined for each experimental time point by subtracting the reading of the blank well from the DMRIE-C-only well and each mRNA-transfected well. Data are presented as the fold increase in relative light units (RLU) over the DMRIE-C only well.

3.2.13 Statistical Analysis

All results are expressed as mean ± SD from at least three independent experiments. Multiple-group comparisons were performed using ANOVA with *post hoc* Fisher PLSD correction testing, and $p < 0.05$ was accepted as statistically significant.

3.3 RESULTS

3.3.1 Ischemia-severity correlates PSI with neuronal viability

We initially sought to establish our primary neuronal culture system coupled with oxygen glucose deprivation (OGD) as a viable model of the persistent PSI observed following *in vivo* ischemia. To accomplish this we needed to model both ischemia-sensitive and –resistant areas of the brain; accordingly, we established both sublethal and lethal durations of OGD. Sublethal, moderately and severely lethal OGD durations were established by measuring cell viability using AlamarBlue reduction assay, measuring necrosis using LDH release and measuring nuclear morphology (a measure of programmed cell death) at 0.5, 1 and 1.5h, respectively. Sublethal OGD did not result in significant amounts of neuronal death as determined by any of the aforementioned assays. However, OGD exposure times of 1.0h and 1.5h decreased viability by 50% and 90% respectively (**Figure 3.1A, C and D**), with corresponding increases in LDH release (**Figure 3.1B**). Sublethal OGD resulted in an initial inhibition of protein synthesis followed by a progressive recovery to control levels by 24h reperfusion (**Figure 3.1E**). Lethal

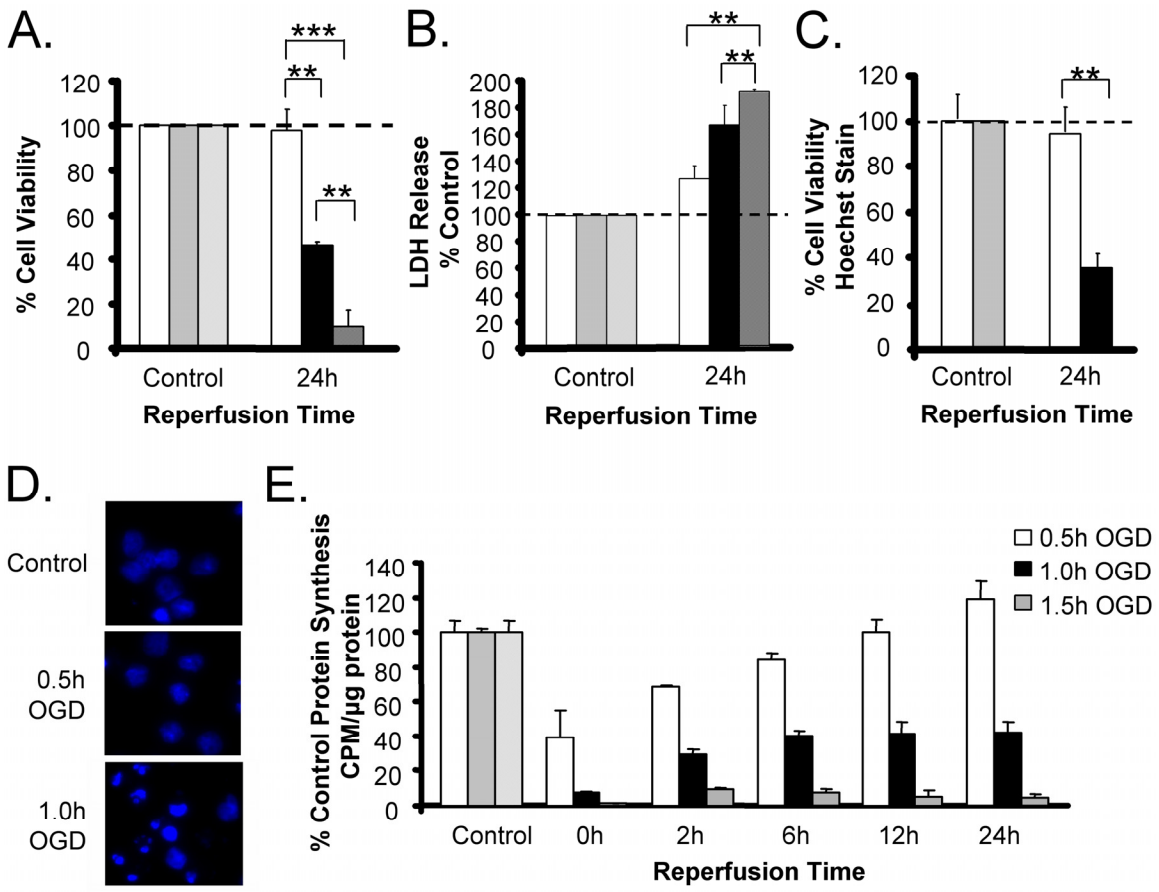

Figure 3.1 Protein synthesis inhibition correlates with cell death. A, Cell viability was determined with the AlamarBlue reduction assay, **B,** LDH assay, and **C,** by Hoechst staining. **D,** Representative images of control neurons and neurons subjected to 0.5 and 1h of OGD stained with Hoechst. Note the condensed nuclei in the 1h OGD neurons. **E,** Protein synthesis was measured by incorporation of ^{35}S-methionine into nascent peptides (relative to total protein content of each well) following various OGD durations at indicated reperfusion times. Bars represent mean ± SD values of n = 3-4 independent experiments. ANOVA with Fisher PLSD was conducted to determine statistical significance: **p<0.01, ***p<0.001.

levels of OGD caused a similar initial inhibition of protein synthesis but with recovery to 45% and 10% control translation for 1h and 1.5h OGD, respectively. The levels of protein synthesis recovered by 24h reperfusion showed a positive correlation with the amount of cell viability as measured by the Alamar Blue reduction assay and Hoechst staining and necrosis measured by LDH release.

3.3.2 Levels of eIF4G correlate with persistent PSI

Continuing to validate our model, we compared the changes in the initiation factor levels and phosphorylation states induced by *in vitro* ischemia to the results of the *in vivo* literature. As seen *in vivo* (DeGracia et al., 1996; Garcia et al., 2004b; Martin de la Vega et al., 2001; Mengesdorf et al., 2002) , there were no changes in most of the major regulatory initiation factors following 1h OGD (**Figure 3.2A and D**). Lethal but not sublethal OGD, however, resulted in the progressive decrease of eIF4G from 2h to 24h reperfusion (**Figure 3.2B and D**). Notably, the decreases in the levels of eIF4G strongly correlate with decreased neuronal viability and persistent PSI presented in **Figure 3.1**. This initial evidence supports our hypothesis that loss of baseline levels of eIF4G could be responsible for persistent PSI following ischemia, and ultimately cell death. Of note, total levels of 4EBP did decrease at 6-12h, but since it is a negative regulator of translation, lower levels of this protein are not expected to contribute to PSI.

Phosphorylation of eIF2α is a known mechanism to inhibit translation by blocking delivery of the tRNA to the ribosome (Kimball, 2001). Transient increases in the phosphorylation of eIF2α with levels returning to baseline by 6 hours of reperfusion have been

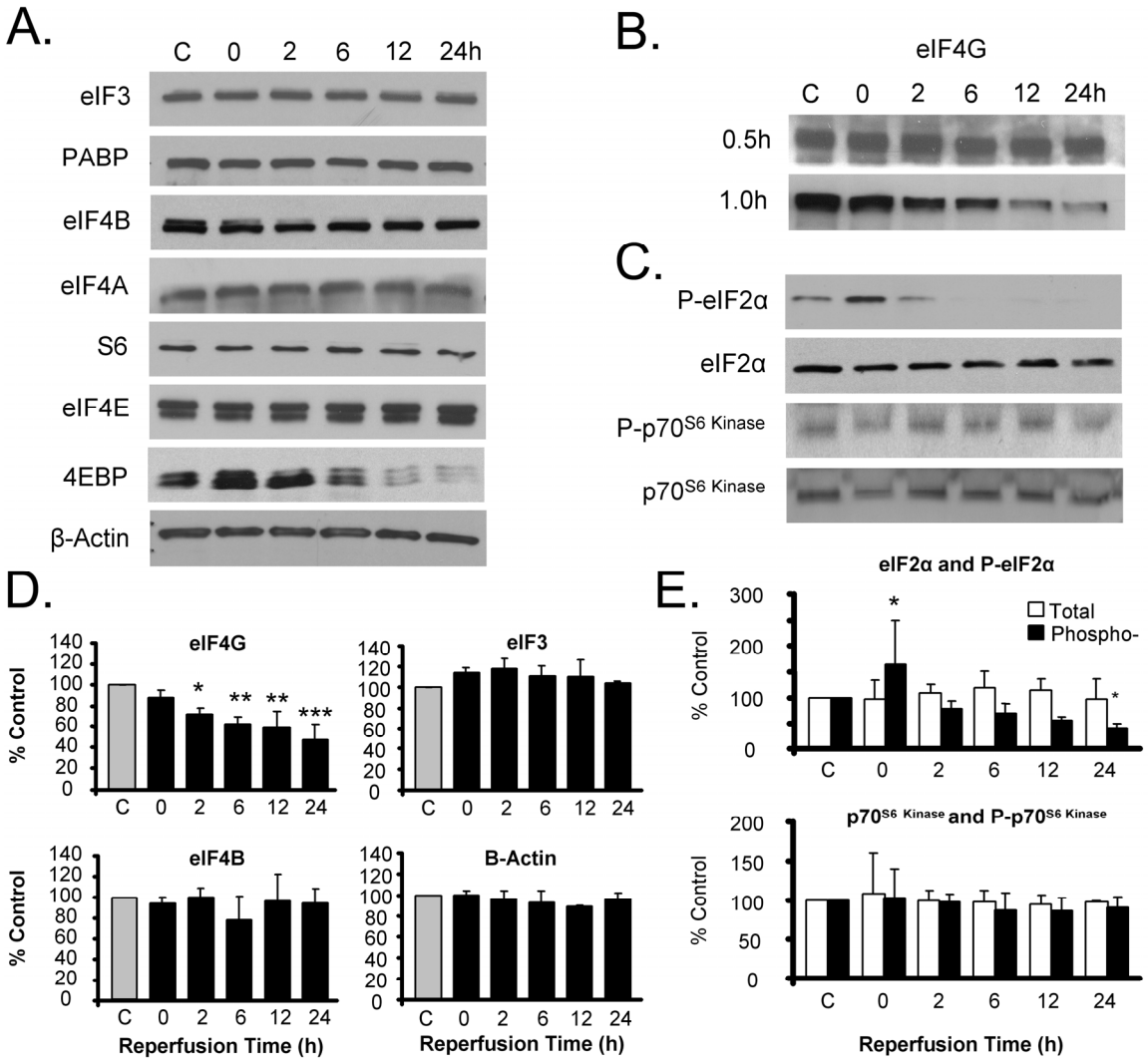

Figure 3.2 Decreased levels of eIF4G correlate with persistent PSI. A, Western analysis of various translation initiation factors after 1.0h OGD at indicated reperfusion time. Note there were no changes in initiation factor levels that would be associated with inhibition of translation at any reperfusion time. **B,** Levels of eIF4G following sublethal OGD did not result in decreases in eIF4G levels while lethal OGD of 1.0h showed a progressive decrease starting at 2h reperfusion. **C,** Western blot images of the total and phosphorylated levels of two major translation initiation regulators following OGD. **D,** Relative optical density was measured and compared to control values for indicated initiation factors and β-actin loading control after 1h OGD. **E,** Levels of total and phospho proteins were compared following 1.0h OGD. Bars represent mean ± SD of n = 4-6 independent experiments. ANOVA with Fisher PLSD determined statistical significance: *p<0.05, **,p<0.01, ***p<0.001. Abbreviations: 4EBP, 4E binding protein; PABP, poly(A) binding protein; S6, small ribosomal subunit 6 protein.

repeatedly observed following *in vivo* ischemia (DeGracia et al., 1996; DeGracia et al., 1997; Althausen et al., 2001; Kumar et al., 2001; Martin de la Vega et al., 2001; Mengesdorf et al., 2002; Garcia et al., 2004b; Owen et al., 2005). Following OGD the levels of phosphorylated eIF2α mimicked that seen *in vivo* as there was 2-fold increase in phosphorylation followed by a rapid return to baseline by 2h reperfusion (Figure 3.2C and E). The level and phosphorylation state of $p70^{S6\ kinase}$, the regulator of 5'TOP mRNA and a indicator of global protein synthesis (Fumagall and Thomas, 2000), was not significantly altered during *in vitro* ischemia or reperfusion Figure 3.2C and E). This also corresponds to the status of $p70^{S6\ kinase}$ in ischemia-sensitive brain regions (Martin de la Vega et al., 2001). This data provides evidence that validates our *in vitro* model as an adequate representation of *in vivo* ischemia. Furthermore, the onset and duration of eIF2α phosphorylation indicates that it is probably mediating the initiation of PSI but it is not involved with persistent PSI.

3.3.3 Calpain is activated following *in vitro* ischemia

Neuronal cell death following OGD has been linked to both caspase and calpain-dependent mechanisms (Newcomb-Fernandez et al., 2001; Cho et al., 2004; Malagelada et al., 2005), and eIF4G has been shown to be both a substrate of caspase-3 (Clemens et al., 1998; Marissen and Lloyd, 1998; Bushell et al., 1999; Bushell et al., 2000) and calpain (Wycoff et al., 1990; Neumar et al., 1998). Therefore, we attempted to determine if these proteases are involved with the decreases in eIF4G following *in vitro* ischemia.

We first evaluated the cleavage products of the caspase-3 and calpain substrate α-spectrin following OGD. Both proteases cleave the 240kDa protein into a 150kDa fragment, but calpain

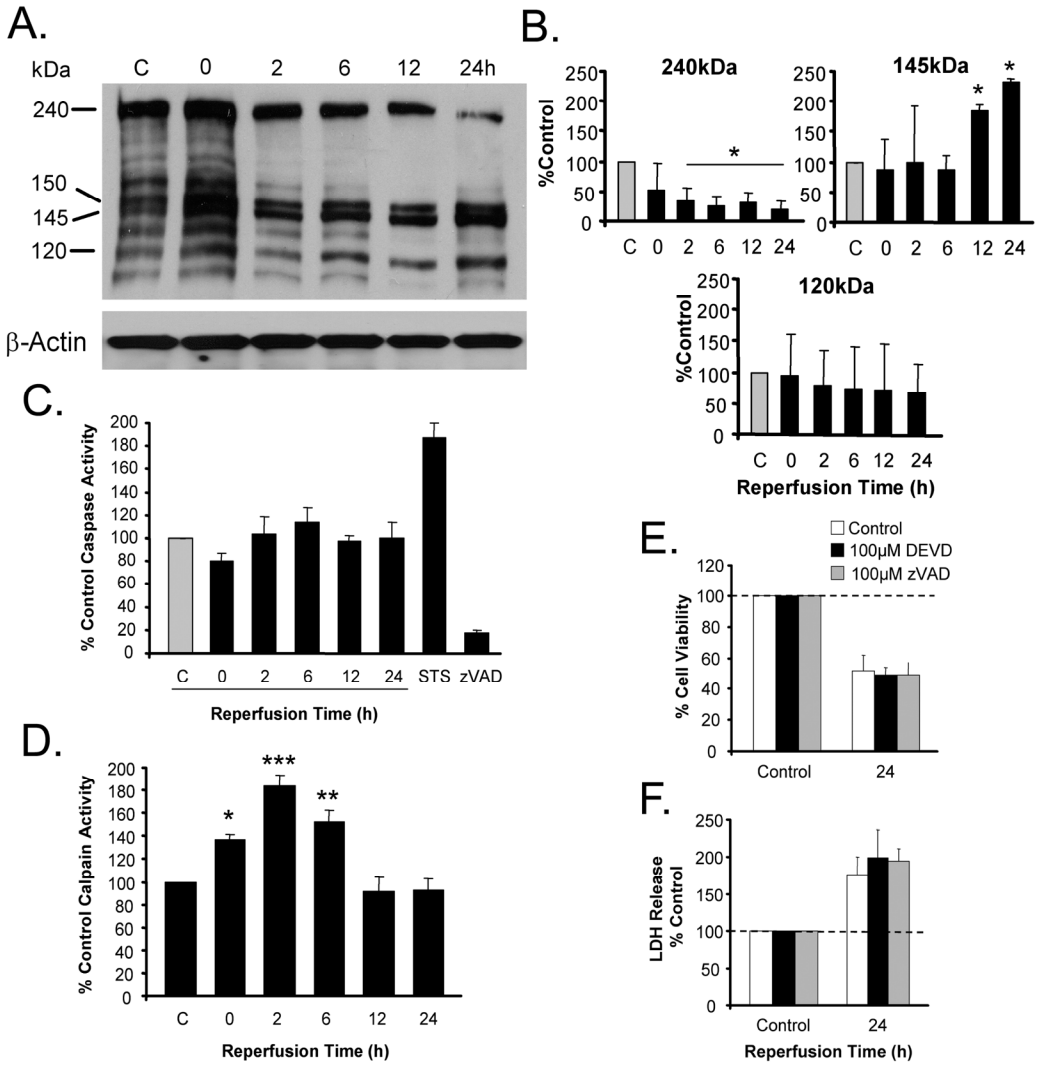

Figure 3.3: Evaluation of caspase and calpain activation following OGD. A, Primary neurons were subjected to 1h OGD, lysates were taken at the indicated reperfusion times, and Western blot was performed using an antibody directed against α-spectrin. Immunoblots show increased calpain-generated α-spectrin fragments (145kDa) but not caspase-generated fragments (120kDa). **B,** Relative optical density of α-spectrin fragments following OGD and reperfusion. **C,** Caspase activity assay was performed as described in the methods section. Neuorns were also treated with 200nM staurospaurine (STS) as a positive control or 200nM STS and 100μM of the caspase inhibitor zVAD as a negative control for 1h. **D,** Calpain activity assay revealed increased calpain activity immediately after OGD. **E and F,** Primary neurons were treated with the indicated concentrations of the caspase inhibitors for 1h prior to OGD and throughout 1h OGD and reperfusion. Cell viability (Alamar Blue), **E**, and necrosis (LDH), **F**, were assessed at 24h reperfusion. Inhibitor concentration was optimized to allow highest concentration without causing cell death. Bars represent mean ± SD of n = 3-4 independent experiments. ANOVA with Fisher PLSD determined statistical significance: *p<0.05, **,p<0.01, ***p<0.001.

further cleaves it into a 145kDa fragment while caspase-3 produces a 120kDa fragment. Following OGD there is a decrease in the full length protein. This corresponded to an increase in the appearance of the calpain-induced 145kDa fragment, while there is no change in the caspase-induced 120kDa fragment (**Figure 3.3A and B**). This suggests that calpain rather than caspase is activated in our model. These results were confirmed with caspase and calpain activity assays. Caspase activity did not increase above control following OGD. In contrast, calpain activity was increased immediately after OGD and continued for 6h of reperfusion (**Figure 3.3C and D**).

To further confirm that caspases were not involved with the neurotoxicity seen in our model, we examined the effect of caspase inhibition on neuronal viability and necrosis. Inhibition of caspases using the effector caspase specific inhibitor DEVD or the pan caspase inhibitor zVAD failed to provide neuroprotection (**Figure 3.3E and F**). This is in agreement with previous studies of ODG in mixed glial and neuronal cultures (Newcomb-Fernandez et al., 2001).

3.3.4 Calpain inhibition blocks eIF4G cleavage

Based on these findings we examined the role of calpain on cell viability, protein synthesis and eIF4G levels after OGD by inhibiting calpain. Calpain inhibition was achieved by overexpression of calpastatin, the only known endogenous inhibitor of calpain (Pontremoli et al., 1992). Calpastatin was clearly overexpressed in these neurons as measured by immunoblot and with approximately 50% transfection efficiency measured by immunocytochemistry (**Figure 3.4A and B**). Examination of calpain activity revealed calpastatin overexpression reduced the appearance of the 145kDa band of α-spectrin and inhibited the decrease in full length α-spectrin.

Treatment with zVAD did not alter the α-spectrin cleavage profile following OGD (**Figure 3.4C**).

Analysis of protein synthesis following OGD in calpastatin and GFP-transfected neurons shows an initial inhibition of protein synthesis with increased recovery in the calpastatin-overexpressing neurons compared to time-matched GFP controls at 12 and 24h reperfusion (**Figure 3.4D**). The increase in protein synthesis was associated with increases in cell viability at 24h reperfusion (**Figure 3.4E and F**). Calpain inhibition did not significantly decreased LDH release in our model suggesting calpain is involved with programmed neuronal death in our model and not necrosis (data not shown) Overexpression of calpastatin, but not inhibition of caspases, resulted in significantly increased levels of eIF4G at 24h reperfusion compared to GFP transfected controls (**Figure 3.4G**). This provides further evidence that calpain is mediating eIF4G cleavage following OGD in primary neurons, and decreases in eIF4G potentially account for persistent PSI and, ultimately, neuronal death following ischemia.

3.3.5 eIF4G is a calpain substrate

Confirming that eIF4G is a substrate of calpain (Wyckoff et al., 1990; Neumar et al., 1998), we employed a cell free assay where we coupled recombinant eIF4G with recombinant calpain I (50:1 molar ratio of eIF4G: calpain) then activated calpain with 1mM calcium. Calpain I clearly cleaved eIF4G during the incubation. This is an unambiguous effect of calpain as the endogenous calpain inhibitor calpastatin and the pharmacological calpain specific inhibitor ALLN abrogated eIF4G cleavage (**Figure 3.5A**).

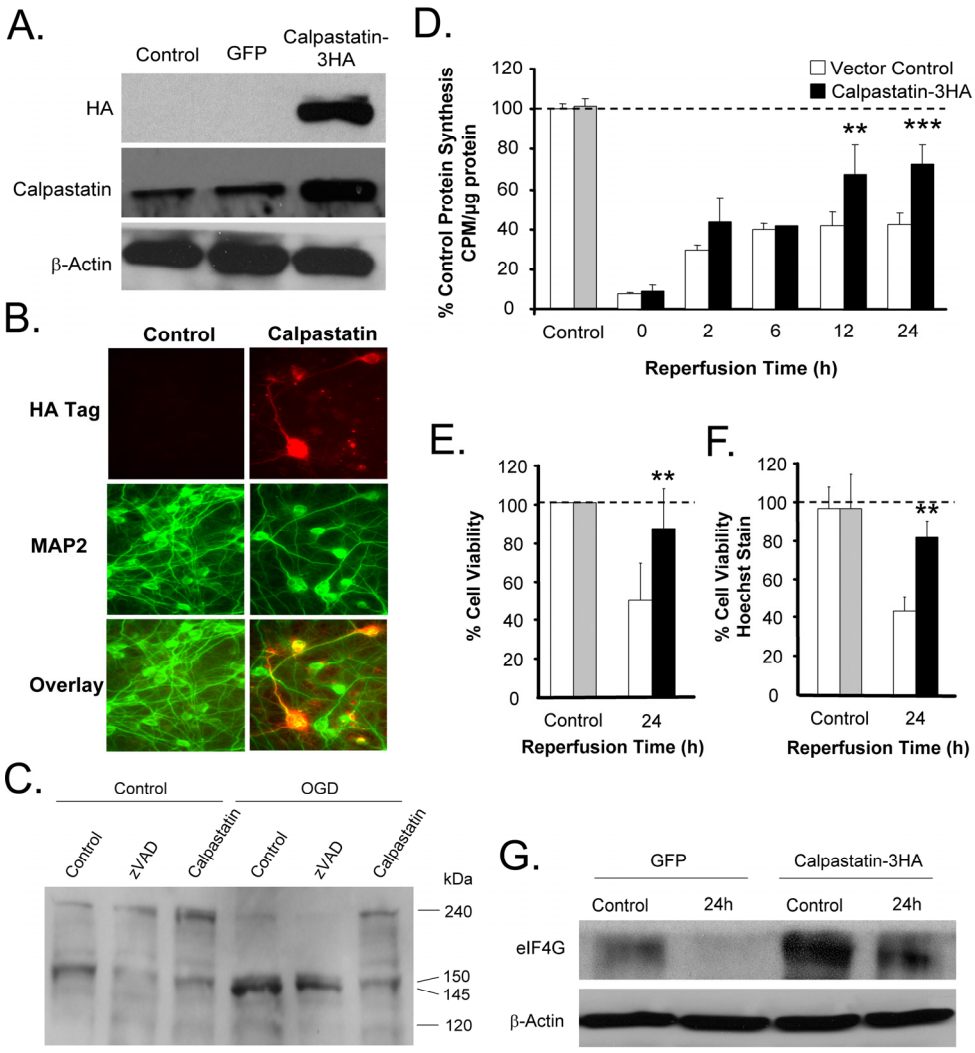

Figure 3.4 Calpain inhibition results in increased translation, cell viability and eIF4G levels following OGD. Rat primary cortical neurons were transfected with HA-tagged calpastatin. Transfection was confirmed by immunoblotting for HA, **A**, and efficiency was assessed by immunocytochemistry, **B**. **C,** Calpastatin overexpression was confirmed to inhibit calpain activity measured by α-spectrin cleavage. Neurons were either transfected with calpastatin or GFP plasmids, or treated with 100µM zVAD for 1h prior to and for 24h after 1h OGD. Overexpression of calpastatin blocked decreases in total α-spectrin and formation of the 145kDA calpain-mediated cleavage product. **D,** Protein synthesis was measured in calpastatin- and GFP transfected controls following 1h OGD for the indicated reperfusion times. Statistical significance represents calpastatin-overexpressing neurons compared to time-matched GFP controls. Cell viability was measured using Alamar Blue, **E**, and Hoechst staining**, F**, at 24h reperfusion. **G,** Calpastatin and GFP transfected neurons were exposed to 1.0h OGD and levels of eIF4G were observed at 24h reperfusion. Bars represent mean ± SD of n = 3-4 independent experiments. ANOVA with Fisher PLSD determined statistical significance: **,$p<0.01$, ***$p<0.001$.

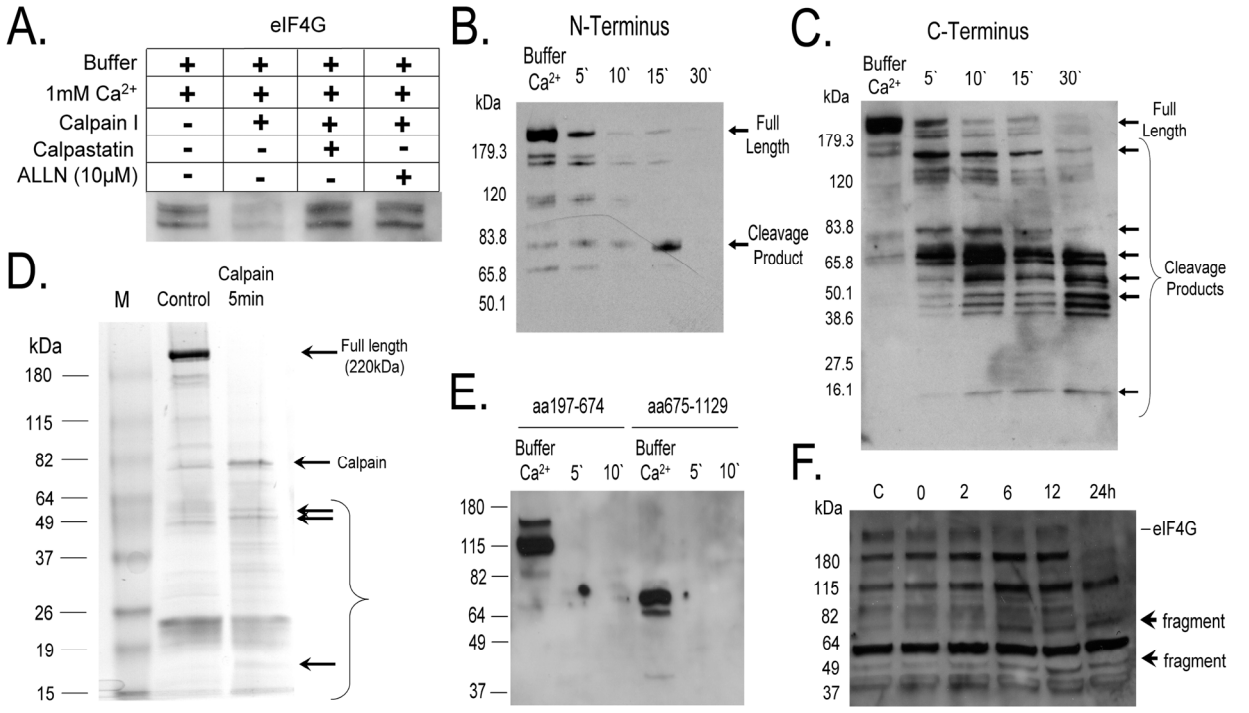

Figure 3.5 Calpain cleaves eIF4G in a cell-free assay. A, Recombinant eIF4G (400ng) was incubated with 10nM calpain I and activated by 1mM Ca^{2+} at 25°C for 1h in a calpain reaction buffer. The reaction was stopped by the addition of 10μM EDTA in an SDS loading buffer. The protein was then resolved on 4-15% gradient gels. Calpain was inhibited with both recombinant calpastatin and the pharmacological calpain inhibitor ALLN. Gels were probed with an N-terminal eIF4G antibody. **B and C**, Reactions were also incubated for the indicated times with the same amounts of recombinant eIF4G and calpain and probed for eIF4G using antibodies directed against the N-, **B**, or C-, **C**, terminus. The figures show potential cleavage bands of eIF4G produced by calpain I. **D**, Recombinant eIF4G (10μg) was incubated with Ca^{2+} (control) or Ca^{2+} and calpain for the indicated time. Coomassie-blue stained eIF4GI cleavage by calpain I was analyzed by mass spectrometry. The three cleavage products were positively identified as eIF4G and molecular weights confirmed at 60, 50 and 16kDa. **E,** Recombinant truncated eIF4G proteins (100ng) were assessed for susceptibility to calpain cleavage as above. Immuoblot probed for C-terminal His tag to visualize recombinant proteins. **F**, Western analysis of primary neuronal lysates at various reperfusion times following 1h OGD and probed with C-terminal eIF4G antibody. The fragments found in neuronal culture correspond to the fragments observed in the cell free assays.

We next examined the time course of eIF4G cleavage by calpain. Incubation of recombinant eIF4G with 10nM calpain for specified times resulted in progressive cleavage of eIF4G into size specific products as shown by probing for eIF4G N- and C-terminal directed antibodies (**Figure 3.5B and C**). Notably, 50 and 66kDa fragments were seen using the C-terminus antibody, which corroborates the findings in the neuronal cultures following OGD (**Figure 3.5F**) and in brain following focal ischemia (Mengesdorf et al., 2002).

In a further attempt to identify the cleavage sites of calpain on eIF4G, we used recombinant protein fragments of eIF4G. Recombinant calpain was also able to completely cleave eIF4G fragments consisting of amino acids 197 to 674 and 675 to 1129 (**Figure 3.5E**). Analysis of the cleavage products by mass spectrometry positively identified the bands as eIF4G and confirmed the molecular weights as 60, 50 and 16kDa (**Figure 3.5D**). Unfortunately, multiple attempts to identify the specific sequence targeted by calpain using Edman degradation have not yielded any results. Together, these results suggest that calpain does not recognize a discrete site on eIF4G, but progressively cleaves the protein to either modify or completely abolish its function.

3.3.6 Overexpression of eIF4G is neuroprotective

We next sought to determine if neuronal death following ischemia was directly related to maintenance of critical levels of eIF4G. To test this hypothesis we overexpressed eIF4GI in primary neurons using a lentiviral vector. The lentivirus expressing HA-eIF4GI under control of the constitutive ubiquitin promoter was able to efficiently overexpress (~75-90%) HA-eIF4G (**Figure 3.6A and B**). Overexpression of eIF4G did not affect the level of other initiation

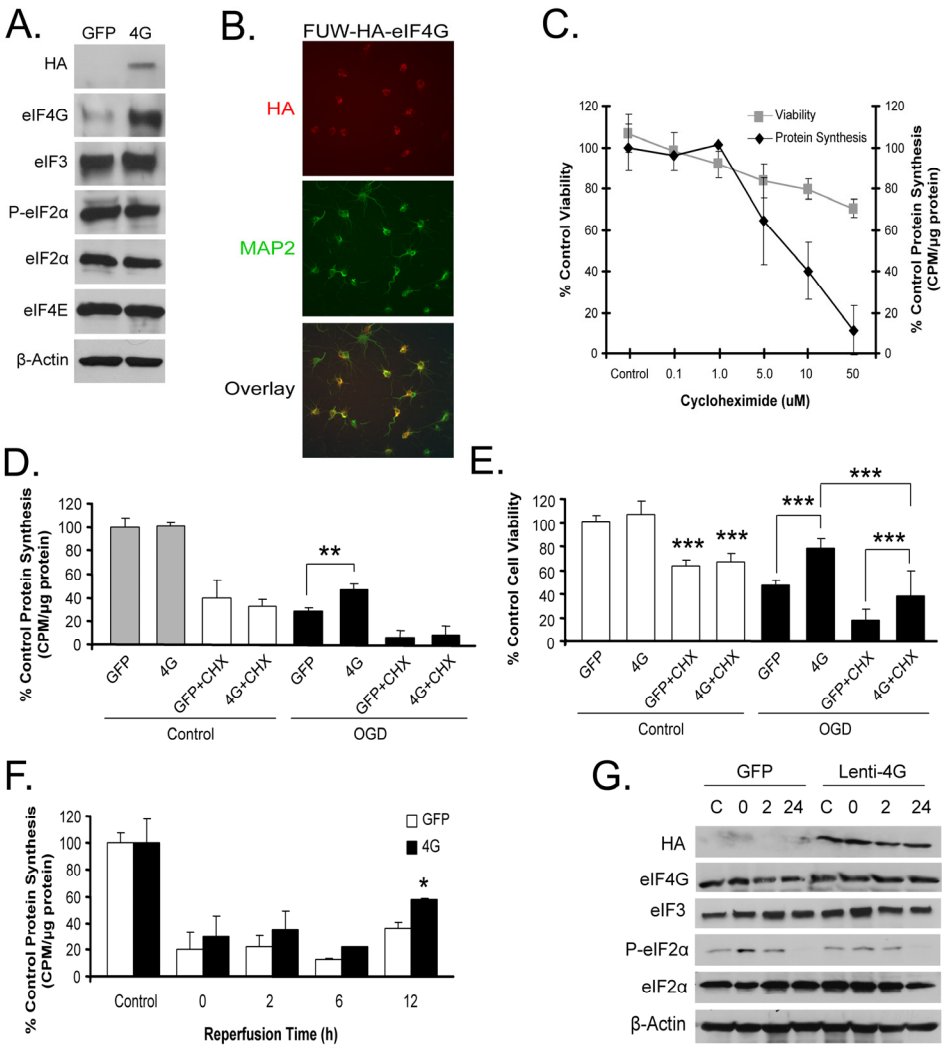

Figure 3.6 Neuroprotection by eIF4G is partially protein synthesis dependent. **A**, Lentiviral-mediated overexpression of eIF4GI under control of the ubuiquitin promoter (FUW) is shown by Western blot of neurons infected with GFP lentivirus and HA-eIF4GI lentivirus. **B**, Immunostaining for the HA tag was performed to assess transfection efficiency, and neuronal co-localization is demonstrated by costaining for MAP2. **C**, Concentration-response of neuronal viability, measured by AlamarBlue, and protein synthesis of neurons exposed to cycloheximide (CHX) for 24h. Note the decrease in viability when protein synthesis inhibition becomes more pronounced. **D and E**, Neurons transfected for 72h were exposed to either 50µM CHX, 1h OGD, or 1h OGD followed by 50µM CHX and protein synthesis (CPM/µg protein), **D**, and neuronal viability (AlamarBlue), **E**, was assessed in GFP- and eIF4G-transfected neurons at 24h. **F**, The effect of eIF4G overexpression on protein sythesis at the early reperfusion times of 0-12h was assessed. **G,** Western blot analysis showing the effect of transfection and 1h OGD on the expression of regulatory translation initiation factors at progressive reperfusion times. Bars represent mean ± SD of n = 3-4 independent experiments. ANOVA with Fisher PLSD determined statistical significance: * $p< 0.05$, **$p<0.01$, ***$p<0.001$.

factors, including the phosphorylation state of eIF2α (**Figure 3.6A**). Of note, we attempted to examine the role of cap-dependent protein synthesis on neuronal viability by constructing a lentiviral vector with a mutant eIF4GI (m4GI). This mutant lacked the cap binding protein (eIF4E) binding domain. Unfortunately we were not able to express the full length mutants in our neurons using our lentiviral expression system.

Overexpression of eIF4GI resulted in increased protein synthesis and neuronal viability 24h following 1h OGD compared to GFP control (**Figure 3.6D and E**, respectively). To determine if the neuroprotective effect of eIF4GI was directly due to protein synthesis, we blocked protein synthesis using cycloheximide (CHX). A concentration response curve of CHX application demonstrates that concentrations of CHX that substantially inhibit protein synthesis for 24h also result in evident neuronal death (**Figure 3.6C**). Protein synthesis was inhibited to 20% of untreated levels following 24h exposure of CHX in all groups under control conditions, and was nearly completely inhibited in all groups after OGD (**Figure 3.6C and D**).

Examination of neuronal viability revealed that concentrations of CHX that inhibited protein synthesis were also mildly, but significantly neurotoxic (**Figure 3.6C and E**). This observation corroborates previous findings in primary neurons (Furukawa et al., 1997). The importance of protein synthesis in maintenance of viability following *in vitro* ischemia was further substantiated as CHX treatment resulted in significantly decreased neuronal viability following OGD in both the GFP and eIF4G overexpressing conditions. Significantly reduced viability was also observed when comparing control CHX-treated cultures treated with CHX to OGD-and CHX-treated cultures (**Figure 3.6E**). Importantly, inhibition of protein synthesis with CHX only partially blocked the neuroprotective effect of eIF4G as eIF4G-overexpressing cultures that were simultaneously treated with CHX had increased viability compared to OGD-

and CHX-treated GFP neurons (**Figure 3.6E**). This suggests suggesting that eIF4G may confer neuroprotection via mechanisms other than simply increasing global translation.

In further support of our hypothesis that transient PSI is an adaptive response to ischemia, while persistent PSI is pathological, we examined the effect of eIF4G overexpression on the time course of protein synthesis following OGD. As seen with control cultures and calpastatin-overexpressing neurons, protein synthesis was immediately inhibited following OGD in both control and eIF4G-overexpressing neurons. However, protein synthesis began to recover at 12h reperfusion in eIF4G overexpressing neurons but not in control (**Figure 3.6F**).

Examination of protein levels following OGD revealed increased eIF4G levels at all times measured following OGD in eIF4G but not GFP overexpressing neurons. Furthermore, OGD resulted in a similar eIF2α phosphorylation profile when comparing GFP and eIF4G overexpressing neurons (**Figure 3.6G**). Again, this suggests that eIF2α does not contribute to persistent PSI or delayed neuronal death. However, these data collectively demonstrate that maintenance of critical levels of eIF4G is essential for neuronal survival in both a translation dependent and perhaps a translation independent manner.

3.3.7 shRNA silencing of eIF4G exacerbates neuronal death

Our overexpression experiments demonstrate that maintenance of eIF4G levels is sufficient to restore protein synthesis and provide neuroprotection from OGD. The next step was to determine if eIF4G was necessary for neuronal survival following *in vitro* ischemia. To accomplish this we transfected a lentiviral vector with shRNA targeting rat eIF4G into our

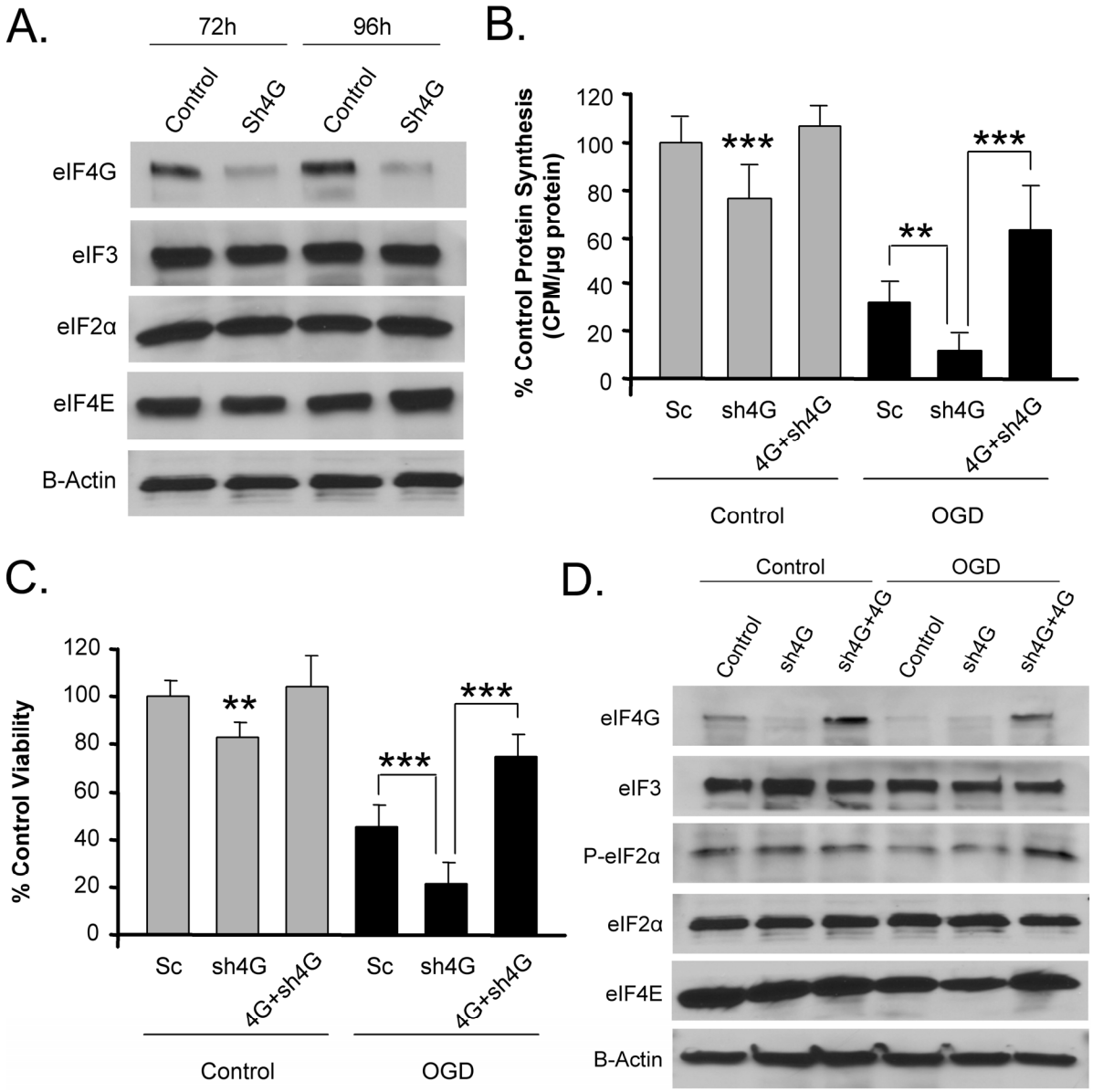

Figure 3.7 eIF4G silencing is detrimental to neurons and exacerbates ischemic injury. A, Neurons plated in 6-well dishes were infected with either 10µl of shRNA lentivirus targeting rat eIF4G or control shRNA virus for 72 and 96h. Cell lysates were analyzed by Western blot and probed with an eIF4G N-terminus antibody to determine protein knockdown. **B**, Analysis of protein synthesis in control shRNA- and GFP-transfected, eIF4G shRNA-transfected (sh4G) and co-transfection of human HA-eIF4G and eIF4G shRNA (4G+sh4G) under control conditions and 24h after 1h OGD. **C**, Viability analysis using AlamarBlue under the same conditions as in **B**. **D**, Western blot analysis of initiation factors after eIF4G silencing and restoration under control conditions and 24h after 1h OGD. Bars represent mean ± SD of n = 3-4 independent experiments. ANOVA with Fisher PLSD determined statistical significance: **p<0.01, ***p<0.001.

primary cultures. Knockdown of eIF4G to approximately 20% of control values was observed at 72h and 96h post infection without affecting levels of other initiation factors (**Figure 3.7A**).

Short hairpin RNA-mediated knockdown of eIF4G resulted in a 24% and 17% decrease in protein synthesis and neuronal viability, respectively (**Figure 3.7B and C**). The decreases in translation are similar to eIF4G silencing in a recent study in a breast cancer cell line (Ramirez-Valle et al., 2008). Ischemia-induced decreases in protein synthesis and viability were also exacerbated by loss of eIF4G. To determine if the exacerbation of injury was specific to loss of eIF4G, concomitant overexpression of human eIF4G was performed. Importantly, overexpression of human eIF4G in endogenous eIF4G-depleted neurons resulted in increased protein synthesis and neuronal viability (**Figure 3.7B and C**). Recovery of protein synthesis and viability was again associated with eIF4G as there were no changes in levels of other regulatory translation initiation factors and eIF4G levels were increased compared to control and shRNA-treated neurons (**Figure 3.7D**).

3.3.8 Cap-dependent translation is inhibited following OGD

It is established that select viral and cellular mRNAs have a 5'UTR that functions as an internal ribosomal entry sequence (IRES), allowing for translation to proceed in a cap-independent manner. Moreover, different IRESs possess various requirements for eIF4G. For example, picornaviruses such as encephalomyocarditis virus (EMCV) require only the central portion of eIF4G for translation of its uncapped messages. Other IRESs such as hepatitis C virus (HCV) do not require eIF4G, but require other initiation factors for efficient translation. Cellular IRESs

have recently been discovered; however, much less is known about the initiation factor requirements for their translation (Jackson, 2005).

We thus wanted to determine if cleavage of eIF4GI by calpain following OGD would differentially affect translation of various cellular and viral IRESs. Additionally, we sought to confirm that cap-dependent translation was indeed inhibited following OGD. Both cellular (β-globin, c-myc and vascular endothelial growth factor) and viral (EMCV and HCV) 5'UTRs were inserted upstream of the *Renilla* luciferase open reading frame. In vitro transcription was performed either in the presence of the methyl-7-guanosine cap to produce capped mRNA or the G(ppp)A cap analog structure to produced uncapped mRNA. The various mRNAs were then transfected into the primary neurons for 2h at the times indicated. Following incubation, the cells were lysed and luciferase activity was measured.

Under control conditions, the capped β-globin, HCV and VEGF 5'UTRs were robustly translated, while the c-myc and EMCV mRNAs underwent more moderate translation (**Figure 3.8A**). Interestingly, the inverted c-myc 5'UTR was more efficiently translated than c-myc itself. The uncapped HCV 5'UTR was also robustly translated under control conditions. No other uncapped mRNAs were translated with greater efficiency than capped mRNAs. It is notable that both uncapped β-globin and VEGF mRNAs translated significantly less than the capped forms under control conditions.

Following OGD, capped β-globin translation was severely inhibited throughout all measurement times while translation of the uncapped mRNA did not change. Similarly, both capped and uncapped HCV mRNA translation was strongly reduced. Translation of the VEGF 5'UTR was also decreased; however, the decrease was more gradual, progressively decreasing

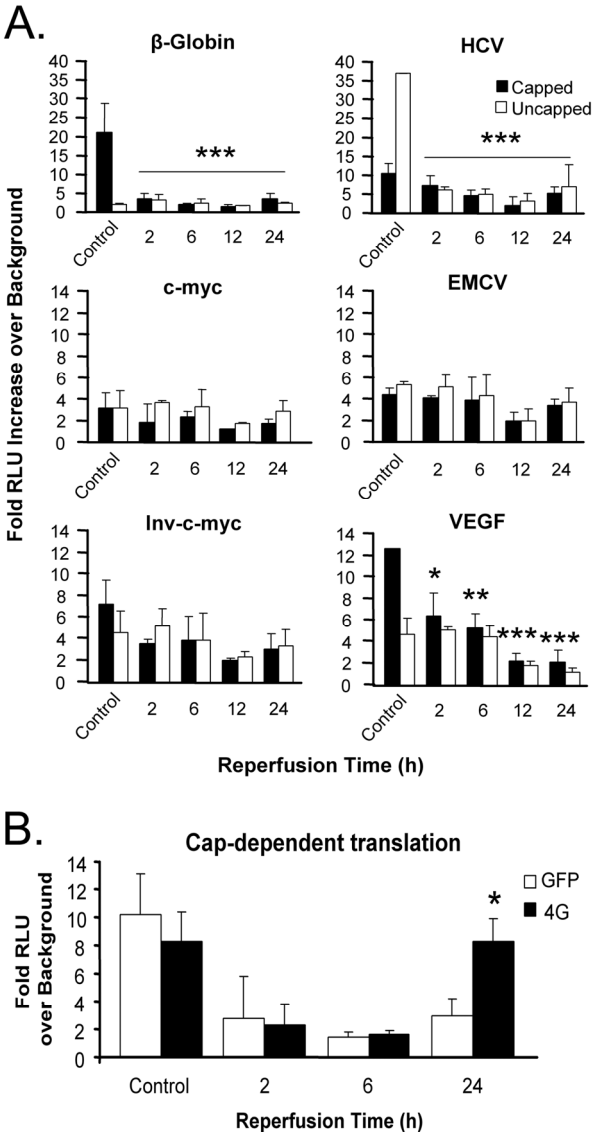

Figure 3.8 Cap- and IRES-dependent translation following *in vitro* ischemia. **A**, Plasmid DNA carrying indicated 5'UTRs upstream of the *Renilla* luciferase reporter ORF were linearlized and mRNA transcription was performed in the presence of the 7-methyl guanosine cap or the G(ppp)A cap analog to produce capped and uncapped mRNA . Neurons were exposed to 1h OGD, and mRNA was transfected into neurons 1h before indicated reperfusion time and neurons were lysed 2h later. The fold relative light units (RLU) were determined for each transcript at each time and are presented above. Note the pronounced and persistent decrease in cap-dependent translation during reperfusion. **B**, Neurons were infected with GFP and eIF4G (4G) lentivirus for 72h wherein neurons underwent 1h OGD. Infected neurons were then transfected with the β-globin mRNA to examine the effect of eIF4G overexpression on cap-dependent translation. Bars represent mean ± SD of n = 3-4 independent experiments. ANOVA with Fisher PLSD determined statistical significance: *p<0.05, **p<0.01, ***p<0.001.

from 2h to 24h reperfusion. Interestingly, the cap and uncapped VEGF mRNA were translated with equal efficiency following OGD. There were no changes in the translation of c-myc and EMCV mRNAs at any of the reperfusion times measured. These data demonstrate that cap-dependent translation is impaired following OGD. In addition, translation of the 5'UTRs examined did not correspond to eIF4G cleavage.

Lastly, we wanted to determine if the restoration of protein synthesis due to eIF4G overexpression was due to restoration of cap-dependent translation. As in the previous experiments, capped β-globin mRNA was transfected into eIF4G- and GFP- transfected neurons at the indicated times after OGD. Luciferase activity indicating cap-dependent translation was continually inhibited following OGD in GFP-transfected neurons (**Figure 3.8B**). Overexpression of eIF4G, however, increased cap-dependent translation 24h after the insult. These results indicate that the increase in protein synthesis caused by increasing eIF4G levels was, at least in part, due to increased cap-dependent translation.

3.4 DISCUSSION

It has been known for nearly 40 years that protein synthesis is inhibited in all ischemia-affected brain regions (Kleihues and Hossmann, 1971), and that persistent inhibition of protein synthesis is a robust predictor of eventual neuronal death in both global (Dienel et al., 1980; Thilmann et al., 1986; Araki et al., 1990) and focal (Hata et al., 2000a, b) models of ischemia. Despite this knowledge, protein synthesis inhibition has never been directly linked to neuronal death. In fact,

persistent PSI was thought to be a mere epiphenomenon of ischemic injury (Heiss, 1992) and persisted due to repeated peri-infarct depolarizations (Hata et al., 2000b) or was secondary to eventual energy failure (Hata et al., 2000a).

Here we provide compelling evidence of a direct link between ischemic neuronal death and persistent PSI. The mechanistic connection between neuronal death and PSI is the pathological degradation of eIF4G mediated by excitotoxicity-induced calpain activation. Calpain inhibition increased protein synthesis and blocked ischemia-induced decreases in eIF4G. Maintenance of critical levels of eIF4G by overexpression resulted in increased neuronal viability that was in part due to increased cap-dependent protein synthesis. Complementing this finding was the depletion of eIF4G resulting in decreased protein synthesis and exacerbating ischemic neuronal injury.

To our knowledge, this is a novel finding demonstrating that a translation initiation factor is directly involved in neuronal death. The decrease in overall translation rate caused by multiple death stimuli are known to correlate with eIF4G levels in a number of cell types (Clemens et al., 1998; Marissen et al., 2000; Morley et al., 2000; Constantinou and Clemens, 2007). Decreases in eIF4G have also been implicated in previous *in vivo* studies that repeatedly demonstrated persistently decreased levels of 4G up to 4h of reperfusion in global ischemia models (DeGracia et al., 1996; Neumar et al., 1998; Martin de la Vega et al., 2001; Garcia et al., 2004b) and up to 24h following focal ischemia (Mengesdorf et al., 2002). Importantly, the complete loss of eIF4G at 24h after focal ischemia is highly correlated with the time of final infarction area (Hata et al., 1998).

In order to adequately study the role of eIF4G in ischemic neuronal death we therefore needed to apply an *in vitro* approach. Previous studies have used either cancer cell lines or other

immortalized cell lines to study PSI following ischemic-like injury. Examination of the effect of OGD on differentiated PC-12 cells failed to show the persistent inhibition of protein synthesis, the activation of any of the eIF2α kinases or the decreases in eIF4G levels that are seen following ischemia *in vivo* (Martin et al., 2000; Munoz et al., 2000). This information combined with the knowledge that both the major regulatory aspects of translation initiation (eIF2-Met-tRNA complex and eIF4F transport of mRNA) are likely to be altered in certain cancers (Clemens, 2004) suggest that the processes involved with PSI following ischemia could be fundamentally altered in these cell types; hence, they are not adequate models for the study of PSI. As demonstrated in our model, the activation state of a number of important translation initiation regulatory proteins nearly completely recapitulate that seen *in vivo* (Figure 3.2).

In the present study, we confirmed that calpain was activated following OGD, and that inhibition of calpain by overexpression of its endogenous inhibitor calpastatin was sufficient to block decreases in eIF4G. Calpain has been demonstrated to degrade eIF4G in a cell free-assay (Wyckoff et al., 1990), and it has been implicated in the degradation of eIF4G in brain following ischemia (Neumar et al., 1996; Neumar et al., 1998). Importantly, our findings show that not only does calpain inhibition by calpastatin block decreases in eIF4G, it also abrogates ischemia-induced persistent PSI and increases neuronal viability.

Calpain inhibition was recently shown to block NMDA- and nitric oxide- mediated decreases in eIF4G in rat primary cortical cultures (Petegnief et al., 2008). However, an increase in protein synthesis was not observed with calpain inhibition. The discrepancy between this study and ours could be explained by the pharmacologic agents used to inhibit calpain as opposed to the molecular inhibition used in this study. The pharmacologic agents could have unknown off-target effects including inhibition of protein synthesis. Indeed, the authors did not

find that calpain inhibition decreased NMDA-induced neuronal death (Petegnief et al., 2008). This is in stark contrast to many studies demonstrating that calpain inhibition is neuroprotective following excitotoxicity [for review see (Ray, 2006)].

Numerous attempts to identify preferential calpain cleavage sites have been unsuccessful (Tompa et al., 2004; Cuerrier et al., 2005); therefore we employed a cell-free system in an attempt to identify the calpain-mediated cleavage products of eIF4G. Our cell-free assay demonstrated that calpain readily cleaves eIF4G in to progressively smaller fragments with increased time. This result was unexpected as calpain activation generally results in cleavage at discrete sites on its substrates (Goll et al., 2003). Instead, the progressive cleavage of eIF4G is more reminiscent of degradation as seen with 20S proteasomal processing of eIF4G than the site-specific cleavage of calpain (Baugh and Pilipenko, 2004).

Despite many efforts, we were not able to identify the calpain cleavage sites or the fragments of eIF4G produced by proteolysis. However, we were able to detect an approximately 65kDa cleavage product with a C-terminal directed antibody in both our cell free assay and our neuronal cultures following OGD that is similar to a band observed following focal ischemia (Mengesdorf et al., 2002). This suggests that at least one product of calpain-mediated 4G cleavage is conserved *in vivo* and may play a role in translation.

In an attempt to determine the biological significance of ischemia-induced eIF4G degradation on translation we examined the translation of various mRNA 5'UTRs linked to a *Renilla* luciferase reporter. Our results confirmed our hypothesis that cap-dependent translation is robustly and persistently inhibited due to decreased levels of eIF4G. Interestingly, none of the viral or cellular IRES sequences were preferentially translated following *in vitro* ischemia, including the HCV IRES which does not require eIF4G for translation (Jackson, 2005). This

suggests that other factors regulating IRES translation may be compromised. Of note, translation of the VEGF IRES was sustained for up to 6 hours after ischemia. The reason for the sustained translation of VEGF mRNA is not known, and the luciferase reporter method used may not reveal other aspects governing VEGF mRNA stability. However, since VEGF is known to be neuroprotective, further examination is warranted (Hansen et al., 2008; Lee et al., 2009).

The importance of protein synthesis in cell death is controversial as application of protein synthesis inhibitors has been shown to induce programmed cell death in some cell types (Cotter et al., 1990; Martin et al., 1990; Bushell et al., 2000) and to prevent death in others—especially in neurons. Inhibition of protein synthesis with cycloheximide was shown to be neuroprotective in cultured sympathetic neurons deprived of nerve growth factor (NGF) (Martin et al., 1988; Scott and Davies, 1990), and pretreatment of cultured neurons with cycloheximide protected neurons from OGD (Lobner and Choi, 1996; Meloni et al., 2002).

There are important differences between these studies and the current study in terms of the models used, the time when CHX was applied and the concentration CHX used. First, the insult of NGF deprivation is expectedly different from *in vitro* ischemia. Therefore induction of programmed cell death may proceed by different mechanisms. Second, in the OGD studies, CHX was applied 24h before the insult and could have resulted in altered gene transcription that was neuroprotective when CHX was removed (i.e. preconditioning). Finally, the concentration of CHX used, 1μg/ml (~3.6μM) for NGF deprivation (Martin et al., 1988) and 0.5 μg/ml (~1.8μM) for protection from OGD (Lobner and Choi, 1996; Meloni et al., 2002), were much less than was necessary in the current experiment to inhibit protein synthesis for 24h (50μM corresponds to 14μg/ml CHX) (Figure 3.6C). This discrepancy could be due to different culture densities plated and culture conditions compared with the current study. However, these studies

did not present data demonstrating the effect of CHX treatment on viability. Baseline viability data should be required when analyzing the effect of protein synthesis inhibitors in models of cell death.

The results presented in this paper suggest that persistent PSI following OGD is related to delayed neuronal death. Accordingly, addition of CHX at concentrations that severely decrease protein synthesis for 24h exacerbated ischemia-induced neuronal death, while neuroprotection provided by overexpression of either calpastatin or eIF4G increased protein synthesis. An important finding of this paper is that the neuroprotective proteins did not prevent PSI, they restored translation. This is an important distinction in terms of eventual neuroprotective strategies as the aim for clinical neuroprotection is to prevent loss of brain after ischemia onset where protein synthesis is already inhibited.

Restoration of protein synthesis is clearly important for maintenance of neuronal viability following ischemia. Neuroprotection provided by eIF4G overexpression significantly increased protein synthesis; however, neuroprotection by eIF4G was only partially due to restoration of translation as treatment with CHX did not completely block the neuroprotective effect. Other mechanisms must therefore be involved with the protective effect of eIF4G. Recently, it was demonstrated that eIF4G was involved with preservation of bioenergetics and mitochondrial activity along with suppression of autophagy (Ramirez-Valle et al., 2008). The potential role of eIF4G in regulating mitochondrial biogenesis and autophagy via protein synthesis-dependent and –independent mechanisms is an enticing prospect for further study as both phenomena are burgeoning fields in ischemia research (Vosler et al., 2009a).

In conclusion, we provide evidence that calpain-mediated degradation of eIF4G is the link between neuronal death and persistent PSI. Notably, neuroprotection provided by

preservation of eIF4G levels is only partly due to restoration of ischemia-induced PSI. Future studies should examine alternative mechanisms whereby eIF4G confers neuroprotection. Additional assessment of the types of mRNA translated and the mechanism of translation following ischemia are also warranted. Further understanding of the role of eIF4G and potentially other factors regulating persistent PSI may lead to the development of novel neuroprotective strategies.

4.0 DISCUSSION OF THE FUTURE DIRECTION OF SECONDARY ENERGY DEPLETION AND PERSISTENT PROTEIN SYNTHESIS INHIBITION

4.1 INTRODUCTION

The previous chapters provide detailed experimental evidence regarding two major components of ischemia research—secondary energy depletion and persistent protein synthesis inhibition. Considering the extensive literature regarding energy depletion and PSI it would appear that these two phenomena are independent of each other. The apparent commonality between them is calpain activation. However, one piece of experimental evidence is lacking. That is the demonstration that restoration of NAD^+ levels blocks subsequent mitochondrial calcium dysregulation, thus providing a connection between loss of NAD^+ and calpain. While there is limited data available to support this statement, there is a possibility that the neuroprotective mechanism of eIF4G, other than its restoration of protein synthesis, is its involvement in maintenance of cellular bioenergetics. These possibilities will be discussed in the following sections. In addition, the main contemporary theories of the mechanisms governing persistent PSI are discussed in relation to pathologic eIF4G degradation.

4.2 SECONDARY ENERGY DEPLETION

Focal ischemia results in lack of blood flow and energy depletion below a CBF of 18ml/100mg/min. Upon reperfusion, however, energy is restored to baseline levels. Secondary energy depletion is observed in the gradually progressing infarct area, suggesting that it is involved in delayed neuronal death. The intracellular mechanisms governing energy depletion have been worked out in great detail.

Briefly, increased intracellular calcium caused by NMDA receptor activation is buffered by various cellular organelles including mitochondria. The increased calcium load increases production of superoxide radicals that diffuse into the cytosol and interact with the NO produced during NMDA receptor activation and form peroxynitrite. This is a ROS that potently damages DNA, activating the DNA damage detection enzyme PARP-1. Overactivation of PARP-1 due to extensive DNA damage severely depletes energy stores in the form of NAD^+ and concomitantly releases PAR polymer.

Currently it is unknown whether NAD^+ depletion or excess PAR polymer formation mediates mitochondrial calcium dysregulation. Furthermore, it is not known exactly how mitochondrial calcium dysregulation occurs due to the two putative stimuli. A reasonable hypothesis is that either NAD^+ depletion or PAR cause VDAC channels to open and allow excess calcium entry. What is known is that mitochondrial calcium dysregulation activates calpain that resides in its inner mitochondrial membrane. Activated calpain then cleaves a number of substrates, including AIF to actuate delayed neuronal death.

Recently our lab examined the involvement of NAD^+ in the context of DNA repair instigated by OGD in primary neurons (Wang et al., 2008). Repletion of NAD^+ prior to or up to

1h after OGD profoundly increased neuronal viability and reduced DNA damage. The reduction in DNA damage was associated with increased base-excision repair (BER); however, the protective effect of NAD^+ was only partially due to restoration of BER activity, as genetic silencing of the rate limiting BER enzyme, APE1, did not completely block neuroprotection (Wang et al., 2008).

Collectively, this study demonstrates that preservation of NAD^+ is critical to maintain activity of the essential process of DNA repair in response to ischemic injury. There are other targets that also rely upon NAD^+ as an energy substrate that may also be involved with the prosurvival effect of NAD^+. Oxidative phosphorylation in the mitochondria is a process that necessitates large amounts of NAD^+ to produce the majority of cellular ATP. It has been argued that since NAD^+ is compartmentalized in neurons that the mitochondrial store of NAD^+ is resistant to PARP-1-mediated NAD^+ depletion in the nucleus (Ying et al., 2005; Alano et al., 2007).

The counter argument can be provided that while initial depletion of NAD^+ may not deplete mitochondrial pools, sustained activation of PARP-1 with continued depletion of nuclear and cytosolic NAD^+ may indirectly decrease mitochondrial energy stores by increasing overall intracellular energy demand. Further increases in energy demand following ischemia could push the mitochondrial past a functional threshold leading to membrane compromise. This could explain how PARP-1 overactivation and subsequent NAD^+ depletion would lead to mitochondrial calcium dysregulation observed in our model (**Figure 2.7**). This would also correlate well with the onset of secondary energy failure observed following focal ischemia.

Another plausible mechanism underlying NAD^+ protection is restoring the activity of the class III histone deacetylases, particularly SIRT1. These NAD^+-dependent nuclear enzymes

function by deacetylating targets such as histones and transcription factors, and they have been associated with increased life span promoted by calorie restriction (Fulco and Sartorelli, 2008). Decreased SIRT1 activity is seen following PARP-1 mediated NAD^+-depletion and cell death in heart (Pillai et al., 2005). Activity of SIRT1 is also important for protection against axonal degeneration (Araki et al., 2004), and it is involved in the protective preconditioning effect of resveratrol against OGD in brain slice (Raval et al., 2006).

We are currently exploring the role of SIRT1 involvement in NAD^+-dependent neuroprotection following NMDA exposure. We are examining the effect of NAD^+ on maintenance of mitochondrial calcium regulation. The results of these studies will provide vital understanding of the mechanisms underlying secondary energy failure provoked by ischemic insult.

4.3 PERSISTENT PROTEIN SYNTHESIS INHIBITION

The data from Chapter 3 demonstrate that preventing degradation of eIF4G is critical to recovery of protein synthesis following ischemia and preservation of neuronal viability. The mechanisms governing the neuroprotective effect of eIF4G are both translation-dependent and –independent. This forms the molecular basis underlying persistent PSI. In addition to the hypothesis that eIF4G degradation mediates persistent PSI, other postulates exist. Phenomena such as formation of irreversible protein aggregates, stress granule and P-body (RNA degradation) formation,

formation and persistence of RNA granules and translation-associated dysfunction of stress responses are all implicated in persistent PSI (DeGracia et al., 2008). These phenomena are discussed in relation to the pathological degradation of eIF4G.

Stress-induced PSI is a universal phenomenon, and transient PSI is an adaptive response to manage stress. The function of PSI is suggested to serve a two-fold purpose. The first is to block nascent peptide synthesis as increases in unfolded proteins would contribute to increased cellular damage. The second function is to initiate the heat shock response, which consists of selective translation of chaperone proteins that serve to reverse any damage caused by the stress by refolding proteins and eventually restore normal translation (DeGracia and Hu, 2007).

The inhibition of protein synthesis caused by all stresses including ischemia has been divided into three phases: initiation, maintenance, and termination (DeGracia and Hu, 2007). The stages were recently refined to incorporate mRNA regulation or ribonomics (Tenenbaum et al., 2002). The initiation phase is associated with protein synthesis regulation at the ribosomal level, the maintenance phase refers to mRNA regulation and termination is governed by successful execution of stress-response programs such as the UPR and heat shock response (DeGracia et al., 2008). To facilitate discussion relevant to contemporary theory concerning persistent PSI (DeGracia et al., 2008) the following sections discuss ischemia-related PSI in terms of these three stages.

4.3.1 Initiation phase of translation arrest

One of the initial events following ischemia is dissociation of polysomes to block translation initiation (Cooper et al., 1977). Dissociated polysomes, comprised of ribosomes, translation

initiation factors and mRNA are released into the cytoplasm. It is known that ischemia results in the formation of ubiquinated proteins in all ischemia-affected neurons (Hu et al., 2000; Hu et al., 2001). The ubiquinated protein clusters are cleared in ischemia-resistant neurons, but remain in the sensitive neurons such as the CA1 field (Hu et al., 2000; Hu et al., 2001; Liu et al., 2005b).

Ischemia-sensitive neurons additionally possess co-translational aggregates that sequester components of the disassociated polysome including ribosomal subunits, initiation factors, co-chaperones and components of the ubiquitin-proteasome apparatus (Liu et al., 2005b). The co-translational protein aggregates were regarded as irreversible and were thus associated with persistent PSI. Furthermore, reductions of co-translational aggregates were found following ischemic preconditioning, a phenomenon of increased resistance to subsequent ischemia following a sublethal insult (Liu et al., 2005a). The decreases in aggregates were associated with preconditioning-induced upregulation of chaperones and of the ubiquitin-proteasomal response.

The sequestration of ribosomes into protein aggregates is not complete. Examination of the relation between S6 ribosomal subunit and ubiquinated proteins in post-ischemia neurons revealed only a partial co-localization as there was a large proportion of free-cytosolic S6 (DeGracia et al., 2007). Therefore, protein aggregation may only play a part in persistent PSI. However, the S6 subunit and ubiquinated proteins were also associated with components of stress granules (DeGracia et al., 2007), which leads to the maintenance stage of PSI.

4.3.2 Maintenance of PSI by RNA regulation

Stress granules (SGs) are dynamic cytoplasmic foci consisting of arrested translation initiation complexes induced in cells by environmental stresses (Anderson and Kedersha, 2002; Kedersha

and Anderson, 2002). The formation of SGs is thought to be an adaptive cellular mechanism whereby the translation of housekeeping genes is suppressed while repair or cell death program expression is enhanced (Kedersha and Anderson, 2002). The RNA-binding/prion-like protein, T-cell internal antigen-1 (TIA-1), is an essential component of SGs. It exports out of the nucleus following stress-induced phosphorylation of eIF2, the key component of the ternary complex that transports the initiator methionyl-transfer RNA to the ribosome (Kedersha et al., 1999). TIA-1 forms SGs in the cytoplasm by binding untranslated mRNA and its associated translation initiation machinery via its RNA-recognition motifs (RRM) and self-aggregating via its prion-related domain (PRD) (Gilks et al., 2004). Removal of the RRM of TIA-1 prevents SG formation and may attenuate the PSI caused by cellular stress (Gilks et al., 2004). Furthermore, inhibition of TIA-1 increases translation of TIA-targeted mRNA (Lopez de Silanes et al., 2005).

SGs are formed in ischemia-exposed neurons *in vivo* (Kayali et al., 2005; DeGracia et al., 2006). These studies revealed that TIA-1 co-localized with two markers of SGs, the small ribosomal subunit (S6) and eIF4G, in the hippocampus following global ischemia (Kayali et al., 2005; DeGracia et al., 2006). Subsequent examination of the involvement of SGs in persistent translation arrest revealed that SGs increased in all ischemia-affected brain regions, and that sequestration of the small ribosomal subunit into SGs represented only a fraction of total 40S ribosomes in neurons. Thus, regulation of 40S subunit by SGs cannot account for persistent PSI (DeGracia et al., 2007).

Another process of mRNA maintenance during translation arrest involves selective mRNA degradation. SGs confine select mRNAs until a molecular decision is made to either reinitiate translation, store, or degrade the mRNA (Anderson and Kedersha, 2002; Kedersha and Anderson, 2002; Kedersha et al., 2005). Following cellular stress, SGs can co-localize with

another type of cytoplasmic foci, processing bodies (PBs), that contain mRNA degradation enzymes (Kedersha et al., 2005). While there are many proteins exclusive to either SGs or PBs, there are some common to both. One of these proteins, tristetraprolin (TTP), is associated with both mRNA binding in SGs and mRNA decay (Lykke-Andersen and Wagner, 2005; Murata et al., 2005). Overexpression of TTP results in an increase in SG and PB co-localization (Kedersha et al., 2005). TTP may then bind to mRNA destined for degradation in SGs and transport them into PBs where RNA degradation enzymes are located. However, degradation of mRNA does not appear to play a role in persistent PSI as the co-localization of TTP with SGs occurs at approximately 16h in all ischemia-affected neurons (Jamison et al., 2008).

Although RNA-degradation does not seem to play a role in persistent PSI, another possibility has been revealed. Following ischemia, there is a redistribution of mRNA from a diffuse cytoplasmic staining into a punctate pattern. These puncta, which are termed mRNA granules, were present in all reperfused neurons. However, they eventually resolved in ischemia-resistant neurons while they persisted in CA1 neurons. The mRNA granules contained poly-A-binding protein (PABP), eIF4G and mRNA (Jamison et al., 2008). Importantly, TIA-1 and S6 were absent from the granules suggesting they are not components of SGs.

An interesting finding was that the mRNA granules also co-localized with HuR, a protein that binds adenine-uridine rich elements (ARE) on specific mRNA and aids in their stabilization (Brennan and Steitz, 2001). Additionally, the protein is involved in sequestering functionally similar mRNA to putatively activate coordinated translation programs (Keene, 2007). Association of HuR with mRNA granules was observed in all ischemia-resistant neurons; however HuR did not associate with ischemia-sensitive neurons until 36h reperfusion (Jamison et al., 2008), suggesting an impaired signaling to mRNA granules.

4.3.3 Termination phase of PSI by activation of stress responses

The final phase of PSI following stress is the activation of the stress response. This phase is mediated by the unfolded protein response (UPR) caused by ER-stress (Kaufman, 1999), and by the heat shock response (HSR) to increase translation of chaperone proteins. An increase in unfolded proteins or denatured proteins results in chaperones dissociating from stress actuators in the ER and the cytosol. The ER stress response, mediated by the chaperone GRP-78 release of PERK with subsequent PERK-dependent phosphorylation of eIF2α (Kumar et al., 2001), inhibits synthesis of constitutive proteins. The HSR is induced by an increase in dysfunctional proteins in the cytosol (Voellmy and Boellmann, 2007).

As was previously discussed in the introduction, the UPR is rendered dysfunctional by ischemia since translation is persistently inhibited (Kumar et al., 2003; Paschen et al., 2003). Evidence has long been known of an impairment of the heat shock response in ischemia-sensitive brain regions (Nowalk et al., 1985). It was discovered that mRNA of HSP70, an inducible heat shock protein robustly increased with cellular stress, is present for prolonged periods in ischemia-sensitive brain regions, but only transiently in ischemia-resistant areas (Welsh et al., 1992). Moreover, successful translation of HSP70 only occurred in ischemia-resistant neurons of the penumbra (Kinouchi et al., 1993).

This ties in with HuR localization to mRNA granules because translation of the heat shock protein HSP70 correlates with early HuR localization to mRNA granules in ischemia-resistant neurons, but HuR fails to localize to mRNA granules until 36h reperfusion in ischemia-sensitive neurons (Jamison et al., 2008). This supports the suggestion that successful mounting

of the HSR early after stress protects neurons from delayed death (DeGracia and Hu, 2007). Indeed, HSP70 can reverse SG formation (Gilks et al., 2004) and may result in resumption of translation. However, this remains to be demonstrated in post-ischemic neurons.

4.3.4 Relationship between eIF4G and the phases of ischemia-induced PSI

Overall, in ischemia-sensitive neurons there appears to be a dysfunctional termination phase of ischemia-induced PSI. One explanation is neurons that do not mount a HSR cannot alleviate the stimuli that caused the initial PSI inhibition, thus PSI persists and there is a toxic accumulation of misfolded proteins and protein aggregates. Neurons that can successfully mount and HSR produce chaperone proteins that aid in refolding some proteins and may increase degradation of severely damaged proteins. A flaw to this logic is that while PSI persists, the signals that initiate PSI are transient. Namely, phosphorylation of eIF2α by PERK is transient and translation inhibition is unaffected in PERK knock out mice following ischemia (Owen et al., 2005).

Another explanation is that ischemia-resistant neurons maintain levels of eIF4G, while eIF4G is decreased in ischemia-sensitive neurons. Therefore, functional eIF4G may be necessary to form the eIF4F complex to translate heat shock mRNA to mount the HSR and to restore protein synthesis. This is suggested in our study examining the role of eIF4G in persistent PSI and neuronal death. The maintenance of critical levels of eIF4G may be necessary for translation of HSR proteins such as HSP70. Indeed, the protective effect of eIF4G maybe partially due to restoration of translation of HSP70. An experiment examining the induction of HSP70 was not examined in our study, but it could easily be tested in subsequent experiments.

Additionally, the restoration of protein synthesis by overexpression of eIF4G may restore the UPR to produce neuroprotection. Again, this could also be studied in our model.

Successful expression of the stress response could also alleviate the co-translational aggregates seen in ischemia-sensitive neurons (Hu et al., 2000; Hu et al., 2001; Liu et al., 2005a; Liu et al., 2005b). A functional HSR would increase chaperone function to decrease misfolded proteins and increase elimination of defunct proteins. Thus, prolonged presence of co-translational aggregates is the result of an impaired stress response, and theoretically can be reversed if the stress response is repaired in a timely fashion.

Currently, it is not clear how HuR interacts with mRNA granules to induce HSP translation. The mRNA granules consist of eIF4G, PABP and mRNA in both ischemia-resistant and –sensitive brain regions. Since eIF4G is degraded in ischemia-sensitive neurons, the signal for HuR to colocalize with mRNA granules may be lacking. Indeed, there is altered subcellular localization of eIF4G (DeGracia et al., 2006) that could account for lack of HuR localization. However, it is unlikely that HSP70 would be translated even if HuR was located in the mRNA granule because eIF4G is functionally compromised.

4.4 A POTENTIAL LINK BETWEEN EIF4G, SECONDARY ENERGY FAILURE AND PERSITENT PROTEIN SYNTHESIS INHIBITION

Our results demonstrate that the neuroprotective effect of eIF4G is both protein synthesis-dependent and –independent. The previous sections postulate a mechanism for the protein-

synthesis dependent component of eIF4G to provide neuroprotection. A recent study has provided a possibility for a protein-synthesis independent mechanism. By silencing eIF4G expression in MCF10A immortalized breast epithelial cells, the authors demonstrate that eIF4G is responsible not only for the translation of important mRNA involved with bioenergetics and mitochondrial activity, but it is linked to intracellular signaling involving nutrient sensing, mitochondrial dysfunction and autophagy (Ramirez-Valle et al., 2008).

The mRNA regulated by eIF4G included mitochondrial ribosomal proteins and proteins involved with glucose homeostasis. It was also discovered that eIF4G silencing induced an increase in the phosphorylation of the energy sensing kinase AMP kinase (AMPK) possibly due to a decrease in ATP production. Phosphorylation of AMPK occurs when energy metabolism is decreased as indicated by an increase in the AMP/ATP ratio (Fulco and Sartorelli, 2008). Activated AMPK inhibits mammalian target of rapamycin (mTOR) (Inoki et al., 2003), an important translation regulator that is activated by Akt in response to growth factors to increase translation via eIF4G (Holcik and Sonenberg, 2005).

It can be postulated that a decrease in eIF4G could impair mitochondrial bioenergetics, leading to an increased AMP/ATP ratio and the activation of AMPK, or eIF4G could be involved with the signaling of AMPK. The increase in AMPK activation due to eIF4G depletion could be caused by direct activation of a signaling cascade or indirectly by impairing mitochondrial bioenergetics, leading to eventual decrease in ATP production and an increase in AMP/ATP ratio. Degradation of eIF4G could thus simultaneously be linked to persistent PSI and secondary energy failure. Indeed, activation of AMPK is known to be detrimental for ischemic brain as genetic knockdown or pharmacologic inhibition of the α subunit of AMPK reduces infarct

volume (Li et al., 2007). However, a direct relationship between eIF4G and AMPK in ischemic brain has not been established.

Maintenance of eIF4G levels in ischemic brain may also exert neuroprotective effects through preservation of mitochondria and increased mitochondrial biogenesis. As stated above, eIF4G is involved with translation of mitochondrial ribosomal proteins and depletion of eIF4G results in impaired mitochondrial membrane potential (Ramirez-Valle et al., 2008). Mitochondrial biogenesis has recently received attention as a potential endogenous neuroprotective mechanism (Vosler et al., 2009b). Future experiments could examine the effect of eIF4G overexpression on mitochondrial membrane potential, ATP levels, mitochondrial DNA content and mitochondrial proteins following ischemia to determine if eIF4G is involved with mitochondrial biogenesis.

Finally, depletion of eIF4G was associated with an increase in autophagy as measured by increased myosin light chain (LC) 3-II expression and increased binding of the autophagosome specific dye monodansylcadaverine (Ramirez-Valle et al., 2008). The role of autophagy has recently received substantial attention in ischemia research. Conditional genetic knock out of important autophagy regulating proteins is neuroprotective in neonatal hypoxia-ischemia (Koike et al., 2008) and pharmacologic inhibition of autophagy reduces infarct volume caused by focal ischemia (Wen et al., 2008). Thus, maintenance of eIF4G levels could function to decrease autophagy following ischemia to provide neuroprotection.

4.5 SUMMARY

The purpose of this dissertation was to examine two major metabolic mediators of delayed neuronal death caused by ischemia—secondary energy depletion and persistent protein synthesis inhibition. Secondary energy depletion was indirectly examined in chapter 2 as a direct mechanism linking decreased NAD^+ and mitochondrial dysfunction has not been provided. However, a novel connection between PARP-1 activation and calpain-mediated AIF release was established via mitochondrial calcium dysregulation.

Chapter 3 examined the role degradation of the important translation initiation factor eIF4G had in mediating persistent protein synthesis inhibition and delayed neuronal death. The data clearly demonstrate that maintenance of critical levels of eIF4G is essential to preserving neuronal viability. Neuroprotection due to increased protein synthesis was discussed in terms of enabling damaged neurons to enact a functional stress response.

Interestingly, protection due to increased levels of a translation initiation factor was also due to a protein synthesis-independent mechanism. Prospective mechanisms of protein synthesis-independent eIF4G mediated neuroprotection are via increased mitochondrial biogenesis, decreasing autophagy and possibly via protection against secondary energy depletion. Thus, eIF4G could be involved with both major metabolic disturbances governing ischemia-induced neuronal death.

Eukaryotic initiation factor 4G thus plays an extremely important role in maintenance of cellular viability. It will be of great interest to entirely delineate the breadth of the function of

eIF4G in ischemia and under physiologic conditions. The research presented in this dissertation provides a novel perspective regarding the mechanisms underlying delayed neuronal death and may eventually lead to the development of clinically applicable neuroprotective strategies.

BIBLIOGRAPHY

(1995) Tissue plasminogen activator for acute ischemic stroke. The National Institute of Neurological Disorders and Stroke rt-PA Stroke Study Group. N Engl J Med 333:1581-1587.

(1997) CAST: randomised placebo-controlled trial of early aspirin use in 20,000 patients with acute ischaemic stroke. CAST (Chinese Acute Stroke Trial) Collaborative Group. Lancet 349:1641-1649.

(2005) Emergency administration of abciximab for treatment of patients with acute ischemic stroke: results of a randomized phase 2 trial. Stroke 36:880-890.

(CDC) CfDCaP (2001) Prevalence of disabilities and associated health conditions among adults--United States, 1999. MMWR Morb Mortal Wkly Rep 50:120-125.

Adams HP, Jr., Bendixen BH, Kappelle LJ, Biller J, Love BB, Gordon DL, Marsh EE, 3rd (1993) Classification of subtype of acute ischemic stroke. Definitions for use in a multicenter clinical trial. TOAST. Trial of Org 10172 in Acute Stroke Treatment. Stroke 24:35-41.

Adams HP, Jr., Effron MB, Torner J, Davalos A, Frayne J, Teal P, Leclerc J, Oemar B, Padgett L, Barnathan ES, Hacke W (2008) Emergency administration of abciximab for treatment of patients with acute ischemic stroke: results of an international phase III trial: Abciximab in Emergency Treatment of Stroke Trial (AbESTT-II). Stroke 39:87-99.

Alano CC, Beutner G, Dirksen RT, Gross RA, Sheu SS (2002) Mitochondrial permeability transition and calcium dynamics in striatal neurons upon intense NMDA receptor activation. J Neurochem 80:531-538.

Alano CC, Tran A, Tao R, Ying W, Karliner JS, Swanson RA (2007) Differences among cell types in NAD(+) compartmentalization: a comparison of neurons, astrocytes, and cardiac myocytes. J Neurosci Res 85:3378-3385.

Almeida A, Bolanos JP (2001) A transient inhibition of mitochondrial ATP synthesis by nitric oxide synthase activation triggered apoptosis in primary cortical neurons. J Neurochem 77:676-690.

Althausen S, Mengesdorf T, Mies G, Olah L, Nairn AC, Proud CG, Paschen W (2001) Changes in the phosphorylation of initiation factor eIF-2alpha, elongation factor eEF-2 and p70 S6 kinase after transient focal cerebral ischaemia in mice. J Neurochem 78:779-787.

Anderson P, Kedersha N (2002) Visibly stressed: the role of eIF2, TIA-1, and stress granules in protein translation. Cell Stress Chaperones 7:213-221.

Andrabi SA, Kim NS, Yu SW, Wang H, Koh DW, Sasaki M, Klaus JA, Otsuka T, Zhang Z, Koehler RC, Hurn PD, Poirier GG, Dawson VL, Dawson TM (2006) Poly(ADP-ribose) (PAR) polymer is a death signal. Proc Natl Acad Sci U S A 103:18308-18313.

Arai H, Passonneau JV, Lust WD (1986) Energy metabolism in delayed neuronal death of CA1 neurons of the hippocampus following transient ischemia in the gerbil. Metab Brain Dis 1:263-278.

Araki T, Sasaki Y, Milbrandt J (2004) Increased nuclear NAD biosynthesis and SIRT1 activation prevent axonal degeneration. Science 305:1010-1013.

Araki T, Kato H, Inoue T, Kogure K (1990) Regional impairment of protein synthesis following brief cerebral ischemia in the gerbil. Acta Neuropathol (Berl) 79:501-505.

Arrington DD, Van Vleet TR, Schnellmann RG (2006) Calpain 10: a mitochondrial calpain and its role in calcium-induced mitochondrial dysfunction. Am J Physiol Cell Physiol 291:C1159-1171.

Arthur JS, Elce JS, Hegadorn C, Williams K, Greer PA (2000) Disruption of the murine calpain small subunit gene, Capn4: calpain is essential for embryonic development but not for cell growth and division. Mol Cell Biol 20:4474-4481.

Astrup J, Blennow G, Nilsson B (1979) Effects of reduced cerebral blood flow upon EEG pattern, cerebral extracellular potassium, and energy metabolism in the rat cortex during bicuculline-induced seizures. Brain Res 177:115-126.

Astrup J, Siesjo BK, Symon L (1981) Thresholds in cerebral ischemia - the ischemic penumbra. Stroke 12:723-725.

Astrup J, Symon L, Branston NM, Lassen NA (1977) Cortical evoked potential and extracellular K+ and H+ at critical levels of brain ischemia. Stroke 8:51-57.

Avaria LG, Krivanek J (1973) Double labelling study of the spreading depression effect on the incorporation of labelled leucine into the proteins of the brain mitochondrial subfractions. J Neurochem 20:905-908.

Back T, Kohno K, Hossmann KA (1994) Cortical negative DC deflections following middle cerebral artery occlusion and KCl-induced spreading depression: effect on blood flow, tissue oxygenation, and electroencephalogram. J Cereb Blood Flow Metab 14:12-19.

Badugu R, Garcia M, Bondada V, Joshi A, Geddes JW (2008) N terminus of calpain 1 is a mitochondrial targeting sequence. J Biol Chem 283:3409-3417.

Bano D, Young KW, Guerin CJ, Lefeuvre R, Rothwell NJ, Naldini L, Rizzuto R, Carafoli E, Nicotera P (2005) Cleavage of the plasma membrane Na+/Ca2+ exchanger in excitotoxicity. Cell 120:275-285.

Baugh JM, Pilipenko EV (2004) 20S proteasome differentially alters translation of different mRNAs via the cleavage of eIF4F and eIF3. Mol Cell 16:575-586.

Bertolotti A, Zhang Y, Hendershot LM, Harding HP, Ron D (2000) Dynamic interaction of BiP and ER stress transducers in the unfolded-protein response. Nat Cell Biol 2:326-332.

Bevers MB, Neumar RW (2008) Mechanistic role of calpains in postischemic neurodegeneration. J Cereb Blood Flow Metab 28:655-673.

Bi R, Bi X, Baudry M (1998a) Phosphorylation regulates calpain-mediated truncation of glutamate ionotropic receptors. Brain Res 797:154-158.

Bi X, Chen J, Baudry M (1998b) Calpain-mediated proteolysis of GluR1 subunits in organotypic hippocampal cultures following kainic acid treatment. Brain Res 781:355-357.

Bi X, Bi R, Baudry M (2000) Calpain-mediated truncation of glutamate ionotropic receptors. Methods for studying the effects of calpain activation in brain tissue. Methods Mol Biol 144:203-217.

Blanchard H, Grochulski P, Li Y, Arthur JS, Davies PL, Elce JS, Cygler M (1997) Structure of a calpain Ca(2+)-binding domain reveals a novel EF-hand and Ca(2+)-induced conformational changes. Nat Struct Biol 4:532-538.

Blumenfeld H (2002) Neuroanatomy Through Clinical Cases. Sunderland, MA: Sinauer Associates.

Bodsch W, Barbier A, Oehmichen M, Grosse Ophoff B, Hossmann KA (1986) Recovery of monkey brain after prolonged ischemia. II. Protein synthesis and morphological alterations. J Cereb Blood Flow Metab 6:22-33.

Boujrad H, Gubkina O, Robert N, Krantic S, Susin SA (2007) AIF-mediated programmed necrosis: a highly regulated way to die. Cell Cycle 6:2612-2619.

Bradrick SS, Dobrikova EY, Kaiser C, Shveygert M, Gromeier M (2007) Poly(A)-binding protein is differentially required for translation mediated by viral internal ribosome entry sites. Rna 13:1582-1593.

Branston NM, Symon L, Crockard HA, Pasztor E (1974) Relationship between the cortical evoked potential and local cortical blood flow following acute middle cerebral artery occlusion in the baboon. Exp Neurol 45:195-208.

Brennan CM, Steitz JA (2001) HuR and mRNA stability. Cell Mol Life Sci 58:266-277.

Bretin S, Rogemond V, Marin P, Maus M, Torrens Y, Honnorat J, Glowinski J, Premont J, Gauchy C (2006) Calpain product of WT-CRMP2 reduces the amount of surface NR2B NMDA receptor subunit. J Neurochem 98:1252-1265.

Burda J, Martin ME, Gottlieb M, Chavko M, Marsala J, Alcazar A, Pavon M, Fando JL, Salinas M (1998) The intraischemic and early reperfusion changes of protein synthesis in the rat brain. eIF-2 alpha kinase activity and role of initiation factors eIF-2 alpha and eIF-4E. J Cereb Blood Flow Metab 18:59-66.

Bushell M, McKendrick L, Janicke RU, Clemens MJ, Morley SJ (1999) Caspase-3 is necessary and sufficient for cleavage of protein synthesis eukaryotic initiation factor 4G during apoptosis. FEBS Lett 451:332-336.

Bushell M, Poncet D, Marissen WE, Flotow H, Lloyd RE, Clemens MJ, Morley SJ (2000) Cleavage of polypeptide chain initiation factor eIF4GI during apoptosis in lymphoma cells: characterisation of an internal fragment generated by caspase-3-mediated cleavage. Cell Death Differ 7:628-636.

Cao G, Clark RS, Pei W, Yin W, Zhang F, Sun FY, Graham SH, Chen J (2003) Translocation of apoptosis-inducing factor in vulnerable neurons after transient cerebral ischemia and in neuronal cultures after oxygen-glucose deprivation. J Cereb Blood Flow Metab 23:1137-1150.

Cao G, Xing J, Xiao X, Liou AK, Gao Y, Yin XM, Clark RS, Graham SH, Chen J (2007) Critical role of calpain I in mitochondrial release of apoptosis-inducing factor in ischemic neuronal injury. J Neurosci 27:9278-9293.

Cao G, Pei W, Lan J, Stetler RA, Luo Y, Nagayama T, Graham SH, Yin XM, Simon RP, Chen J (2001) Caspase-activated DNase/DNA fragmentation factor 40 mediates apoptotic DNA fragmentation in transient cerebral ischemia and in neuronal cultures. J Neurosci 21:4678-4690.

Chaitanya GV, Babu PP (2008) Activation of Calpain, Cathepsin-b and Caspase-3 during Transient Focal Cerebral Ischemia in Rat Model. Neurochem Res.

Chan SL, Mattson MP (1999) Caspase and calpain substrates: roles in synaptic plasticity and cell death. J Neurosci Res 58:167-190.

Chee PY, Dahl JL (1978) Measurement of protein turnover in rat brain. J Neurochem 30:1485-1493.

Chen J, Nagayama T, Jin K, Stetler RA, Zhu RL, Graham SH, Simon RP (1998) Induction of caspase-3-like protease may mediate delayed neuronal death in the hippocampus after transient cerebral ischemia. J Neurosci 18:4914-4928.

Chen ZM, Sandercock P, Pan HC, Counsell C, Collins R, Liu LS, Xie JX, Warlow C, Peto R (2000) Indications for early aspirin use in acute ischemic stroke : A combined analysis of 40 000 randomized patients from the chinese acute stroke trial and the international stroke trial. On behalf of the CAST and IST collaborative groups. Stroke 31:1240-1249.

Cheung EC, Joza N, Steenaart NA, McClellan KA, Neuspiel M, McNamara S, MacLaurin JG, Rippstein P, Park DS, Shore GC, McBride HM, Penninger JM, Slack RS (2006) Dissociating the dual roles of apoptosis-inducing factor in maintaining mitochondrial structure and apoptosis. Embo J 25:4061-4073.

Cho S, Liu D, Fairman D, Li P, Jenkins L, McGonigle P, Wood A (2004) Spatiotemporal evidence of apoptosis-mediated ischemic injury in organotypic hippocampal slice cultures. Neurochem Int 45:117-127.

Choi DW (1987) Ionic dependence of glutamate neurotoxicity. J Neurosci 7:369-379.

Chu CT, Zhu JH, Cao G, Signore A, Wang S, Chen J (2005) Apoptosis inducing factor mediates caspase-independent 1-methyl-4-phenylpyridinium toxicity in dopaminergic cells. J Neurochem 94:1685-1695.

Clark WM, Albers GW, Madden KP, Hamilton S (2000) The rtPA (alteplase) 0- to 6-hour acute stroke trial, part A (A0276g) : results of a double-blind, placebo-controlled, multicenter study. Thromblytic therapy in acute ischemic stroke study investigators. Stroke 31:811-816.

Clark WM, Wissman S, Albers GW, Jhamandas JH, Madden KP, Hamilton S (1999) Recombinant tissue-type plasminogen activator (Alteplase) for ischemic stroke 3 to 5 hours after symptom onset. The ATLANTIS Study: a randomized controlled trial. Alteplase Thrombolysis for Acute Noninterventional Therapy in Ischemic Stroke. Jama 282:2019-2026.

Clemens MJ (2004) Targets and mechanisms for the regulation of translation in malignant transformation. Oncogene 23:3180-3188.

Clemens MJ, Bushell M, Morley SJ (1998) Degradation of eukaryotic polypeptide chain initiation factor (eIF) 4G in response to induction of apoptosis in human lymphoma cell lines. Oncogene 17:2921-2931.

Clemens MJ, Bushell M, Jeffrey IW, Pain VM, Morley SJ (2000) Translation initiation factor modifications and the regulation of protein synthesis in apoptotic cells. Cell Death Differ 7:603-615.

Cohen-Armon M, Visochek L, Katzoff A, Levitan D, Susswein AJ, Klein R, Valbrun M, Schwartz JH (2004) Long-term memory requires polyADP-ribosylation. Science 304:1820-1822.

Coldwell MJ, Mitchell SA, Stoneley M, MacFarlane M, Willis AE (2000) Initiation of Apaf-1 translation by internal ribosome entry. Oncogene 19:899-905.

Collins RC, Nandi N, Smith CB, Sokoloff L (1980) Focal seizures inhibit brain protein synthesis. Trans Am Neurol Assoc 105:43-46.

Constantinou C, Clemens MJ (2007) Regulation of translation factors eIF4GI and 4E-BP1 during recovery of protein synthesis from inhibition by p53. Cell Death Differ 14:576-585.

Cooper HK, Zalewska T, Kawakami S, Hossmann KA, Kleihues P (1977) The effect of ischaemia and recirculation on protein synthesis in the rat brain. J Neurochem 28:929-934.

Cotter TG, Lennon SV, Glynn JG, Martin SJ (1990) Cell death via apoptosis and its relationship to growth, development and differentiation of both tumour and normal cells. Anticancer Res 10:1153-1159.

Cozzi A, Cipriani G, Fossati S, Faraco G, Formentini L, Min W, Cortes U, Wang ZQ, Moroni F, Chiarugi A (2006) Poly(ADP-ribose) accumulation and enhancement of postischemic brain damage in 110-kDa poly(ADP-ribose) glycohydrolase null mice. J Cereb Blood Flow Metab 26:684-695.

Cregan SP, Fortin A, MacLaurin JG, Callaghan SM, Cecconi F, Yu SW, Dawson TM, Dawson VL, Park DS, Kroemer G, Slack RS (2002) Apoptosis-inducing factor is involved in the regulation of caspase-independent neuronal cell death. J Cell Biol 158:507-517.

Cuerrier D, Moldoveanu T, Davies PL (2005) Determination of peptide substrate specificity for mu-calpain by a peptide library-based approach: the importance of primed side interactions. J Biol Chem 280:40632-40641.

Culmsee C, Landshamer S (2006) Molecular insights into mechanisms of the cell death program: role in the progression of neurodegenerative disorders. Curr Alzheimer Res 3:269-283.

Culmsee C, Zhu C, Landshamer S, Becattini B, Wagner E, Pellecchia M, Blomgren K, Plesnila N (2005) Apoptosis-inducing factor triggered by poly(ADP-ribose) polymerase and Bid mediates neuronal cell death after oxygen-glucose deprivation and focal cerebral ischemia. J Neurosci 25:10262-10272.

Czogalla A, Sikorski AF (2005) Spectrin and calpain: a 'target' and a 'sniper' in the pathology of neuronal cells. Cell Mol Life Sci 62:1913-1924.

D'Amours D, Desnoyers S, D'Silva I, Poirier GG (1999) Poly(ADP-ribosyl)ation reactions in the regulation of nuclear functions. Biochem J 342 (Pt 2):249-268.

Davidovic L, Vodenicharov M, Affar EB, Poirier GG (2001) Importance of poly(ADP-ribose) glycohydrolase in the control of poly(ADP-ribose) metabolism. Exp Cell Res 268:7-13.

Dawson VL, Dawson TM, London ED, Bredt DS, Snyder SH (1991) Nitric oxide mediates glutamate neurotoxicity in primary cortical cultures. Proc Natl Acad Sci U S A 88:6368-6371.

Dawson VL, Kizushi VM, Huang PL, Snyder SH, Dawson TM (1996) Resistance to neurotoxicity in cortical cultures from neuronal nitric oxide synthase-deficient mice. J Neurosci 16:2479-2487.

De Jongh KS, Colvin AA, Wang KK, Catterall WA (1994) Differential proteolysis of the full-length form of the L-type calcium channel alpha 1 subunit by calpain. J Neurochem 63:1558-1564.

de Murcia JM, Niedergang C, Trucco C, Ricoul M, Dutrillaux B, Mark M, Oliver FJ, Masson M, Dierich A, LeMeur M, Walztinger C, Chambon P, de Murcia G (1997) Requirement of poly(ADP-ribose) polymerase in recovery from DNA damage in mice and in cells. Proc Natl Acad Sci U S A 94:7303-7307.

DeGracia DJ, Hu BR (2007) Irreversible translation arrest in the reperfused brain. J Cereb Blood Flow Metab 27:875-893.

DeGracia DJ, Neumar RW, White BC, Krause GS (1996) Global brain ischemia and reperfusion: modifications in eukaryotic initiation factors associated with inhibition of translation initiation. J Neurochem 67:2005-2012.

DeGracia DJ, Rafols JA, Morley SJ, Kayali F (2006) Immunohistochemical mapping of total and phosphorylated eukaryotic initiation factor 4G in rat hippocampus following global brain ischemia and reperfusion. Neuroscience 139:1235-1248.

DeGracia DJ, Jamison JT, Szymanski JJ, Lewis MK (2008) Translation arrest and ribonomics in post-ischemic brain: layers and layers of players. J Neurochem 106:2288-2301.

DeGracia DJ, Rudolph J, Roberts GG, Rafols JA, Wang J (2007) Convergence of stress granules and protein aggregates in hippocampal cornu ammonis 1 at later reperfusion following global brain ischemia. Neuroscience 146:562-572.

DeGracia DJ, Sullivan JM, Neumar RW, Alousi SS, Hikade KR, Pittman JE, White BC, Rafols JA, Krause GS (1997) Effect of brain ischemia and reperfusion on the localization of phosphorylated eukaryotic initiation factor 2 alpha. J Cereb Blood Flow Metab 17:1291-1302.

DeMartino GN, Wachendorfer R, McGuire MJ, Croall DE (1988) Proteolysis of the protein inhibitor of calcium-dependent proteases produces lower molecular weight fragments that retain inhibitory activity. Arch Biochem Biophys 262:189-198.

Dienel GA, Pulsinelli WA, Duffy TE (1980) Regional protein synthesis in rat brain following acute hemispheric ischemia. J Neurochem 35:1216-1226.

Dirnagl U, Iadecola C, Moskowitz MA (1999) Pathobiology of ischaemic stroke: an integrated view. Trends Neurosci 22:391-397.

Dobrikova EY, Grisham RN, Kaiser C, Lin J, Gromeier M (2006) Competitive translation efficiency at the picornavirus type 1 internal ribosome entry site facilitated by viral cis and trans factors. J Virol 80:3310-3321.

Du L, Zhang X, Han YY, Burke NA, Kochanek PM, Watkins SC, Graham SH, Carcillo JA, Szabo C, Clark RS (2003) Intra-mitochondrial poly(ADP-ribosylation) contributes to NAD+ depletion and cell death induced by oxidative stress. J Biol Chem 278:18426-18433.

Duan Y, Gross RA, Sheu SS (2007) Ca2+-dependent generation of mitochondrial reactive oxygen species serves as a signal for poly(ADP-ribose) polymerase-1 activation during glutamate excitotoxicity. J Physiol 585:741-758.

Dutt P, Croall DE, Arthur JS, Veyra TD, Williams K, Elce JS, Greer PA (2006) m-Calpain is required for preimplantation embryonic development in mice. BMC Dev Biol 6:3.

Dwyer BE, Wasterlain CG (1984) Selective focal inhibition of brain protein synthesis during generalized bicuculline seizures in newborn marmoset monkeys. Brain Res 308:109-121.

Edvinsson LaK, DN (2002) Cerebral Blood Flow and Metabolism, 2nd Edition: Lippincott Williams and Wilkins.

Eliasson MJ, Sampei K, Mandir AS, Hurn PD, Traystman RJ, Bao J, Pieper A, Wang ZQ, Dawson TM, Snyder SH, Dawson VL (1997) Poly(ADP-ribose) polymerase gene disruption renders mice resistant to cerebral ischemia. Nat Med 3:1089-1095.

Endres M, Wang ZQ, Namura S, Waeber C, Moskowitz MA (1997) Ischemic brain injury is mediated by the activation of poly(ADP-ribose)polymerase. J Cereb Blood Flow Metab 17:1143-1151.

Evenson KR, Rosamond WD, Morris DL (2001) Prehospital and in-hospital delays in acute stroke care. Neuroepidemiology 20:65-76.

French JP, Quindry JC, Falk DJ, Staib JL, Lee Y, Wang KK, Powers SK (2006) Ischemia-reperfusion-induced calpain activation and SERCA2a degradation are attenuated by exercise training and calpain inhibition. Am J Physiol Heart Circ Physiol 290:H128-136.

Fulco M, Sartorelli V (2008) Comparing and contrasting the roles of AMPK and SIRT1 in metabolic tissues. Cell Cycle 7:3669-3679.

Fumagall S, Thomas G (2000) S6 phosphorylation and signal transduction In: Translational Control and Gene Expression (Sonenberg N, Hershey JWB, Mathews MB, eds), pp 695-718. New York: Cold Spring Harbor Laboratory Press.

Furlan A, Higashida R, Wechsler L, Gent M, Rowley H, Kase C, Pessin M, Ahuja A, Callahan F, Clark WM, Silver F, Rivera F (1999) Intra-arterial prourokinase for acute ischemic stroke. The PROACT II study: a randomized controlled trial. Prolyse in Acute Cerebral Thromboembolism. Jama 282:2003-2011.

Furukawa K, Estus S, Fu W, Mark RJ, Mattson MP (1997) Neuroprotective action of cycloheximide involves induction of bcl-2 and antioxidant pathways. J Cell Biol 136:1137-1149.

Garcia L, O'Loghlen A, Martin ME, Burda J, Salinas M (2004a) Does phosphorylation of eukaryotic elongation factor eEF2 regulate protein synthesis in ischemic preconditioning? J Neurosci Res 77:292-298.

Garcia L, Burda J, Hrehorovska M, Burda R, Martin ME, Salinas M (2004b) Ischaemic preconditioning in the rat brain: effect on the activity of several initiation factors, Akt and extracellular signal-regulated protein kinase phosphorylation, and GRP78 and GADD34 expression. J Neurochem 88:136-147.

Garcia M, Bondada V, Geddes JW (2005) Mitochondrial localization of mu-calpain. Biochem Biophys Res Commun 338:1241-1247.

Gascon S, Sobrado M, Roda JM, Rodriguez-Pena A, Diaz-Guerra M (2008) Excitotoxicity and focal cerebral ischemia induce truncation of the NR2A and NR2B subunits of the NMDA receptor and cleavage of the scaffolding protein PSD-95. Mol Psychiatry 13:99-114.

Gascon S, Deogracias R, Sobrado M, Roda JM, Renart J, Rodriguez-Pena A, Diaz-Guerra M (2005) Transcription of the NR1 subunit of the N-methyl-D-aspartate receptor is down-regulated by excitotoxic stimulation and cerebral ischemia. J Biol Chem 280:35018-35027.

Ghosh M, Shanker S, Siwanowicz I, Mann K, Machleidt W, Holak TA (2005) Proteolysis of insulin-like growth factor binding proteins (IGFBPs) by calpain. Biol Chem 386:85-93.

Gil J, Esteban M (2000) Induction of apoptosis by the dsRNA-dependent protein kinase (PKR): mechanism of action. Apoptosis 5:107-114.

Gilks N, Kedersha N, Ayodele M, Shen L, Stoecklin G, Dember LM, Anderson P (2004) Stress granule assembly is mediated by prion-like aggregation of TIA-1. Mol Biol Cell 15:5383-5398.

Gill R, Foster AC, Woodruff GN (1987) Systemic administration of MK-801 protects against ischemia-induced hippocampal neurodegeneration in the gerbil. J Neurosci 7:3343-3349.

Gingras AC, Raught B, Sonenberg N (1999) eIF4 initiation factors: effectors of mRNA recruitment to ribosomes and regulators of translation. Annu Rev Biochem 68:913-963.

Goll DE, Thompson VF, Taylor RG, Zalewska T (1992) Is calpain activity regulated by membranes and autolysis or by calcium and calpastatin? Bioessays 14:549-556.

Goll DE, Thompson VF, Li H, Wei W, Cong J (2003) The calpain system. Physiol Rev 83:731-801.

Gradi A, Imataka H, Svitkin YV, Rom E, Raught B, Morino S, Sonenberg N (1998) A novel functional human eukaryotic translation initiation factor 4G. Mol Cell Biol 18:334-342.

Greenberg JH, Uematsu D, Araki N, Hickey WF, Reivich M (1990) Cytosolic free calcium during focal cerebral ischemia and the effects of nimodipine on calcium and histologic damage. Stroke 21:IV72-77.

Gubitz G, Sandercock P, Counsell C (2004) Anticoagulants for acute ischaemic stroke. Cochrane Database Syst Rev:CD000024.

Guttmann RP, Baker DL, Seifert KM, Cohen AS, Coulter DA, Lynch DR (2001) Specific proteolysis of the NR2 subunit at multiple sites by calpain. J Neurochem 78:1083-1093.

Guttmann RP, Sokol S, Baker DL, Simpkins KL, Dong Y, Lynch DR (2002) Proteolysis of the N-methyl-d-aspartate receptor by calpain in situ. J Pharmacol Exp Ther 302:1023-1030.

Hacke W, Kaste M, Fieschi C, Toni D, Lesaffre E, von Kummer R, Boysen G, Bluhmki E, Hoxter G, Mahagne MH, et al. (1995) Intravenous thrombolysis with recombinant tissue plasminogen activator for acute hemispheric stroke. The European Cooperative Acute Stroke Study (ECASS). Jama 274:1017-1025.

Hacke W, Kaste M, Fieschi C, von Kummer R, Davalos A, Meier D, Larrue V, Bluhmki E, Davis S, Donnan G, Schneider D, Diez-Tejedor E, Trouillas P (1998) Randomised double-blind placebo-controlled trial of thrombolytic therapy with intravenous alteplase in acute ischaemic stroke (ECASS II). Second European-Australasian Acute Stroke Study Investigators. Lancet 352:1245-1251.

Hacke W, Kaste M, Bluhmki E, Brozman M, Davalos A, Guidetti D, Larrue V, Lees KR, Medeghri Z, Machnig T, Schneider D, von Kummer R, Wahlgren N, Toni D (2008) Thrombolysis with alteplase 3 to 4.5 hours after acute ischemic stroke. N Engl J Med 359:1317-1329.

Hacke W, Donnan G, Fieschi C, Kaste M, von Kummer R, Broderick JP, Brott T, Frankel M, Grotta JC, Haley EC, Jr., Kwiatkowski T, Levine SR, Lewandowski C, Lu M, Lyden P, Marler JR, Patel S, Tilley BC, Albers G, Bluhmki E, Wilhelm M, Hamilton S (2004) Association of outcome with early stroke treatment: pooled analysis of ATLANTIS, ECASS, and NINDS rt-PA stroke trials. Lancet 363:768-774.

Hansen TM, Moss AJ, Brindle NP (2008) Vascular endothelial growth factor and angiopoietins in neurovascular regeneration and protection following stroke. Curr Neurovasc Res 5:236-245.

Hara MR, Snyder SH (2007) Cell signaling and neuronal death. Annu Rev Pharmacol Toxicol 47:117-141.

Harding HP, Zhang Y, Ron D (1999) Protein translation and folding are coupled by an endoplasmic-reticulum-resident kinase. Nature 397:271-274.

Harding HP, Zhang Y, Bertolotti A, Zeng H, Ron D (2000) Perk is essential for translational regulation and cell survival during the unfolded protein response. Mol Cell 5:897-904.

Hata R, Maeda K, Hermann D, Mies G, Hossmann KA (2000a) Evolution of brain infarction after transient focal cerebral ischemia in mice. J Cereb Blood Flow Metab 20:937-946.

Hata R, Maeda K, Hermann D, Mies G, Hossmann KA (2000b) Dynamics of regional brain metabolism and gene expression after middle cerebral artery occlusion in mice. J Cereb Blood Flow Metab 20:306-315.

Hata R, Mies G, Wiessner C, Fritze K, Hesselbarth D, Brinker G, Hossmann KA (1998) A reproducible model of middle cerebral artery occlusion in mice: hemodynamic, biochemical, and magnetic resonance imaging. J Cereb Blood Flow Metab 18:367-375.

Heikkila JJ, Brown IR (1979a) Hyperthermia and disaggregation of brain polysomes induced by bacterial pyrogen. Life Sci 25:347-352.

Heikkila JJ, Brown IR (1979b) Disaggregation of brain polysomes after LSD in vivo. Involvement of LSD-induced hyperthermia. Neurochem Res 4:763-776.

Heiss WD (1992) Experimental evidence of ischemic thresholds and functional recovery. Stroke 23:1668-1672.

Hell JW, Westenbroek RE, Breeze LJ, Wang KK, Chavkin C, Catterall WA (1996) N-methyl-D-aspartate receptor-induced proteolytic conversion of postsynaptic class C L-type calcium channels in hippocampal neurons. Proc Natl Acad Sci U S A 93:3362-3367.

Henis-Korenblit S, Strumpf NL, Goldstaub D, Kimchi A (2000) A novel form of DAP5 protein accumulates in apoptotic cells as a result of caspase cleavage and internal ribosome entry site-mediated translation. Mol Cell Biol 20:496-506.

Hirtz D, Thurman DJ, Gwinn-Hardy K, Mohamed M, Chaudhuri AR, Zalutsky R (2007) How common are the "common" neurologic disorders? Neurology 68:326-337.

Holcik M, Sonenberg N (2005) Translational control in stress and apoptosis. Nat Rev Mol Cell Biol 6:318-327.

Hossmann KA (1971) Cortical steady potential, impedance and excitability changes during and after total ischemia of cat brain. Exp Neurol 32:163-175.

Hossmann KA (1993) Disturbances of cerebral protein synthesis and ischemic cell death. Prog Brain Res 96:161-177.

Hossmann KA (1994) Viability thresholds and the penumbra of focal ischemia. Ann Neurol 36:557-565.

Hossmann KA (2006) Pathophysiology and therapy of experimental stroke. Cell Mol Neurobiol 26:1057-1083.

Hossmann KA, Zimmermann V (1974) Resuscitation of the monkey brain after 1 h complete ischemia. I. Physiological and morphological observations. Brain Res 81:59-74.

Hossmann KA, Schmidt-Kastner R, Grosse Ophoff B (1987) Recovery of integrative central nervous function after one hour global cerebro-circulatory arrest in normothermic cat. J Neurol Sci 77:305-320.

Hou ST, Jiang SX, Desbois A, Huang D, Kelly J, Tessier L, Karchewski L, Kappler J (2006) Calpain-cleaved collapsin response mediator protein-3 induces neuronal death after glutamate toxicity and cerebral ischemia. J Neurosci 26:2241-2249.

Hu BR, Martone ME, Jones YZ, Liu CL (2000) Protein aggregation after transient cerebral ischemia. J Neurosci 20:3191-3199.

Hu BR, Janelidze S, Ginsberg MD, Busto R, Perez-Pinzon M, Sick TJ, Siesjo BK, Liu CL (2001) Protein aggregation after focal brain ischemia and reperfusion. J Cereb Blood Flow Metab 21:865-875.

Hyrc K, Handran SD, Rothman SM, Goldberg MP (1997) Ionized intracellular calcium concentration predicts excitotoxic neuronal death: observations with low-affinity fluorescent calcium indicators. J Neurosci 17:6669-6677.

Imataka H, Olsen HS, Sonenberg N (1997) A new translational regulator with homology to eukaryotic translation initiation factor 4G. Embo J 16:817-825.

Inoki K, Zhu T, Guan KL (2003) TSC2 mediates cellular energy response to control cell growth and survival. Cell 115:577-590.

Jackson RJ (2005) Alternative mechanisms of initiating translation of mammalian mRNAs. Biochem Soc Trans 33:1231-1241.

Jamison JT, Kayali F, Rudolph J, Marshall M, Kimball SR, DeGracia DJ (2008) Persistent redistribution of poly-adenylated mRNAs correlates with translation arrest and cell death following global brain ischemia and reperfusion. Neuroscience 154:504-520.

Jamsa A, Backstrom A, Gustafsson E, Dehvari N, Hiller G, Cowburn RF, Vasange M (2006) Glutamate treatment and p25 transfection increase Cdk5 mediated tau phosphorylation in SH-SY5Y cells. Biochem Biophys Res Commun 345:324-331.

Jiang SX, Kappler J, Zurakowski B, Desbois A, Aylsworth A, Hou ST (2007) Calpain cleavage of collapsin response mediator proteins in ischemic mouse brain. Eur J Neurosci 26:801-809.

Johnston SC, Gress DR, Browner WS, Sidney S (2000) Short-term prognosis after emergency department diagnosis of TIA. Jama 284:2901-2906.

Jones TH, Morawetz RB, Crowell RM, Marcoux FW, FitzGibbon SJ, DeGirolami U, Ojemann RG (1981) Thresholds of focal cerebral ischemia in awake monkeys. J Neurosurg 54:773-782.

Joy J, Nalabothula N, Ghosh M, Popp O, Jochum M, Machleidt W, Gil-Parrado S, Holak TA (2006) Identification of calpain cleavage sites in the G1 cyclin-dependent kinase inhibitor p19(INK4d). Biol Chem 387:329-335.

Kaiser C, Dobrikova EY, Bradrick SS, Shveygert M, Herbert JT, Gromeier M (2008) Activation of cap-independent translation by variant eukaryotic initiation factor 4G in vivo. Rna 14:2170-2182.

Kataoka K, Graf R, Rosner G, Heiss WD (1987) Experimental focal ischemia in cats: changes in multimodality evoked potentials as related to local cerebral blood flow and ischemic brain edema. Stroke 18:188-194.

Kaufman RJ (1999) Stress signaling from the lumen of the endoplasmic reticulum: coordination of gene transcriptional and translational controls. Genes Dev 13:1211-1233.

Kayali F, Montie HL, Rafols JA, DeGracia DJ (2005) Prolonged translation arrest in reperfused hippocampal cornu Ammonis 1 is mediated by stress granules. Neuroscience 134:1223-1245.

Kedersha N, Anderson P (2002) Stress granules: sites of mRNA triage that regulate mRNA stability and translatability. Biochem Soc Trans 30:963-969.

Kedersha N, Stoecklin G, Ayodele M, Yacono P, Lykke-Andersen J, Fitzler MJ, Scheuner D, Kaufman RJ, Golan DE, Anderson P (2005) Stress granules and processing bodies are dynamically linked sites of mRNP remodeling. J Cell Biol 169:871-884.

Kedersha NL, Gupta M, Li W, Miller I, Anderson P (1999) RNA-binding proteins TIA-1 and TIAR link the phosphorylation of eIF-2 alpha to the assembly of mammalian stress granules. J Cell Biol 147:1431-1442.

Keene JD (2007) RNA regulons: coordination of post-transcriptional events. Nat Rev Genet 8:533-543.

Kesner RP, Partlow LM, Bush LG, Berman RF (1981) A quantitative regional analysis of protein synthesis inhibition in the rat brain following localized injection of cycloheximide. Brain Res 209:159-176.

Kiessling M, Kleihues P (1981) Regional protein synthesis in the rat brain during bicuculline-induced epileptic seizures. Acta Neuropathol 55:157-162.

Kiessling M, Xie Y, Kleihues P (1984) Regionally selective inhibition of cerebral protein synthesis in the rat during hypoglycemia and recovery. J Neurochem 43:1507-1514.

Kiessling M, Auer RN, Kleihues P, Siesjo BK (1986) Cerebral protein synthesis during long-term recovery from severe hypoglycemia. J Cereb Blood Flow Metab 6:42-51.

Kim MY, Zhang T, Kraus WL (2005) Poly(ADP-ribosyl)ation by PARP-1: 'PAR-laying' NAD+ into a nuclear signal. Genes Dev 19:1951-1967.

Kimball SR (2001) Regulation of translation initiation by amino acids in eukaryotic cells. Prog Mol Subcell Biol 26:155-184.

Kinouchi H, Sharp FR, Hill MP, Koistinaho J, Sagar SM, Chan PH (1993) Induction of 70-kDa heat shock protein and hsp70 mRNA following transient focal cerebral ischemia in the rat. J Cereb Blood Flow Metab 13:105-115.

Kintner DB, Luo J, Gerdts J, Ballard AJ, Shull GE, Sun D (2007) Role of Na+-K+-Cl- cotransport and Na+/Ca2+ exchange in mitochondrial dysfunction in astrocytes following in vitro ischemia. Am J Physiol Cell Physiol 292:C1113-1122.

Kirino T (1982) Delayed neuronal death in the gerbil hippocampus following ischemia. Brain Res 239:57-69.

Kleihues P, Hossmann KA (1971) Protein synthesis in the cat brain after prolonged cerebral ischemia. Brain Res 35:409-418.

Kleihues P, Hossmann KA (1973) Regional incorporation of L-(3-3H)tyrosine into cat brain proteins after 1 hour of complete ischemia. Acta Neuropathol 25:313-324.

Kleihues P, Hossmann KA, Pegg AE, Kobayashi K, Zimmermann V (1975) Resuscitation of the monkey brain after one hour complete ischemia. III. Indications of metabolic recovery. Brain Res 95:61-73.

Klein JA, Longo-Guess CM, Rossmann MP, Seburn KL, Hurd RE, Frankel WN, Bronson RT, Ackerman SL (2002) The harlequin mouse mutation downregulates apoptosis-inducing factor. Nature 419:367-374.

Knowles RG, Moncada S (1994) Nitric oxide synthases in mammals. Biochem J 298 (Pt 2):249-258.

Koh JY, Choi DW (1987) Quantitative determination of glutamate mediated cortical neuronal injury in cell culture by lactate dehydrogenase efflux assay. J Neurosci Methods 20:83-90.

Koike M, Shibata M, Tadakoshi M, Gotoh K, Komatsu M, Waguri S, Kawahara N, Kuida K, Nagata S, Kominami E, Tanaka K, Uchiyama Y (2008) Inhibition of autophagy prevents hippocampal pyramidal neuron death after hypoxic-ischemic injury. Am J Pathol 172:454-469.

Krivanek J (1978) On the mechanism of the inhibitory effect of potasium ions on amino acid incorporation into rat cerebral cortex proteins in vivo. Physiol Bohemoslov 27:117-124.

Kumar R, Krause GS, Yoshida H, Mori K, DeGracia DJ (2003) Dysfunction of the unfolded protein response during global brain ischemia and reperfusion. J Cereb Blood Flow Metab 23:462-471.

Kumar R, Azam S, Sullivan JM, Owen C, Cavener DR, Zhang P, Ron D, Harding HP, Chen JJ, Han A, White BC, Krause GS, DeGracia DJ (2001) Brain ischemia and reperfusion activates the eukaryotic initiation factor 2alpha kinase, PERK. J Neurochem 77:1418-1421.

Lee HT, Chang YC, Tu YF, Huang CC (2009) VEGF-A/VEGFR-2 signaling leading to cAMP response element-binding protein phosphorylation is a shared pathway underlying the protective effect of preconditioning on neurons and endothelial cells. J Neurosci 29:4356-4368.

Li J, Zeng Z, Viollet B, Ronnett GV, McCullough LD (2007) Neuroprotective effects of adenosine monophosphate-activated protein kinase inhibition and gene deletion in stroke. Stroke 38:2992-2999.

Liu B, Liao M, Mielke JG, Ning K, Chen Y, Li L, El-Hayek YH, Gomez E, Zukin RS, Fehlings MG, Wan Q (2006) Ischemic insults direct glutamate receptor subunit 2-lacking AMPA receptors to synaptic sites. J Neurosci 26:5309-5319.

Liu C, Chen S, Kamme F, Hu BR (2005a) Ischemic preconditioning prevents protein aggregation after transient cerebral ischemia. Neuroscience 134:69-80.

Liu CL, Ge P, Zhang F, Hu BR (2005b) Co-translational protein aggregation after transient cerebral ischemia. Neuroscience 134:1273-1284.

Lloyd-Jones D, Adams R, Carnethon M, De Simone G, Ferguson TB, Flegal K, Ford E, Furie K, Go A, Greenlund K, Haase N, Hailpern S, Ho M, Howard V, Kissela B, Kittner S, Lackland D, Lisabeth L, Marelli A, McDermott M, Meigs J, Mozaffarian D, Nichol G, O'Donnell C, Roger V, Rosamond W, Sacco R, Sorlie P, Stafford R, Steinberger J, Thom T, Wasserthiel-Smoller S, Wong N, Wylie-Rosett J, Hong Y (2009) Heart disease and stroke statistics -- 2009 update: a report from the American Heart Association Statistics Committee and Stroke Statistics Subcommittee. Circulation 119:480-486.

Lobner D, Choi DW (1996) Preincubation with protein synthesis inhibitors protects cortical neurons against oxygen-glucose deprivation-induced death. Neuroscience 72:335-341.

Lopez de Silanes I, Galban S, Martindale JL, Yang X, Mazan-Mamczarz K, Indig FE, Falco G, Zhan M, Gorospe M (2005) Identification and functional outcome of mRNAs associated with RNA-binding protein TIA-1. Mol Cell Biol 25:9520-9531.

Lucas DR, Newhouse JP (1957) The effects of nutritional and endocrine factors on an inherited retinal degeneration in the mouse. AMA Arch Ophthalmol 57:224-235.

Lykke-Andersen J, Wagner E (2005) Recruitment and activation of mRNA decay enzymes by two ARE-mediated decay activation domains in the proteins TTP and BRF-1. Genes Dev 19:351-361.

MacInnes JW, Luttges MW (1973) Interactive effects of cycloheximide and puromycin in altering brain polyribosomes and neutral and behavioural responses to electroshock in mice. J Neurochem 21:775-781.

Magistretti PJ PJ, Martin JL ed (1995) Brain Energy Metabolism: An Integrated Cellular Perspective New York: Raven Press.

Magnusson A, Haug LS, Walaas SI, Ostvold AC (1993) Calcium-induced degradation of the inositol (1,4,5)-trisphosphate receptor/Ca(2+)-channel. FEBS Lett 323:229-232.

Malagelada C, Xifro X, Minano A, Sabria J, Rodriguez-Alvarez J (2005) Contribution of caspase-mediated apoptosis to the cell death caused by oxygen-glucose deprivation in cortical cell cultures. Neurobiol Dis 20:27-37.

Mandir AS, Poitras MF, Berliner AR, Herring WJ, Guastella DB, Feldman A, Poirier GG, Wang ZQ, Dawson TM, Dawson VL (2000) NMDA but not non-NMDA excitotoxicity is mediated by Poly(ADP-ribose) polymerase. J Neurosci 20:8005-8011.

Mao X, Moerman AM, Barger SW (2002) Neuronal kappa B-binding factors consist of Sp1-related proteins. Functional implications for autoregulation of N-methyl-D-aspartate receptor-1 expression. J Biol Chem 277:44911-44919.

Mao X, Yang SH, Simpkins JW, Barger SW (2007) Glutamate receptor activation evokes calpain-mediated degradation of Sp3 and Sp4, the prominent Sp-family transcription factors in neurons. J Neurochem 100:1300-1314.

Marissen WE, Lloyd RE (1998) Eukaryotic translation initiation factor 4G is targeted for proteolytic cleavage by caspase 3 during inhibition of translation in apoptotic cells. Mol Cell Biol 18:7565-7574.

Marissen WE, Gradi A, Sonenberg N, Lloyd RE (2000) Cleavage of eukaryotic translation initiation factor 4GII correlates with translation inhibition during apoptosis. Cell Death Differ 7:1234-1243.

Marks JD, Boriboun C, Wang J (2005) Mitochondrial nitric oxide mediates decreased vulnerability of hippocampal neurons from immature animals to NMDA. J Neurosci 25:6561-6575.

Martin de la Vega C, Burda J, Nemethova M, Quevedo C, Alcazar A, Martin ME, Danielisova V, Fando JL, Salinas M (2001) Possible mechanisms involved in the down-regulation of translation during transient global ischaemia in the rat brain. Biochem J 357:819-826.

Martin DP, Schmidt RE, DiStefano PS, Lowry OH, Carter JG, Johnson EM, Jr. (1988) Inhibitors of protein synthesis and RNA synthesis prevent neuronal death caused by nerve growth factor deprivation. J Cell Biol 106:829-844.

Martin ME, Munoz FM, Salinas M, Fando JL (2000) Ischaemia induces changes in the association of the binding protein 4E-BP1 and eukaryotic initiation factor (eIF) 4G to eIF4E in differentiated PC12 cells. Biochem J 351 Pt 2:327-334.

Martin SJ, Lennon SV, Bonham AM, Cotter TG (1990) Induction of apoptosis (programmed cell death) in human leukemic HL-60 cells by inhibition of RNA or protein synthesis. J Immunol 145:1859-1867.

Matsumoto K, Graf R, Rosner G, Shimada N, Heiss WD (1992) Flow thresholds for extracellular purine catabolite elevation in cat focal ischemia. Brain Res 579:309-314.

Mattson MP, Kumar KN, Wang H, Cheng B, Michaelis EK (1993) Basic FGF regulates the expression of a functional 71 kDa NMDA receptor protein that mediates calcium influx and neurotoxicity in hippocampal neurons. J Neurosci 13:4575-4588.

McCaig D, Imai H, Gallagher L, Graham DI, Harland J, Moira Brown S, Mhairi Macrae I (2005) Evolution of GADD34 expression after focal cerebral ischaemia. Brain Res 1034:51-61.

McCullough KD, Martindale JL, Klotz LO, Aw TY, Holbrook NJ (2001) Gadd153 sensitizes cells to endoplasmic reticulum stress by down-regulating Bcl2 and perturbing the cellular redox state. Mol Cell Biol 21:1249-1259.

McGinnis KM, Gnegy ME, Park YH, Mukerjee N, Wang KK (1999) Procaspase-3 and poly(ADP)ribose polymerase (PARP) are calpain substrates. Biochem Biophys Res Commun 263:94-99.

Meloni BP, Majda BT, Knuckey NW (2002) Evaluation of preconditioning treatments to protect near-pure cortical neuronal cultures from in vitro ischemia induced acute and delayed neuronal death. Brain Res 928:69-75.

Memezawa H, Smith ML, Siesjo BK (1992) Penumbral tissues salvaged by reperfusion following middle cerebral artery occlusion in rats. Stroke 23:552-559.

Mengesdorf T, Proud CG, Mies G, Paschen W (2002) Mechanisms underlying suppression of protein synthesis induced by transient focal cerebral ischemia in mouse brain. Exp Neurol 177:538-546.

Metter EJ, Yanagihara T (1979) Protein synthesis in rat brain in hypoxia, anoxia and hypoglycemia. Brain Res 161:481-492.

Mies G, Iijima T, Hossmann KA (1993a) Correlation between peri-infarct DC shifts and ischaemic neuronal damage in rat. Neuroreport 4:709-711.

Mies G, Kohno K, Hossmann KA (1993b) MK-801, a glutamate antagonist, lowers flow threshold for inhibition of protein synthesis after middle cerebral artery occlusion of rat. Neurosci Lett 155:65-68.

Mies G, Kohno K, Hossmann KA (1994) Prevention of periinfarct direct current shifts with glutamate antagonist NBQX following occlusion of the middle cerebral artery in the rat. J Cereb Blood Flow Metab 14:802-807.

Mies G, Ishimaru S, Xie Y, Seo K, Hossmann KA (1991) Ischemic thresholds of cerebral protein synthesis and energy state following middle cerebral artery occlusion in rat. J Cereb Blood Flow Metab 11:753-761.

Miramar MD, Costantini P, Ravagnan L, Saraiva LM, Haouzi D, Brothers G, Penninger JM, Peleato ML, Kroemer G, Susin SA (2001) NADH oxidase activity of mitochondrial apoptosis-inducing factor. J Biol Chem 276:16391-16398.

Morimoto K, Yanagihara T (1981) Cerebral ischemia in gerbils: polyribosomal function during progression and recovery. Stroke 12:105-110.

Morimoto K, Brengman J, Yanagihara T (1978) Further evaluation of polypeptide synthesis in cerebral anoxia, hypoxia and ischemia. J Neurochem 31:1277-1282.

Morley SJ, McKendrick L, Bushell M (1998) Cleavage of translation initiation factor 4G (eIF4G) during anti-Fas IgM-induced apoptosis does not require signalling through the p38 mitogen-activated protein (MAP) kinase. FEBS Lett 438:41-48.

Morley SJ, Coldwell MJ, Clemens MJ (2005) Initiation factor modifications in the preapoptotic phase. Cell Death Differ 12:571-584.

Morley SJ, Jeffrey I, Bushell M, Pain VM, Clemens MJ (2000) Differential requirements for caspase-8 activity in the mechanism of phosphorylation of eIF2alpha, cleavage of eIF4GI and signaling events associated with the inhibition of protein synthesis in apoptotic Jurkat T cells. FEBS Lett 477:229-236.

Moubarak RS, Yuste VJ, Artus C, Bouharrour A, Greer PA, Menissier-de Murcia J, Susin SA (2007) Sequential activation of poly(ADP-ribose) polymerase 1, calpains, and Bax is essential in apoptosis-inducing factor-mediated programmed necrosis. Mol Cell Biol 27:4844-4862.

Munoz F, Martin ME, Manso-Tomico J, Berlanga J, Salinas M, Fando JL (2000) Ischemia-induced phosphorylation of initiation factor 2 in differentiated PC12 cells: role for initiation factor 2 phosphatase. J Neurochem 75:2335-2345.

Murachi T, Tanaka K, Hatanaka M, Murakami T (1980) Intracellular Ca2+-dependent protease (calpain) and its high-molecular-weight endogenous inhibitor (calpastatin). Adv Enzyme Regul 19:407-424.

Murata T, Morita N, Hikita K, Kiuchi K, Kaneda N (2005) Recruitment of mRNA-destabilizing protein TIS11 to stress granules is mediated by its zinc finger domain. Exp Cell Res 303:287-299.

Nedergaard M, Astrup J (1986) Infarct rim: effect of hyperglycemia on direct current potential and [14C]2-deoxyglucose phosphorylation. J Cereb Blood Flow Metab 6:607-615.

Neumar RW, Hagle SM, DeGracia DJ, Krause GS, White BC (1996) Brain mu-calpain autolysis during global cerebral ischemia. J Neurochem 66:421-424.

Neumar RW, DeGracia DJ, Konkoly LL, Khoury JI, White BC, Krause GS (1998) Calpain mediates eukaryotic initiation factor 4G degradation during global brain ischemia. J Cereb Blood Flow Metab 18:876-881.

Newcomb-Fernandez JK, Zhao X, Pike BR, Wang KK, Kampfl A, Beer R, DeFord SM, Hayes RL (2001) Concurrent assessment of calpain and caspase-3 activation after oxygen-glucose deprivation in primary septo-hippocampal cultures. J Cereb Blood Flow Metab 21:1281-1294.

Nixon RA (1986) Fodrin degradation by calcium-activated neutral proteinase (CANP) in retinal ganglion cell neurons and optic glia: preferential localization of CANP activities in neurons. J Neurosci 6:1264-1271.

Nowak TS, Jr., Fried RL, Lust WD, Passonneau JV (1985) Changes in brain energy metabolism and protein synthesis following transient bilateral ischemia in the gerbil. J Neurochem 44:487-494.

Olney JW (1969) Brain lesions, obesity, and other disturbances in mice treated with monosodium glutamate. Science 164:719-721.

Owen CR, Kumar R, Zhang P, McGrath BC, Cavener DR, Krause GS (2005) PERK is responsible for the increased phosphorylation of eIF2alpha and the severe inhibition of protein synthesis after transient global brain ischemia. J Neurochem 94:1235-1242.

Ozaki T, Tomita H, Tamai M, Ishiguro S (2007) Characteristics of mitochondrial calpains. J Biochem 142:365-376.

Parsons JT, Churn SB, DeLorenzo RJ (1999) Global ischemia-induced inhibition of the coupling ratio of calcium uptake and ATP hydrolysis by rat whole brain microsomal Mg(2+)/Ca(2+) ATPase. Brain Res 834:32-41.

Paschen W, Mies G, Hossmann KA (1992) Threshold relationship between cerebral blood flow, glucose utilization, and energy metabolites during development of stroke in gerbils. Exp Neurol 117:325-333.

Paschen W, Gissel C, Linden T, Doutheil J (1998a) Erp72 expression activated by transient cerebral ischemia or disturbance of neuronal endoplasmic reticulum calcium stores. Metab Brain Dis 13:55-68.

Paschen W, Aufenberg C, Hotop S, Mengesdorf T (2003) Transient cerebral ischemia activates processing of xbp1 messenger RNA indicative of endoplasmic reticulum stress. J Cereb Blood Flow Metab 23:449-461.

Paschen W, Hayashi T, Saito A, Chan PH (2004) GADD34 protein levels increase after transient ischemia in the cortex but not in the CA1 subfield: implications for post-ischemic recovery of protein synthesis in ischemia-resistant cells. J Neurochem 90:694-701.

Paschen W, Gissel C, Linden T, Althausen S, Doutheil J (1998b) Activation of gadd153 expression through transient cerebral ischemia: evidence that ischemia causes endoplasmic reticulum dysfunction. Brain Res Mol Brain Res 60:115-122.

Patrick GN, Zukerberg L, Nikolic M, de la Monte S, Dikkes P, Tsai LH (1999) Conversion of p35 to p25 deregulates Cdk5 activity and promotes neurodegeneration. Nature 402:615-622.

Pattni K, Millard TH, Banting G (2003) Calpain cleavage of the B isoform of Ins(1,4,5)P3 3-kinase separates the catalytic domain from the membrane anchoring domain. Biochem J 375:643-651.

Pelletier J, Sonenberg N (1988) Internal initiation of translation of eukaryotic mRNA directed by a sequence derived from poliovirus RNA. Nature 334:320-325.

Peng PL, Zhong X, Tu W, Soundarapandian MM, Molner P, Zhu D, Lau L, Liu S, Liu F, Lu Y (2006) ADAR2-dependent RNA editing of AMPA receptor subunit GluR2 determines vulnerability of neurons in forebrain ischemia. Neuron 49:719-733.

Petegnief V, Font-Nieves M, Martin ME, Salinas M, Planas AM (2008) Nitric oxide mediates NMDA-induced persistent inhibition of protein synthesis through dephosphorylation of eukaryotic initiation factor 4E-binding protein 1 and eukaryotic initiation factor 4G proteolysis. Biochem J 411:667-677.

Pillai JB, Isbatan A, Imai S, Gupta MP (2005) Poly(ADP-ribose) polymerase-1-dependent cardiac myocyte cell death during heart failure is mediated by NAD+ depletion and reduced Sir2alpha deacetylase activity. J Biol Chem 280:43121-43130.

Plesnila N, Zhu C, Culmsee C, Groger M, Moskowitz MA, Blomgren K (2004) Nuclear translocation of apoptosis-inducing factor after focal cerebral ischemia. J Cereb Blood Flow Metab 24:458-466.

Polster BM, Basanez G, Etxebarria A, Hardwick JM, Nicholls DG (2005) Calpain I induces cleavage and release of apoptosis-inducing factor from isolated mitochondria. J Biol Chem 280:6447-6454.

Pontremoli S, Viotti PL, Michetti M, Salamino F, Sparatore B, Melloni E (1992) Modulation of inhibitory efficiency of rat skeletal muscle calpastatin by phosphorylation. Biochem Biophys Res Commun 187:751-759.

Pottorf WJ, 2nd, Johanns TM, Derrington SM, Strehler EE, Enyedi A, Thayer SA (2006) Glutamate-induced protease-mediated loss of plasma membrane Ca2+ pump activity in rat hippocampal neurons. J Neurochem 98:1646-1656.

Pulsinelli WA, Brierley JB (1979) A new model of bilateral hemispheric ischemia in the unanesthetized rat. Stroke 10:267-272.

Pulsinelli WA, Buchan AM (1988) The four-vessel occlusion rat model: method for complete occlusion of vertebral arteries and control of collateral circulation. Stroke 19:913-914.

Pulsinelli WA, Brierley JB, Plum F (1982) Temporal profile of neuronal damage in a model of transient forebrain ischemia. Ann Neurol 11:491-498.

Ramezani A, Hawley RG (2002) Generation of HIV-1-based lentiviral vector particles. Curr Protoc Mol Biol Chapter 16:Unit 16 22.

Ramirez-Valle F, Braunstein S, Zavadil J, Formenti SC, Schneider RJ (2008) eIF4GI links nutrient sensing by mTOR to cell proliferation and inhibition of autophagy. J Cell Biol 181:293-307.

Rardon DP, Cefali DC, Mitchell RD, Seiler SM, Hathaway DR, Jones LR (1990) Digestion of cardiac and skeletal muscle junctional sarcoplasmic reticulum vesicles with calpain II. Effects on the Ca2+ release channel. Circ Res 67:84-96.

Rashidian J, Iyirhiaro G, Aleyasin H, Rios M, Vincent I, Callaghan S, Bland RJ, Slack RS, During MJ, Park DS (2005) Multiple cyclin-dependent kinases signals are critical mediators of ischemia/hypoxic neuronal death in vitro and in vivo. Proc Natl Acad Sci U S A 102:14080-14085.

Raval AP, Dave KR, Perez-Pinzon MA (2006) Resveratrol mimics ischemic preconditioning in the brain. J Cereb Blood Flow Metab 26:1141-1147.

Ray SK (2006) Currently evaluated calpain and caspase inhibitors for neuroprotection in experimental brain ischemia. Curr Med Chem 13:3425-3440.

Reeves MJ, Arora S, Broderick JP, Frankel M, Heinrich JP, Hickenbottom S, Karp H, LaBresh KA, Malarcher A, Mensah G, Moomaw CJ, Schwamm L, Weiss P (2005) Acute stroke care in the US: results from 4 pilot prototypes of the Paul Coverdell National Acute Stroke Registry. Stroke 36:1232-1240.

Rogawski MA (2008) Common pathophysiologic mechanisms in migraine and epilepsy. Arch Neurol 65:709-714.

Rothman S (1984) Synaptic release of excitatory amino acid neurotransmitter mediates anoxic neuronal death. J Neurosci 4:1884-1891.

Sandercock PA, Counsell C, Gubitz GJ, Tseng MC (2008) Antiplatelet therapy for acute ischaemic stroke. Cochrane Database Syst Rev:CD000029.

Schlossmann J, Hofmann F (2005) cGMP-dependent protein kinases in drug discovery. Drug Discov Today 10:627-634.

Scott SA, Davies AM (1990) Inhibition of protein synthesis prevents cell death in sensory and parasympathetic neurons deprived of neurotrophic factor in vitro. J Neurobiol 21:630-638.

Seubert P, Baudry M, Dudek S, Lynch G (1987) Calmodulin stimulates the degradation of brain spectrin by calpain. Synapse 1:20-24.

Sharbrough FW, Messick JM, Jr., Sundt TM, Jr. (1973) Correlation of continuous electroencephalograms with cerebral blood flow measurements during carotid endarterectomy. Stroke 4:674-683.

Sharkey J, Butcher SP (1994) Immunophilins mediate the neuroprotective effects of FK506 in focal cerebral ischaemia. Nature 371:336-339.

Shen J, Chen X, Hendershot L, Prywes R (2002) ER stress regulation of ATF6 localization by dissociation of BiP/GRP78 binding and unmasking of Golgi localization signals. Dev Cell 3:99-111.

Shibata A, Maeda D, Ogino H, Tsutsumi M, Nohmi T, Nakagama H, Sugimura T, Teraoka H, Masutani M (2009) Role of Parp-1 in suppressing spontaneous deletion mutation in the liver and brain of mice at adolescence and advanced age. Mutat Res 664:20-27.

Shibata A, Kamada N, Masumura K, Nohmi T, Kobayashi S, Teraoka H, Nakagama H, Sugimura T, Suzuki H, Masutani M (2005) Parp-1 deficiency causes an increase of deletion mutations and insertions/rearrangements in vivo after treatment with an alkylating agent. Oncogene 24:1328-1337.

Shimada N, Graf R, Rosner G, Heiss WD (1990) Differences in ischemia-induced accumulation of amino acids in the cat cortex. Stroke 21:1445-1451.

Shioda N, Moriguchi S, Shirasaki Y, Fukunaga K (2006) Generation of constitutively active calcineurin by calpain contributes to delayed neuronal death following mouse brain ischemia. J Neurochem 98:310-320.

Shioda N, Han F, Moriguchi S, Fukunaga K (2007) Constitutively active calcineurin mediates delayed neuronal death through Fas-ligand expression via activation of NFAT and FKHR transcriptional activities in mouse brain ischemia. J Neurochem 102:1506-1517.

Siman R, Baudry M, Lynch G (1984) Brain fodrin: substrate for calpain I, an endogenous calcium-activated protease. Proc Natl Acad Sci U S A 81:3572-3576.

Simon RP, Swan JH, Griffiths T, Meldrum BS (1984) Blockade of N-methyl-D-aspartate receptors may protect against ischemic damage in the brain. Science 226:850-852.

Simpkins KL, Guttmann RP, Dong Y, Chen Z, Sokol S, Neumar RW, Lynch DR (2003) Selective activation induced cleavage of the NR2B subunit by calpain. J Neurosci 23:11322-11331.

Smith ML, Bendek G, Dahlgren N, Rosen I, Wieloch T, Siesjo BK (1984) Models for studying long-term recovery following forebrain ischemia in the rat. 2. A 2-vessel occlusion model. Acta Neurol Scand 69:385-401.

Smith WS, Sung G, Starkman S, Saver JL, Kidwell CS, Gobin YP, Lutsep HL, Nesbit GM, Grobelny T, Rymer MM, Silverman IE, Higashida RT, Budzik RF, Marks MP (2005) Safety and efficacy of mechanical embolectomy in acute ischemic stroke: results of the MERCI trial. Stroke 36:1432-1438.

Smith WS, Sung G, Saver J, Budzik R, Duckwiler G, Liebeskind DS, Lutsep HL, Rymer MM, Higashida RT, Starkman S, Gobin YP, Frei D, Grobelny T, Hellinger F, Huddle D, Kidwell C, Koroshetz W, Marks M, Nesbit G, Silverman IE (2008) Mechanical thrombectomy for acute ischemic stroke: final results of the Multi MERCI trial. Stroke 39:1205-1212.

Sonenberg N, Hershey JWB, Mathews M (2000) Translational control of gene expression, 2nd Edition. Cold Spring Harbor, NY: Cold Spring Harbor Laboratory Press.

Stansbury JP, Jia H, Williams LS, Vogel WB, Duncan PW (2005) Ethnic disparities in stroke: epidemiology, acute care, and postacute outcomes. Stroke 36:374-386.

Stout AK, Raphael HM, Kanterewicz BI, Klann E, Reynolds IJ (1998) Glutamate-induced neuron death requires mitochondrial calcium uptake. Nat Neurosci 1:366-373.

Susin SA, Lorenzo HK, Zamzami N, Marzo I, Snow BE, Brothers GM, Mangion J, Jacotot E, Costantini P, Loeffler M, Larochette N, Goodlett DR, Aebersold R, Siderovski DP, Penninger JM, Kroemer G (1999) Molecular characterization of mitochondrial apoptosis-inducing factor. Nature 397:441-446.

Suske G (1999) The Sp-family of transcription factors. Gene 238:291-300.

Suzuki R, Yamaguchi T, Li CL, Klatzo I (1983a) The effects of 5-minute ischemia in Mongolian gerbils: II. Changes of spontaneous neuronal activity in cerebral cortex and CA1 sector of hippocampus. Acta Neuropathol 60:217-222.

Suzuki R, Yamaguchi T, Kirino T, Orzi F, Klatzo I (1983b) The effects of 5-minute ischemia in Mongolian gerbils: I. Blood-brain barrier, cerebral blood flow, and local cerebral glucose utilization changes. Acta Neuropathol 60:207-216.

Szabadkai G, Duchen MR (2008) Mitochondria: the hub of cellular Ca2+ signaling. Physiology (Bethesda) 23:84-94.

Takei N, Kawamura M, Hara K, Yonezawa K, Nawa H (2001) Brain-derived neurotrophic factor enhances neuronal translation by activating multiple initiation processes: comparison with the effects of insulin. J Biol Chem 276:42818-42825.

Takei N, Inamura N, Kawamura M, Namba H, Hara K, Yonezawa K, Nawa H (2004) Brain-derived neurotrophic factor induces mammalian target of rapamycin-dependent local activation of translation machinery and protein synthesis in neuronal dendrites. J Neurosci 24:9760-9769.

Tenenbaum SA, Lager PJ, Carson CC, Keene JD (2002) Ribonomics: identifying mRNA subsets in mRNP complexes using antibodies to RNA-binding proteins and genomic arrays. Methods 26:191-198.

Thilmann R, Xie Y, Kleihues P, Kiessling M (1986) Persistent inhibition of protein synthesis precedes delayed neuronal death in postischemic gerbil hippocampus. Acta Neuropathol (Berl) 71:88-93.

Thornton S, Anand N, Purcell D, Lee J (2003) Not just for housekeeping: protein initiation and elongation factors in cell growth and tumorigenesis. J Mol Med 81:536-548.

Tompa P, Buzder-Lantos P, Tantos A, Farkas A, Szilagyi A, Banoczi Z, Hudecz F, Friedrich P (2004) On the sequential determinants of calpain cleavage. J Biol Chem 279:20775-20785.

Towfighi A, Saver JL, Engelhardt R, Ovbiagele B (2007) A midlife stroke surge among women in the United States. Neurology 69:1898-1904.

Tremper-Wells B, Vallano ML (2005) Nuclear calpain regulates Ca2+-dependent signaling via proteolysis of nuclear Ca2+/calmodulin-dependent protein kinase type IV in cultured neurons. J Biol Chem 280:2165-2175.

Trojaborg W, Boysen G (1973) Relation between EEG, regional cerebral blood flow and internal carotid artery pressure during carotid endarterectomy. Electroencephalogr Clin Neurophysiol 34:61-69.

Tsai LH, Delalle I, Caviness VS, Jr., Chae T, Harlow E (1994) p35 is a neural-specific regulatory subunit of cyclin-dependent kinase 5. Nature 371:419-423.

Tsubokawa T, Solaroglu I, Yatsushige H, Cahill J, Yata K, Zhang JH (2006a) Cathepsin and calpain inhibitor E64d attenuates matrix metalloproteinase-9 activity after focal cerebral ischemia in rats. Stroke 37:1888-1894.

Tsubokawa T, Yamaguchi-Okada M, Calvert JW, Solaroglu I, Shimamura N, Yata K, Zhang JH (2006b) Neurovascular and neuronal protection by E64d after focal cerebral ischemia in rats. J Neurosci Res 84:832-840.

Uchino H, Minamikawa-Tachino R, Kristian T, Perkins G, Narazaki M, Siesjo BK, Shibasaki F (2002) Differential neuroprotection by cyclosporin A and FK506 following ischemia corresponds with differing abilities to inhibit calcineurin and the mitochondrial permeability transition. Neurobiol Dis 10:219-233.

Uematsu D, Greenberg JH, Reivich M, Karp A (1988) In vivo measurement of cytosolic free calcium during cerebral ischemia and reperfusion. Ann Neurol 24:420-428.

Uematsu D, Greenberg JH, Araki N, Reivich M (1991a) Mechanism underlying protective effect of MK-801 against NMDA-induced neuronal injury in vivo. J Cereb Blood Flow Metab 11:779-785.

Uematsu D, Araki N, Greenberg JH, Sladky J, Reivich M (1991b) Combined therapy with MK-801 and nimodipine for protection of ischemic brain damage. Neurology 41:88-94.

Urushitani M, Shimohama S, Kihara T, Sawada H, Akaike A, Ibi M, Inoue R, Kitamura Y, Taniguchi T, Kimura J (1998) Mechanism of selective motor neuronal death after

exposure of spinal cord to glutamate: involvement of glutamate-induced nitric oxide in motor neuron toxicity and nonmotor neuron protection. Ann Neurol 44:796-807.

Verkhratsky A (2007) Calcium and cell death. Subcell Biochem 45:465-480.

Voellmy R, Boellmann F (2007) Chaperone regulation of the heat shock protein response. Adv Exp Med Biol 594:89-99.

Vosler P, Chen J (2009) Calpain-modulation of programmed cell death pathways in cerebral ischemia. In: Experimental Stroke (Yang G, Jin K, eds), pp 1-8. Oak Park, IL: Bentham Science Publishers, Ltd.

Vosler PS, Brennan CS, Chen J (2008) Calpain-Mediated Signaling Mechanisms in Neuronal Injury and Neurodegeneration. Mol Neurobiol.

Vosler PS, Graham SH, Wechsler LR, Chen J (2009a) Mitochondrial Targets for Stroke. Focusing Basic Science Research Toward Development of Clinically Translatable Therapeutics. Stroke.

Vosler PS, Sun D, Wang S, Gao Y, Kintner DB, Signore AP, Cao G, Chen J (2009b) Calcium dysregulation induces apoptosis-inducing factor release: Cross-talk between PARP-1- and calpain- signaling pathways. Exp Neurol.

Wang H, Yu SW, Koh DW, Lew J, Coombs C, Bowers W, Federoff HJ, Poirier GG, Dawson TM, Dawson VL (2004) Apoptosis-inducing factor substitutes for caspase executioners in NMDA-triggered excitotoxic neuronal death. J Neurosci 24:10963-10973.

Wang S, Xing Z, Vosler PS, Yin H, Li W, Zhang F, Signore AP, Stetler RA, Gao Y, Chen J (2008) Cellular NAD Replenishment Confers Marked Neuroprotection Against Ischemic Cell Death. Role of Enhanced DNA Repair. Stroke.

Waskiewicz AJ, Flynn A, Proud CG, Cooper JA (1997) Mitogen-activated protein kinases activate the serine/threonine kinases Mnk1 and Mnk2. Embo J 16:1909-1920.

Waskiewicz AJ, Johnson JC, Penn B, Mahalingam M, Kimball SR, Cooper JA (1999) Phosphorylation of the cap-binding protein eukaryotic translation initiation factor 4E by protein kinase Mnk1 in vivo. Mol Cell Biol 19:1871-1880.

Wasterlain CG (1974) Inhibition of cerebral protein synthesis by epileptic seizures without motor manifestations. Neurology 24:175-180.

Welsh FA, Moyer DJ, Harris VA (1992) Regional expression of heat shock protein-70 mRNA and c-fos mRNA following focal ischemia in rat brain. J Cereb Blood Flow Metab 12:204-212.

Wen Y, Yang SH, Liu R, Perez EJ, Brun-Zinkernagel AM, Koulen P, Simpkins JW (2007) Cdk5 is involved in NFT-like tauopathy induced by transient cerebral ischemia in female rats. Biochim Biophys Acta 1772:473-483.

Wen YD, Sheng R, Zhang LS, Han R, Zhang X, Zhang XD, Han F, Fukunaga K, Qin ZH (2008) Neuronal injury in rat model of permanent focal cerebral ischemia is associated with activation of autophagic and lysosomal pathways. Autophagy 4:762-769.

White MJ, DiCaprio MJ, Greenberg DA (1996) Assessment of neuronal viability with Alamar blue in cortical and granule cell cultures. J Neurosci Methods 70:195-200.

White RJ, Reynolds IJ (1996) Mitochondrial depolarization in glutamate-stimulated neurons: an early signal specific to excitotoxin exposure. J Neurosci 16:5688-5697.

Wu HY, Tomizawa K, Matsui H (2007) Calpain-calcineurin signaling in the pathogenesis of calcium-dependent disorder. Acta Med Okayama 61:123-137.

Wu HY, Yuen EY, Lu YF, Matsushita M, Matsui H, Yan Z, Tomizawa K (2005) Regulation of N-methyl-D-aspartate receptors by calpain in cortical neurons. J Biol Chem 280:21588-21593.

Wyckoff EE, Croall DE, Ehrenfeld E (1990) The p220 component of eukaryotic initiation factor 4F is a substrate for multiple calcium-dependent enzymes. Biochemistry 29:10055-10061.

Xie Y, Mies G, Hossmann KA (1989) Ischemic threshold of brain protein synthesis after unilateral carotid artery occlusion in gerbils. Stroke 20:620-626.

Xie Y, Munekata K, Seo K, Hossmann KA (1988) Effect of autologous clot embolism on regional protein biosynthesis of monkey brain. Stroke 19:750-757.

Xu W, Wong TP, Chery N, Gaertner T, Wang YT, Baudry M (2007) Calpain-mediated mGluR1alpha truncation: a key step in excitotoxicity. Neuron 53:399-412.

Yamashima T, Kohda Y, Tsuchiya K, Ueno T, Yamashita J, Yoshioka T, Kominami E (1998) Inhibition of ischaemic hippocampal neuronal death in primates with cathepsin B inhibitor CA-074: a novel strategy for neuroprotection based on 'calpain-cathepsin hypothesis'. Eur J Neurosci 10:1723-1733.

Yamashima T, Tonchev AB, Tsukada T, Saido TC, Imajoh-Ohmi S, Momoi T, Kominami E (2003) Sustained calpain activation associated with lysosomal rupture executes necrosis of the postischemic CA1 neurons in primates. Hippocampus 13:791-800.

Ye H, Cande C, Stephanou NC, Jiang S, Gurbuxani S, Larochette N, Daugas E, Garrido C, Kroemer G, Wu H (2002) DNA binding is required for the apoptogenic action of apoptosis inducing factor. Nat Struct Biol 9:680-684.

Ying W, Alano CC, Garnier P, Swanson RA (2005) NAD+ as a metabolic link between DNA damage and cell death. J Neurosci Res 79:216-223.

Yu SW, Andrabi SA, Wang H, Kim NS, Poirier GG, Dawson TM, Dawson VL (2006) Apoptosis-inducing factor mediates poly(ADP-ribose) (PAR) polymer-induced cell death. Proc Natl Acad Sci U S A 103:18314-18319.

Yu SW, Wang H, Poitras MF, Coombs C, Bowers WJ, Federoff HJ, Poirier GG, Dawson TM, Dawson VL (2002) Mediation of poly(ADP-ribose) polymerase-1-dependent cell death by apoptosis-inducing factor. Science 297:259-263.

Zhou BB, Li H, Yuan J, Kirschner MW (1998) Caspase-dependent activation of cyclin-dependent kinases during Fas-induced apoptosis in Jurkat cells. Proc Natl Acad Sci U S A 95:6785-6790.

Zhu C, Qiu L, Wang X, Hallin U, Cande C, Kroemer G, Hagberg H, Blomgren K (2003) Involvement of apoptosis-inducing factor in neuronal death after hypoxia-ischemia in the neonatal rat brain. J Neurochem 86:306-317.